University of Montana

ScholarWorks at University of Montana

2011

SAMPLING AND MODELING OF SEDIMENT TRANSPORT AND RESERVOIR EROSION FOLLOWING DAM REMOVAL: MILLTOWN DAM, MONTANA

James Walden Johnsen
The University of Montana

Follow this and additional works at: https://scholarworks.umt.edu/etd

Let us know how access to this document benefits you.

SAMPLING AND MODELING OF SEDIMENT TRANSPORT AND RESERVOIR EROSION FOLLOWING
DAM REMOVAL: MILLTOWN DAM, MONTANA

By

JAMES WALDEN JOHNSEN

Bachelors of Science, Utah State University, Logan, Utah, 2003

Thesis

Presented in partial fulfillment of the requirements
for the degree of

Master of Science
in Geosciences

The University of Montana
Missoula, MT
Spring 2011

Approved by:

Dr. Perry Brown, Associate Provost for Graduate Education
Graduate School

Dr. Andrew Wilcox, Chair
Department of Geosciences

Dr. Johnnie Moore
Department of Geosciences

Dr. Lisa Eby
College of Forestry & Conservation

Johnsen, James W., M. S., Spring 2011
     Geosciences

Sampling and Modeling of Sediment Transport and Reservoir Erosion Following Dam Removal: Milltown Dam, Montana

Committee Chair: Dr. Andrew Wilcox

  Measurements of bedload transport in combination with suspended sediment and discharge data collected by the USGS illustrate the rates, magnitudes and processes by which reservoir sediment evacuated the Milltown Reservoir after the 2008 removal of Milltown Dam from just downstream of the confluence of the Blackfoot and Clark Fork Rivers, Montana. Mobilized sediments transported as a series of distinct waves and the speed at which the waves moved downstream was dependent upon the grain size of the sediment. Sand and smaller sized particles were transported out of the reservoir rapidly both as bedload and in suspension with different thresholds for incipient motion between the confined Blackfoot and unconfined alluvial Clark Fork Arms of the reservoir. Bedload sediments, gravel and larger sized, transported downstream as a dispersing and translating wave. Sediment budget calculations, both volumetric and transport derived, illustrate the one-dimensional HEC-6 and DREAM-1 model's inaccuracy in predicting sediment transport in unconfined alluvial deposits while both models predicted accurately confined channel geometry transport settings. Results from sampling and modeling demonstrate that the most important factors in reservoir sediment transport are the channel geometry, hydrology, and grain size and location of the reservoir sediment; which in turn determine distance, processes and timing of transport.

Acknowledgements:

Table of Contents:

List of Figures:

List of Tables:

Chapter 1: Thesis Introduction

The average age of the more than 85,000 dams in the U.S. is over 50 years, and the gap between dams needing repair and those actually repaired is growing significantly (ASCE, 2009). Whether these dams are repaired and relicensed or removed will depend upon the environmental, economic, social and political issues involved. An environmental issue most dams have in common is that they block the delivery of sediment to the downstream reaches of the channel (Heinz Center, 2002). Reservoir sediment accumulation is a key issue when a dam has exceeded its life span and is being considered for relicensing and for a number of dams, sedimentation is soon to be a major problem for their continued sustainability (Graf et al., 2010). Although removal of accumulated sediments is an option, it is expensive. Combining this expense with retrofitting the dam structure, fish passage, public opinion and other issues, the costs can outweigh the benefits, resulting in the dam being removed (Pejchar and Warner, 2001; Poff and Hart, 2002). A growing trend in dam removal is therefore expected, presenting unique challenges for river scientists (Heinz Center, 2003).

There is substantial uncertainty regarding the physical and ecological changes caused by dam removal (Doyle et al., 2002; Rathburn and Wohl, 2001). Field monitoring programs and improved tools to understand the rates, magnitudes, and processes by which sediment evacuates a reservoir and transports downstream following dam removal is needed (Babbitt, 2002; Bushaw-Newton et al., 2002; Grant, 2001; Hart et al., 2002; Nelson et al., 2002; Pizzuto, 2002; Poff et al., 2006; Poff and Hart, 2002; Shuman, 1995; Stanley and Doyle, 2003). In addition, to date the majority of dam removals have taken place on smaller rivers and streams while large river dam removals are rare. The removal of larger dams such as Milltown Dam in Montana presents an opportunity to learn not only about large dam removal, but also about how large rivers function (Hart et al., 2002). For example, a large dam that still maintains mostly natural discharges and limits the sediment influx downstream of the dam will coarsen and armor the downstream channel, causing a stable sediment transport-free reach at most discharges (Schmidt and Wilcock, 2008). Thus, removal of such a dam provides a unique opportunity to sample and understand a large sediment perturbation imposed on a stable, relatively transport-free channel (Grant, 2001).

Numerical models are increasingly used to predict the impacts associated with dam removal. There is a need to validate and develop these models to predict rates, magnitudes, where this sediment will be deposited downstream and its impact to the channel (Doyle et al., 2002). With any model prediction, data can help us understand the limitations of the model and the error in the assumptions made by the modelers. Combining model predictions with empirical data can help researchers and decision makers evaluate the modeling efforts of future dam removals (Doyle et al., 2002; Nelson et al., 2002; Pizzuto, 2002; Rathburn and Wohl, 2001). This can provide others with more confidence in their predictions and show the benefits of using one model over another.

My study investigated the rates, magnitudes, processes and modeling of sediment transport after the removal of Milltown Dam. Using bedload and suspended sediment measurements I evaluated the initial pulse of primarily fine sediment released into a gravel-cobble bedded river. Further, I evaluated the bedload sediment wave that moved out of the reservoir and downstream of the dam. I constructed a sediment budget of the reservoir sediments in transport, taking into account the storage of reservoir sediment downstream of the dam. This budget was compared to volumetric estimates and previous modeling of reservoir sediment erosion. The limitations and assumptions of the previous modeling efforts were identified to understand the possible errors in the results. I also applied another model, designed specifically for dam removal, to the Milltown sediments and evaluated for accuracy.

Milltown Dam Removal:

Milltown Dam was constructed in 1907, immediately downstream of the Blackfoot and Clark Fork River confluence, and had a total drainage area of about 15,700 km^2. The dam impounded both rivers, resulting in two different reservoir arms that joined near the dam. The arm impounding the confined Blackfoot River had a drainage area of about 6100 km^2 while the Clark Fork Arm impounded a wide alluvial floodplain with a drainage area of about 9600 km^2. Blackfoot Arm sediments were composed of sand and silt in the lower 2 km and gravel and cobble in the upper 1 km of the reservoir (Envirocon, 2004a). Sediments in the Clark Fork Arm of the reservoir were composed of silt to fine sands in the lower 1.5 km and coarse sand to fine gravel in the next 1-2 km reach upstream (Harding Lawson Associates, 1986; Titan, 1995). In general, both arms of the reservoir had fine grained sediments in the downstream reaches which coarsened, moving upstream, until particle sizes blended into the active river sediments entering the reservoir.

Both arms of the reservoir had been accumulating sediment since construction of the dam. One flood in particular, a 300 – 500 year flood event in 1908, deposited millions of m^3 of sediment in the reservoir. The total volume of sediment accumulated in the reservoir since the 1907 construction was estimated to be >5 million m^3, the majority of which were deposited in the Clark Fork Arm (Harding Lawson Associates, 1986). Most of these Clark Fork reservoir deposits were contaminated to varying degrees with arsenic, cadmium, zinc, copper and selenium from upstream copper mining and smelting operations near Butte and Anaconda Montana. In 1983, the EPA placed the contaminated Butte and Anaconda mining areas and about 210 km of downstream river length on its list of hazardous waste sites needing cleanup, currently the largest complex of Superfund sites in the nation. The Clark Fork sediments in the former Milltown Reservoir represent the downstream extent of this Superfund area (Moore, 1985). The Blackfoot deposits in the reservoir were not contaminated.

Several issues led decision makers to consider the removal of Milltown Dam:
1. Contaminants from the reservoir sediments had started showing up in local groundwater wells in 1981 (Moore and Woessner, 2003).
2. Periodic ice jams (e.g., 1996) were disturbing and transporting contaminated reservoir sediment downstream (Moore and Landrigan, 1999).

3. The reservoir blocked the migration of native fishes like bull trout and westslope cutthroat trout (USFWS, 2002).
4. The 1998 listing of bull trout as threatened under the Endangered Species Act (USFWS, 1998).
5. The dam structure was nearly 100 years old, past its designed lifespan, no longer economically viable and was classified as "High Hazard Potential" by FERC in 2000 (Hall, 2000).

The selected method for removing the Milltown Dam involved a multiple-stage process. In 2005 the Stimson Dam, built in 1884 and submerged in Milltown Reservoir waters in 1907, was removed from the Blackfoot Arm of the reservoir (Epstein, 2009). After an initial reservoir drawdown of 3.7 m in 2006, an engineered bypass channel was constructed through the lower half of the contaminated Clark Fork sediments. This bypass channel limited sediment erosion in the lower half of the Clark Fork Arm and allowed >2 million m^3 of the most contaminated sediment to be mechanically removed in the dry and shipped by rail. This still left >2 million m^3 of contaminated sediment in the upper half of the Clark Fork Arm susceptible to river transport (Brinkerhoff, 2009). On March 28, 2008 the Milltown Dam was breached, representing the first time in over 100 years that bedload sediments from the Clark Fork and Blackfoot Rivers were able to flow freely past the Milltown Dam area.

Several previous studies documenting the Milltown Reservoir have been used as data sources for this project. A three year site investigation and summary of previous activities, like reservoir sediment characterization, was prepared in 1995 for the Atlantic Richfield Company (Titan, 1995). To evaluate the proposed dam removal strategies and predict the transport of the reservoir sediments during and after the removal, the one-dimensional HEC-6 model was applied to the reservoir sediments(Envirocon, 2004b). As part of dam removal efforts, geomorphic data was collected from the Clark Fork and Blackfoot Rivers in the Milltown area (River Design Group and WestWater Consultants, 2006). In 2006, to monitor the sediments evacuating the reservoir during construction and after the removal, the USGS was asked to provide sampling of the suspended sediment from the Duck Bridge within the Clark Fork Arm of the reservoir (Clark Fork Bypass near Bonner-station 12334570) and at the local gauging stations upstream and downstream of the reservoir as a supplement to the ongoing long term monitoring program in the Upper Clark Fork basin (Dodge et al., 2009; Lambing and Sando, 2009). All suspended sediment results described in this study were collected by the USGS and were obtained from the above reports or the USGS website (USGS, 2010).

Objectives:

Few data sets of large river and large dam removal sediment transport are available. Sediment transport models have little data to verify predictions. My project addresses these gaps in the current knowledge to better understand the rates, magnitudes and processes by which sediment evacuated the Milltown Reservoir after dam removal. My objectives are:

1. Measure bedload transport following the removal of Milltown Dam at locations upstream, within and downstream of Milltown Reservoir to identify the rates, magnitudes, and timing of transport.
2. Construct a sediment budget for the Milltown Dam removal, including determination of the volume of sediment eroded out of Milltown Reservoir and transported downstream, by combining bedload transport data with suspended sediment and discharge data collected by USGS.
3. Develop insights into sediment transport processes, including identification of transport modes (bedload versus suspended load) and thresholds, hysteresis patterns, and grain-size-specific transport across hydrographs.
4. Compare the HEC-6 model predictions of sediment transport out of Milltown Reservoir to measured sediment transport rates to evaluate model accuracy and limitations.
5. Simulate sediment transport out of Milltown Reservoir using an alternative reservoir erosion model, DREAM (Dam Removal Express Assessment Model), for comparison to measured sediment transport rates and to HEC-6 predictions.

Chapter 2: Dam Removal Sediment Transport

Introduction:

There are conditions unique to dam removals that complicate the current understanding of river sediment transport. When in place, dams alter the dynamic equilibrium between natural hydraulic forces and sediment supply (Grant et al., 2003). This leads to deposition of sediment within the impoundment, typically showing a coarsening in grain size moving upstream of the dam. Further, the downstream channel, deprived of coarse sediment in transport, will coarsen the bed material, armor and degrade (Schmidt and Wilcock, 2008). Following dam removal, it is expected that sediment input to the downstream system will increase as the sediment volume stored within the reservoir decreases. The change brought on by the presence of the dam creates uncertainty when we try to predict how the reservoir sediment will erode and transport. Once the dam is removed, the altered channel below the reservoir receives sediment that is changing through time in caliber and volume. Furthermore, the caliber of reservoir sediment in transport is not represented by the grain size distribution of the downstream channel bed material.

To better understand how reservoir sediments will erode and transport we can examine other large scale sediment inputs to rivers. Current theories on how reservoir sediment will transport after removal suggest that it may be translated downstream either as a distinct wave or gradually eroded away (Doyle et al., 2002). If the coarse grained reservoir sediment moves as a wave we can link it to studies of sediment wave propagation. Previous research suggests that bedload waves disperse, translate or disperse and translate downstream (Gilbert, 1917; James, 2010; Lisle et al., 2001; Sklar et al., 2009). Early studies by Gilbert (1917) characterized translational movement of large scale sediment waves produced by hydraulic mining along tributaries of the American and Sacramento Rivers in California. Lisle et al. (2001) revisited the findings from this and other sediment wave studies and concluded that in natural settings the dominant pattern of wave movement is dispersion; and that in rare cases waves transporting in channels with Froude numbers much less than one can have a translational movement downstream. The Froude number is a dimensionless number and is defined as the ratio of a characteristic velocity to a gravitational wave velocity (Equation 1):

$$F_r = \frac{V}{\sqrt{g\frac{A}{B}}}$$

(1)

where F_r is the Froude number in shallow water, V is the characteristic velocity (equal to the average flow velocity over the cross-section perpendicular to the flow direction), g is the acceleration of gravity, A is cross-sectional area and B is surface width.

Flume studies by Sklar et al. (2009) tested the effectiveness of gravel augmentation as a river restoration strategy below dams. They found that pulse translation of added sediment to armored channels can occur where the introduced sediment is finer than the pre existing bed material. The two factors that were found to influence wave behavior are the interactions

between flow, wave topography and bed load transport; and particle sizes of sediment in transport and pre-existing bed material. Supporting previous research, Sklar et al. (2009) also found that low Froude numbers and finer grain sizes in transport than on the channel bed can result in a translating and dispersing wave.

Studies of suspended sediment transport after volcanic eruptions provide insights to the transport of fine grained sediment pulses. The eruption of Mount Pinatubo in the Philippines released extreme quantities of fine sediment to surrounding drainages (Gran and Montgomery, 2005, 2006). Overall, initially high sediment transport rates declined through time as fine sediment availability continued to decline and deposits became more stable. Initial channel response included selective transport of the finer grained sediments at high rates. As fine sediment inputs declined, the channel incised through progressive winnowing into gravel and coarser particles. This developed clast structures which increased roughness and further decreased transport rates.

Mount St. Helens erupted in 1980 and abruptly introduced massive amounts of fine sediment to sediment transport. Twenty years of data illustrate that the moderate magnitude discharges (greater than mean annual flow but less than the 2 year event) transported 60% to 95% of the annual suspended sediment loads (Major, 2004; Major and Mark, 2006). These frequent small discharges transported suspended sediment during rill and gully development. Once the rills and gullies were developed from the small discharges, more moderate magnitude discharges emerged as the dominant sediment transporting flows (Major, 2004). If land sliding delivered sediment to the channel, then large discharges became the more dominant transporting flow. In both eruptions, as the supply of fine grained sediment decreased, suspended sediment transport rates declined (Gran and Montgomery, 2005; Major, 2004).

The next largest dam removal (after Milltown) in terms of sediment exposed to river transport was the Marmot Dam, removed in October of 2007 from Oregon's Sandy River. This removal involved a large river and sediment release, but the Marmot removal released primarily coarse bedload sediment whereas the Milltown removal released mostly sand and smaller sized sediments. Bedload and suspended sediment samples collected after the Marmot Dam removal quantified the rates and magnitudes of sediment transport and constructed a sediment budget (Major et al., 2008a; Major et al., 2008b; Major et al., 2009). Comparison between that study and results from the Milltown removal should allow for a better understanding of the potential responses to future dam removal.

Here I describe the rates, magnitudes and processes by which Milltown Reservoir sediments evacuated and transported downstream after dam removal. Using bedload and suspended sediment results I have quantified the forces at which sediment evacuated and transported downstream of the reservoir, including the shear stress at which grain motion initiated. Bedload sediment rating curves have been developed to demonstrate the differences between the armored channel below the reservoir, the reservoir sediment in transport and the unaltered channel upstream. Dimensionless transport and shear stress calculations of the sample data

contrast the transport of the reservoir sediment with dimensionless ranges. I have identified the patterns and thresholds of transport for the coarse bedload and fine suspended reservoir sediments. My data set is unique. Rarely do studies collect bedload sediment in such conditions. All previous studies of dam removal, except the Marmot Dam removal, have been on smaller rivers, and none have collected bedload data at such high discharges. My study not only is important for dam removal but could also provide insights to large rivers and how they function.

Methods:
Study Area:
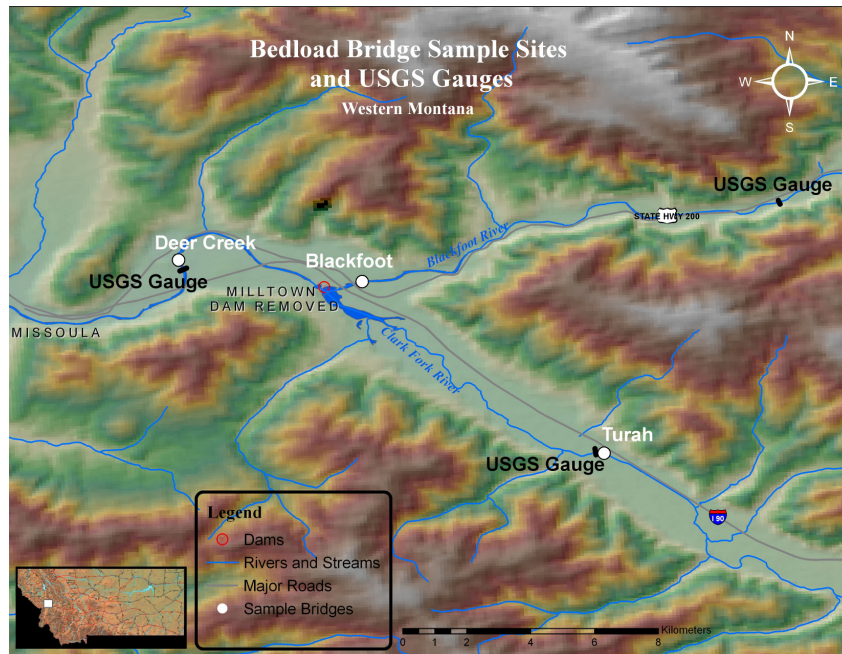
Figure 2.1 Location map of Milltown Dam area where white dot represent bedload sample locations, black bars represent USGS sample locations and open red circle represents the location of the Milltown Dam removal.

My bedload samples were collected at three sites: 1) upstream of the reservoir on the Clark Fork River, 2) within the reservoir on the Blackfoot River and 3) downstream of the reservoir on the Clark Fork River (Figure 2.1). The upstream Clark Fork samples were taken from the Turah Bridge at the USGS 12334550 Clark Fork at Turah Bridge near Bonner, MT Gauge. The Turah Bridge spans a bifurcated alluvial channel with the majority of the water running through the river right channel. Comparisons between surveys collected by the USGS in 2006 and UMT in 2010 showed that the right channel scoured 3-5 m of the island during the 2009 sampling season, matching changes in wetted channel width during the 2009 spring runoff. The Turah Bridge has a pylon in the center of each side channel and the maximum depth at low flow is about 2 m.

Bedload was measured in the Blackfoot River from a pedestrian bridge 0.7 km upstream of the confluence of Blackfoot and Clark Fork Rivers. This site is denoted below as "Black." The resulting bedload rating curves used discharge values from the USGS 12340000 Blackfoot River near Bonner, MT Gauge, which is about 13 km upstream of the sample bridge. There is a difference in drainage area between the gauge and sample site of about 170 km^2. This added un-gauged drainage area is about 3% the total drainage area. Assuming the added area between the sites does not represent a significant difference in discharge, I used the USGS Blackfoot River near Bonner Gauge discharge values to represent the hydrograph of the Black sample site. The Black site underwent significant changes during the sampling period. The original pedestrian bridge that crossed the Blackfoot River was considered unsafe once the dam was removed. In 2008 a temporary construction bridge was available for my sampling. This construction bridge had many I-beam pylons and was about 4 m above the water surface at the time of the 2008 samples. In 2009 I sampled from the newly refurbished pedestrian bridge that is about 12 m above the water surface and spans > 70 m with no pylons, the entire active channel. The channel below the bridge would be classified as a run with a cobble bar in mid channel that becomes inundated at moderate discharges. As of 2010 the maximum depth at low flow is about 1.5 m, and since the dam removal in March 2008 the channel has dropped in mean elevation by about 3-4 m.

The samples I took downstream of the dam were collected from the Deer Creek Bridge, about 4 km below the reservoir and 100 m upstream of the USGS 12340500 Clark Fork above Missoula MT Gauge. This site is denoted below as "Deer." The bridge has two in channel pylons located about 10 m from the left and right edge of water at low flow. The majority of the flow passes between these pylons. The bridge spans a pool with a maximum water depth of 4-5 m at low flow.

Field Methods:
Bedload Sampling:
I sampled bedload sediment in 2008 and 2009 by placing a sampler on the channel bottom for a given duration. A total bedload sample consists of several individual sub-samples, collected across the channel by increments, compiled together. My field sampling methods followed guidelines from various studies (Edwards and Glysson, 1999; Gomez, 1991). In 2008 and 2009, I collected 57 total cross-section integrated bedload samples from the bridges at discharges between 30 and 500 m^3/s (Figure 2.2; Table 2.1). As a result of variable equipment availability, I used three different samplers. Bedload samplers have an intake nozzle and bag for storing the sediment. Each type of sampler has a certain nozzle width, which influences capture efficiency, and also has an expansion ratio to counteract the bag's resistance to flow. In 2008, I used a 15.2-cm Helley Smith sampler with a truck-mounted, one ton Econoton Autocrane and a Warn 4700 winch with a 30 m long, 0.63 cm diameter steel cable. In 2009, I used both BL-84 and Toutle River samplers. The BL-84 sampler was placed using a USGS trolley mounted crane and hand crank with a 40 m, 0.32 cm steel cable at low discharges, and the Toutle sampler was placed using a truck-mounted, Liftmoore one ton bed crane with a retractable 2.1 m boom, and

a WARN 3700 winch with a 30 m, 0.63 cm steel cable at moderate to high discharges (Figure 2.3).

Table 2.1 Summary of the sampler and number of samples collected at each bridge site.

Bridge Sample Site	2008, number of samples collected with the 15.2 cm Helley-Smith sampler.	2009, number of samples collected with the 7.6 cm BL-84 and 30.5 cm Toutle samplers.
Turah	5	11
Black	4	10
Deer	6	21
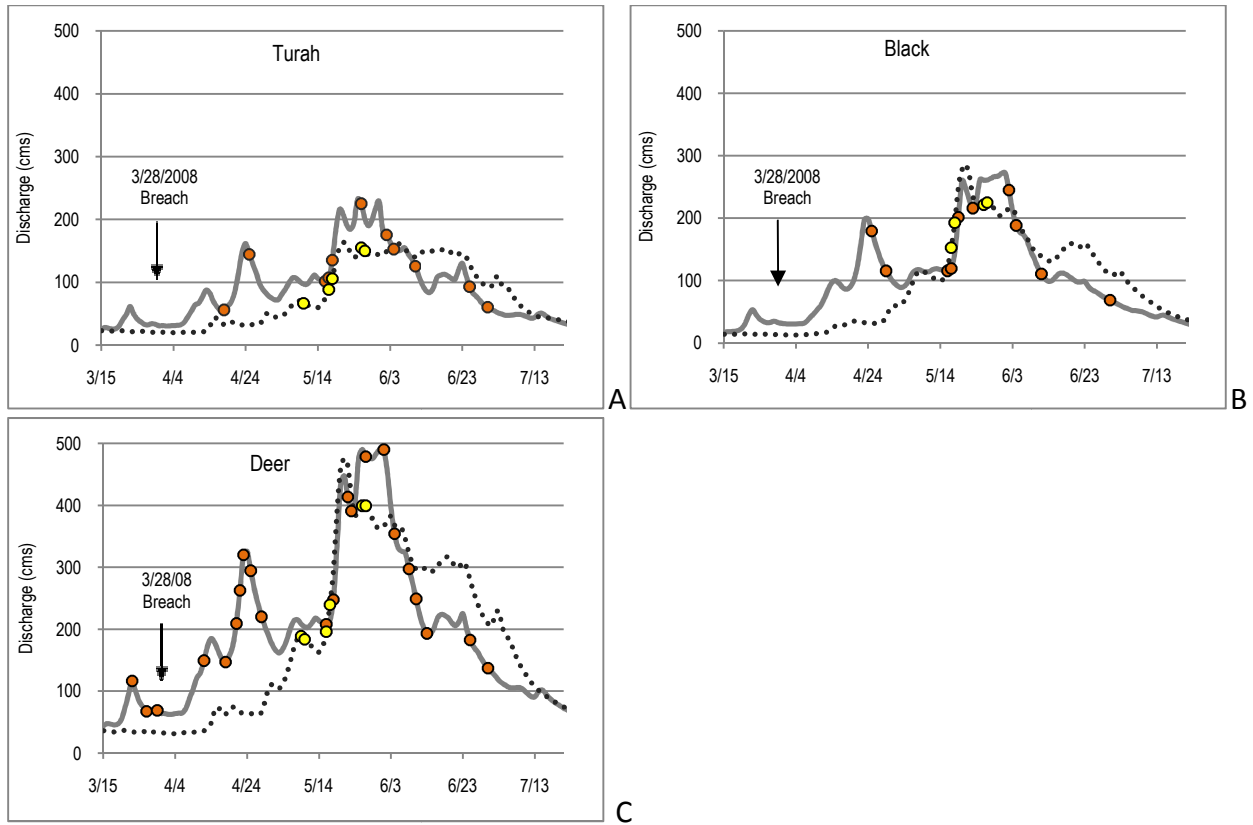
Figure 2.2. Days and discharges sampled at Turah (A), Black (B) and Deer (C) Sites in 2008 and 2009. Grey line represents the 2009 hydrograph, dotted line the 2008 hydrograph, orange dots the 2009 sample days and yellow dots the 2008 sample days.

Figure 2.3 Sampling in 2009 with the Toutle sampler from Deer Creek Bridge.

I took ten sub-samples at each bridge at even intervals across the channel in 2008. In 2009, the new Blackfoot Pedestrian Bridge's spanning framework only allowed me 9 sample points between the support beams. In 2008 all my sub samples were three minutes long for a total sample time of 30 minutes. In 2009, the sub-samples ranged between thirty seconds to three minutes for a total sample time between five and thirty minutes. The shorter sample times prevented the sample bag from filling to greater than 50% capacity (Emmett, 1980). Both the 2008 and 2009 sample seasons occurred during the spring runoff and I took samples at different discharges on both the rising and falling limb of the hydrograph (Figure 2.2). All the bedload samples I collected in 2008 were with a borrowed vehicle and sampler setup. Each set of 2008 samples required ~ 1600 km of driving and two full days of my donated labor. This allowed me to only collect a limited number of bedload samples in 2008.

Bedload samplers used nylon mesh bags to collect and store the sediment. All the samples I collected with bags having pore spaces of 250 or 300 microns, except for samples collected between May 22 and May 26 of 2009. During this time I used a nylon mesh bag with 3 mm pore spaces because the fine pore spaced bag ripped and replacement bags were in transit. A further description of adaptive bedload sampling methods used in 2009 is provided in Appendix A.

Channel Characteristics:
To calculate hydraulic conditions at sampling locations, I documented geometry and roughness of the channel at each bridge by surveying cross-sections and counting pebbles. The cross-sections were surveyed 1 meter downstream of the bridges (i.e., in the same location as bedload measurements) with a total station. Where depth of water prevented me from surveying with standard rod and prism, a 20 kg torpedo depth sounding was taken to get

elevation differences from surveyed points on the bridge. I then modified the elevations of the bridge points to complete the cross-sectional surveys.

I performed pebble counts as close to the bridge locations as possible. The Turah pebble count was collected from a patch that covered the left half of the main channel from 15 to 40 meters downstream of the bridge. The pebble count for the Black site was collected 10 to 20 meters downstream of the bridge in the center of the channel. The Deer pebble count was collected about 100 meters downstream of the bridge, from the USGS cable downstream 20 m along the left bank 15 m into the channel. All my counts followed methods described by Wolman, (1954).

Sample Processing:
Bedload samples were dried and sieved. I sieved with Ro-Tap and Gilson sediment shakers with trays in half-phi increments, from 64 to 0.063 mm. Further, I separated particles larger than 64 mm by hand for grains > 64, > 90 and > 128 mm. After sieving, the sorted sediment was weighed and samples were returned to the original labeled sample bag for preservation. I compiled results from the sieving with the sampler width, width of the channel at the time of the sample, the USGS 15-minute gauge data at the sample time, the start and end time of the sample, the sample location and the date.

Bedload discharge can be extremely variable, spatially and temporally, as a result of variations in discharge and in transport versus supply limitation. For example, river sediment can move in waves or slugs (Edwards and Glysson, 1999), and sample times that do not include the entire wavelength of these sediment waves can over or under-represent the mean transport rate. I evaluated the sampling intensity associated with bedload measurements for this project to assess the proportion of the bedload transport population that was sampled during the sample period. I calculated the sampling intensity by taking the product of the number of sub-samples, nozzle width and duration of a sub-sample and dividing that by the product of the channel width and the total work time required to collect the sample (Bunte et al., 2007). This calculation I applied to each of the samples and summary statistics were reported for each site (Table 2.2).

Table 2.2 Summary statistics for calculations of sampling intensity. Values reported include all samples collected in 2008 and 2009.

Sampling Intensity Statistics	Turah	Black	Deer
Mean	0.0023	0.00076	0.0013
Standard Deviation	0.0013	0.00040	0.00060
Range	0.0039	0.0011	0.0027
Count	16	14	27

Analytical Methods:

Bedload Transport Rates:

The bedload samples I collected from the bridges in 2008 and 2009 represent a sampler width average of the total bedload transport at the cross-section sampled for the duration of the sample period. All sediment transport data are presented in rates of metric tons per day (t/d). To calculate the total transport for any given sample or particle size fraction of a sample, the weight of the sample is multiplied by channel width at the time of the sample over the sampler width and sample duration. The resulting rate then represents the bedload transport at the time, discharge and location of the sample. To compare the sampled transport rates with the current state of knowledge, I converted the sample rates into dimensionless transport rates. The dimensionless transport rate I calculated for this study is W^* (Wilcock et al., 2009):

$$W^* = \frac{(s-1)gq_s}{(\tau/\rho)^{\frac{3}{2}}}$$

(2)

where W^* is the dimensionless transport parameter, s is the ratio of ρ_s/ρ (ρ_s being the density of the sediment and ρ being the density of water), g is the acceleration of gravity, q_s is the volumetric bedload flux per unit width, and τ is shear stress. Assuming steady, uniform flow and a large width to depth ratio (>~20), shear stress can be expressed as:

$$\tau = \rho g d S$$

(3)

where τ is shear stress, d is water depth and S is slope.

Hydraulic Analysis:

To quantify the hydraulic forces acting at each sample site, I entered channel geometry data into WinXSPRO and a user supplied Manning's n option was applied to the cross-section data to match water surface elevations to discharge values at the time of the surveys. Output from WinXSPRO modeling included average shear stress, Froude number and average velocities for the range of discharges sampled. These data were used further to calculate reference shear stress (Wilcock, 1988). Reference shear stress is the shear stress at which a small dimensionless transport rate of W* equals 0.002. To represent the dimensionless shear stress to grain size ratio the Shields number was also calculated using the WinXSPRO output values:

$$\tau^* = \frac{\tau}{(\rho_s - \rho)gD}$$

(4)

where τ^* is Shields number and D is grain diameter (often the grain diameter used is the D50, or median grain size)(Wilcock et al., 2009). My Shields number calculations used grain size values that included the most abundant particle size in transport by weight and year, the largest particle in each sample and the D50 of the channel surface. I presented reference shear stress, reference Shields number and reference discharge values as a range because several groups of bedload calibration data were used. I used two different grain size distributions for the Black site between years. To evaluate the 2008 threshold for sediment motion I used the

D50 and D65 of the reservoir sediment prior to removal. To evaluate the threshold for sediment motion in 2009, at the Black site, I used D50 and D65 values obtained from UMT pebble counts.

Combining the hydraulic analysis results with the dimensionless transport parameter W* allowed me to compare transport rates through time. Although the formula for W* typically requires the proportion of the bed material within various grain size fractions as an input, I did not use it. This is because I noticed the grains in transport were not represented by the bed material in most cases or the bed material was changing through time, downstream and within the reservoir respectively. Instead I used the proportion of sediment in transport within various grain size fractions. I calculated W* for the total bedload in transport with a fraction of one and for individual unit bedload flux of selected grain size categories which individually have a fraction equal to one.

Reference Shear Stress Calculation:
To approximate critical shear stress I used samples of bedload transport to identify a small reference transport rate (Parker and Klingeman, 1982). The shear stress required to transport at the rate of reference transport is called the reference shear stress and was used in place of the critical shear stress (Wilcock, 1988). I applied a spreadsheet authored by Peter Wilcock to calculate reference values. Several different inputs were required for my calculations. I utilized results from WinXSPRO to enter the discharge to mean channel velocity relationship (i.e., hydraulic geometry). Other variables I entered include the slope of the channel, D65 and D50 of the bed material for drag partitioning (the D50 had no influence on the results), width of the bed material (not the channel width), and the volumetric discharge and transport rate of the samples. Once I entered these data, the reference shear stress value was adjusted manually to visually match the sample data until the dimensionless transport rate W* equaled 0.002 (after Wilcock et al., 2009). I then recorded the unique values of reference shear stress (τ_r) and the reference Shields number (τ_r^*) at which grain motion occurred, and relative to the median grain size of the channel sediments. I preformed separate calculations for the 2008 Deer and Black sample data to understand the reference values of the sand pulse that evacuated the reservoir on the rising limb of the 2008 hydrograph.

Rating Curve Calculation:
I used bedload data to develop empirical rating curves by identifying patterns of hysteresis, removing outliers and applying a power function regression to the resulting data sets. Separate rating curves were developed for rising and falling limbs of the hydrograph when a pattern of hysteresis was observed. This hysteresis can be attributed to several conditions, like the channel surface being armored or more sediment being available for transport early in the hydrograph (Moog and Whiting, 1998). If I did not observe hysteresis and results between years demonstrated little to no change in the transport regime, then I compiled the data and a single rating curve was developed for all the sample data.

Outliers were identified and removed from the rating curve regression in two ways. Samples that I determined in the field to have been poorly sampled were removed; usually an additional

sample was collected on site. I further removed points by calculating leverage statistics in SPSS, to identify sample points that had leverage (i.e. an unbalanced influence) on the resulting regression (Figure 2.4).
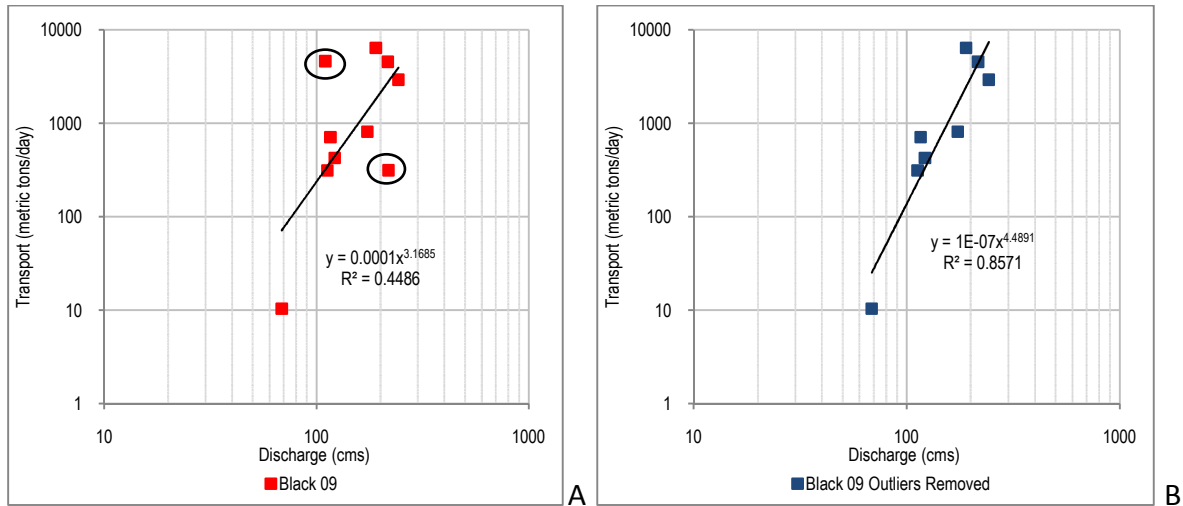
Figure 2.4 Graphic demonstrating leverage statistical analysis results. Original Black 2009 data set with outliers identified from the SPSS leverage statistics analysis (A), and the resulting rating curve once the outliers were removed (B) (circled in black are the outliers identified (A), rating curve regression equations and subsequent R^2 values are reported for each data set).

Because the transport to discharge relationship took the form of a power function the discharge and transport rate values were converted to log form. I entered the resulting values into SPSS, applied a linear regression, and calculated the leverage values for each sample. Using the same discharge values as the sample data a second control data set was created. This time I calculated the transport values from the discharge values to reflect a power function regression with an R^2 value of 1. I converted the control data set to log form and ran it through SPSS. This control run was compared to the sampled leverage values. If any sample leverage values were more than double the control values then I removed the data point from further calculations (Figure 2.4).

Once the outliers were removed, I plotted the remaining data against sample discharge on log-log plots. A power trendline regression was applied with the resulting R^2 value and unique power trendline equation recorded for each rating curve. This calculation is based upon standard statistical methods of fitting a regression to empirical data to obtain the exponent and coefficient of the power equation. Once I developed the rating curves, mean daily discharge values, from the sample site and during the sample period, were plugged into the power equation to calculate the daily bedload transport in t/d. This method was also used to develop rating curves for different grain size fractions in transport.

To address the possible error associated with the rating curve calculation I applied a bootstrapping method to the data after outliers were removed. The bootstrapping method

14

sampled from the data set at random, returning the value selected to the pool after every selection, to calculate a rating curve. Fifteen minute gauge data were used to quantify the bedload sediment transported during the discharge interval and the result was reported. The program then re-sampled from the data and performed the calculation again until 1000 unique transport totals were accomplished. Statistics from these results calculated, with 90% confidence, an interval containing the quantity of bedload sediment transported based on the data set (Efron and Tibshirani, 1994).

Sediment Budget:
To calculate a sediment budget (Dietrich et al., 1982) for Milltown Reservoir, the quantity of the bedload and suspended sediment exiting the reservoir is subtracted from the sediment entering (In - Out = ΔS). All suspended sediment data used in the sediment budget calculations I obtained from the USGS. USGS reports (Dodge et al., 2009; Lambing and Sando, 2009) described the suspended sediment exiting the reservoir in 2008. I used additional USGS sampling results in 2009. I obtained long term data sets of the suspended sediment transport regime entering the reservoir from the USGS for the Clark Fork at Turah Bridge and Blackfoot River near Bonner Gauges. All suspended sediment transport totals are a product of my simply summing the daily suspended sediment transport results published on the USGS website, for the time interval of interest. The analysis of volumetric storage change in Milltown Reservoir has been completed by other UM researchers (Brinkerhoff, 2009; Epstein, 2009).

To quantify the bedload sediment budget, I totaled daily bedload transport rates calculated from the rating curves for the period of interest. A variety of empirical and calibrated rating curves were used to total the bedload sediment out of the reservoir.
1. Input to the reservoir: Bedload input from the Clark Fork drainage relied upon the Turah empirical rating curve. This rating curve was developed from the data I collected in 2008 and 2009, supplemented by 2006 data collected at Turah by River Design Group (River Design Group and WestWater Consultants, 2006). Bedload input from the Blackfoot River was quantified from a rating curve developed from data collected on the Blackfoot along Highway 200, upstream of the extent of reservoir influence, by River Design Group in 2006 (River Design Group and WestWater Consultants, 2006). This rating curve was used here because my Blackfoot data were from a site within the reservoir-influenced reach of the Blackfoot, so did not represent input to the reservoir.
2. Output from the reservoir: The 2008 Deer bedload totals used the Wilcock rating curve I calibrated with the first two samples collected at moderate discharges in 2008. This calibrated rating curve represented the sand bedload transport leading up to the start of the sample period. I used the inverse empirical rating curve developed from the 2008 data to represent the transport during the sampling period. I then applied the Wilcock rating curve that had been calibrated to the last two transport samples in 2008, to represent the transport regime after the sample period. In 2009, the empirically derived rising and falling limb rating curves were used to represent their respective limbs of the hydrograph.

Additional methods can be found in Appendix A.

Results:

Bedload Transport, Rates and Grain Sizes in Transport:

Bedload transport results are presented in several different forms to illustrate the spatial and temporal variability in transport rates and grain sizes in transport. I have presented rates of transport in t/d with the respective discharge values while dimensionless transport rates of individual size fractions are graphed against calculated shear stress values (Figures 2.5-2.7). Empirical rating curve regression equations and R^2 values are reported in the text and Table 2.3. The application of the rating curves for the 2009 sample season is shown in Figure 2.8. A summary of the changing grain sizes in bedload transport at the Black and Deer sites is provided in Figure 2.9.

Sample results from the Turah site are provided to demonstrate patterns of transport typical of a river not transporting high volumes of reservoir sediment. The consistent relationship between transport and discharge at Turah allows me to develop of a single empirical rating curve for the three years of data (Figure 2.5.A). In 2009, 3 samples transported particles > 64 mm at high rates (Figure 2.5.B), potentially as a result of local channel geometry adjustments. Regardless of this variability, I developed a single regression ($y=5E-10x^{5.43}$) with a resulting R^2 value of 0.82 (Figure 2.5.A). Turah dimensionless transport rates increased consistently with increasing shear stress. All grains in transport show an increasing trend in transport with increasing shear stress (Figure 2.5.B).
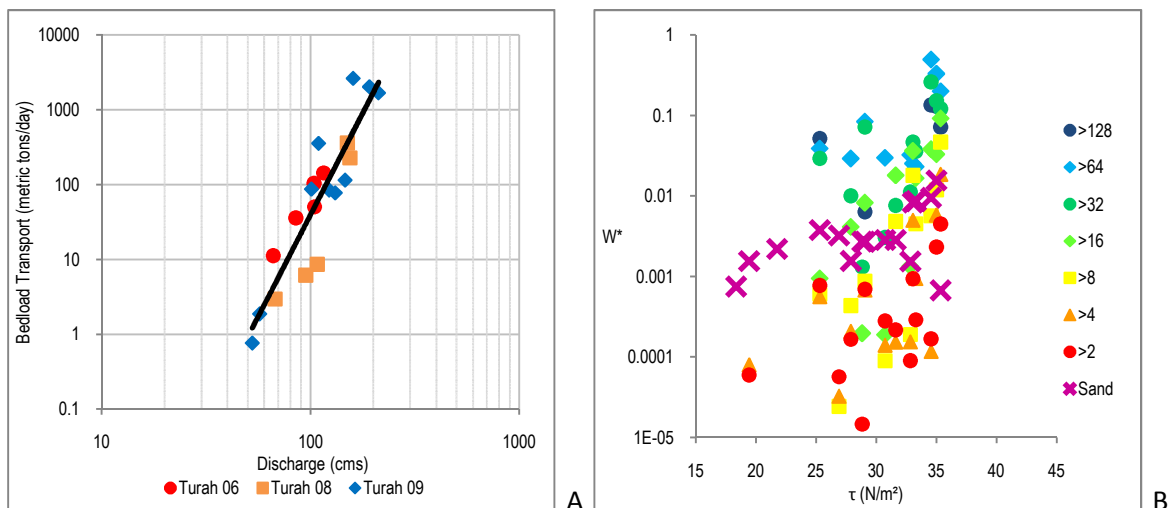
Figure 2.5 Turah 2008 and 2009 bedload sampling and empirical rating curve results. (A) Measured bedload transport rates (t/d) graphed against sample discharge (Supplemental 2006 bedload results included). Black line represents the regression of all data points (power equation and R^2 value presented with text). (B) Dimensionless transport rates of grain size categories graphed against sample shear stress.

Figure 2.6.A shows rating curves for two sample sites on the Blackfoot River. The black sample points and trend line represent the bedload samples collected upstream of the reservoir in 2006 ($y=2E-07x^{3.78}$)(River Design Group and WestWater Consultants, 2006). The remaining

sample points and empirical rating curve represent the transport within the Blackfoot Arm of the reservoir in 2008 and 2009 (y=1E-07x$^{4.49}$, R^2=0.86; Figure 2.6A). I excluded several sample points from this rating curve. Two sample points collected within the reservoir on the 2008 rising limb transported mostly sand at rates similar to those expected entering the reservoir (Figure 2.6.A). These points were subsequently removed from the combined 2008-2009 empirical regression (Figure 2.6.A and B). I sampled highly variable transport rates within the reservoir in 2009, resulting in two of the 2009 data points being removed from the regression (Figure 2.4). Description of Figures 2.6.B-D is provided below.
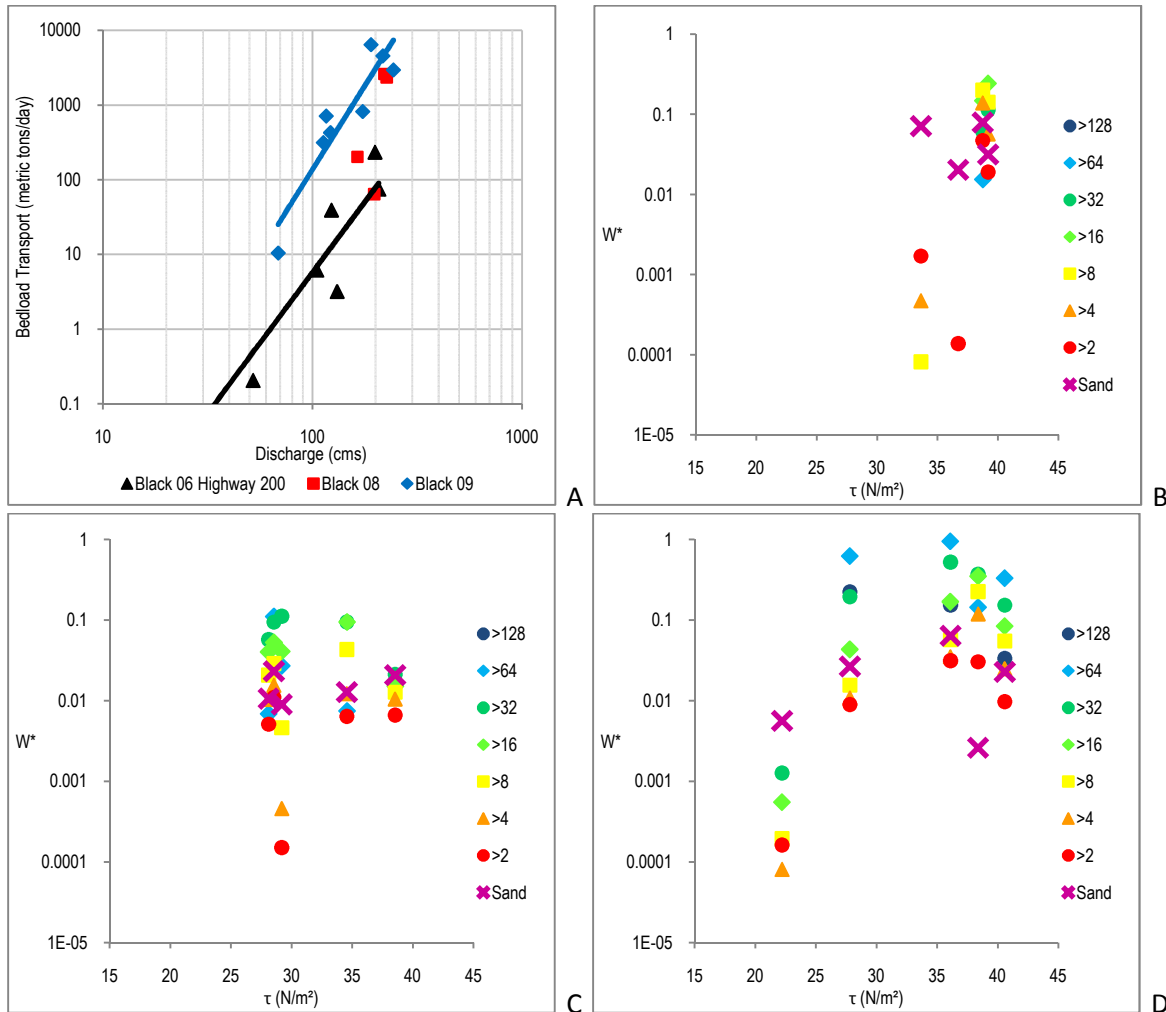
Figure 2.6 Black 2006, 2008 and 2009 bedload sampling and empirical rating curve results. (A) Bedload calculated rates, presented as t/d, graphed against sample discharge (Supplemental 2006 bedload results and trendline represent bedload input from Blackfoot drainage (River Design Group and WestWater Consultants, 2006)). Blue line represents the regression of selected 2008 and all 2009 data, excluding two outliers (Figure 2.4). Black line represents regression of 2006 data (power equations and R^2 values presented with text). (B) 2008 dimensionless transport rates of grain size categories graphed against sample shear stress. (C) 2009 rising limb dimensionless transport rates of grain size categories graphed against sample shear stress. (D) 2009 falling limb dimensionless transport rates of grain size categories graphed against sample shear stress.
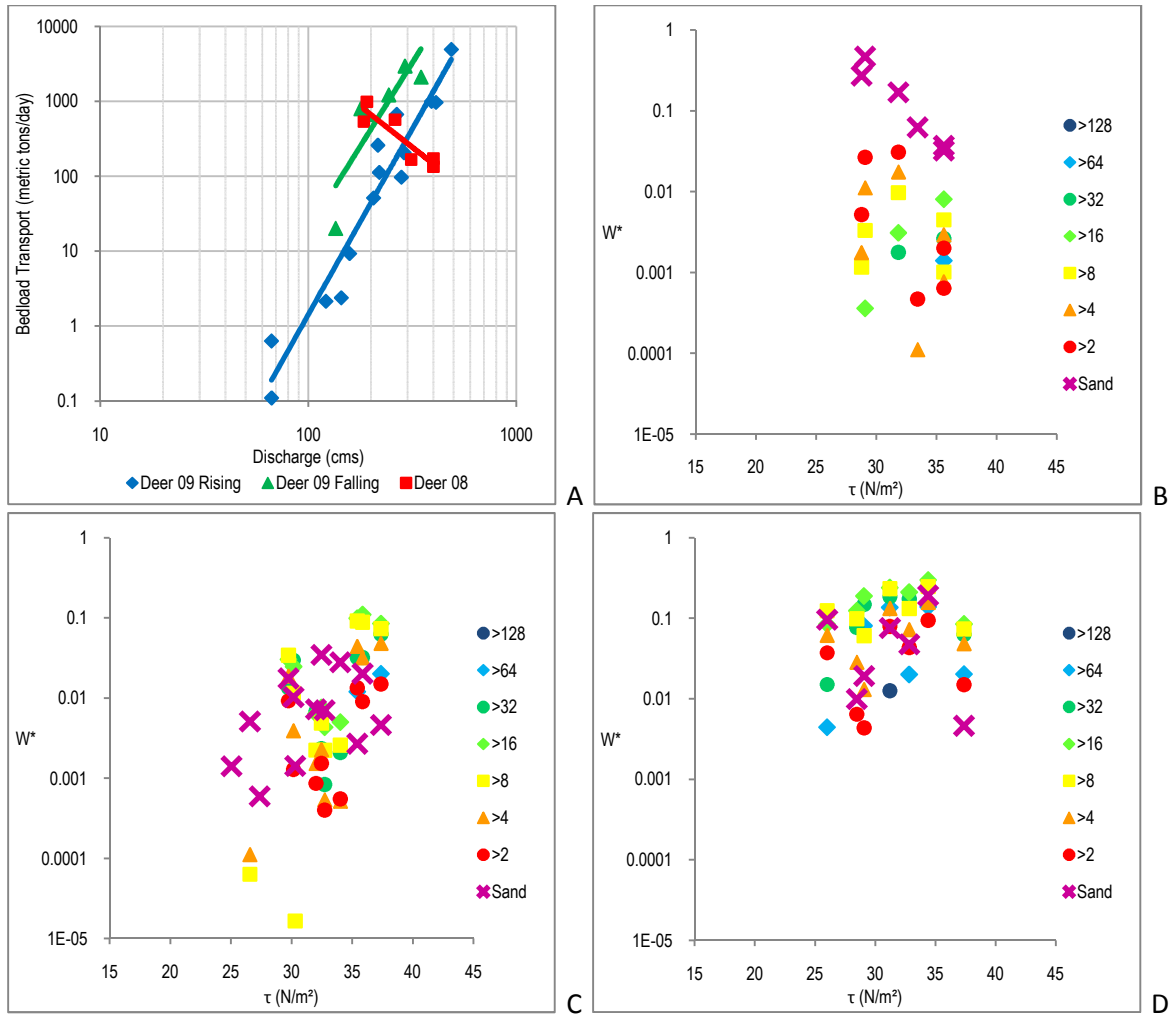
Figure 2.7 Deer 2008 and 2009 bedload sampling and empirical rating curve results. (A) Bedload calculated rates, presented as t/d, graphed against sample discharge. Red line represents regression of 2008 data. Blue line represents regression of 2009 rising limb data. Green line represents regression of 2009 falling limb data (power equations and R^2 values presented with text). (B) 2008 dimensionless transport rates of grain size categories graphed against sample shear stress. (C) 2009 rising limb dimensionless transport rates of grain size categories graphed against sample shear stress. (D) 2009 falling limb dimensionless transport rates of grain size categories graphed against sample shear stress.

At the Deer site sediment transport rates in 2008 showed an inverse correlation to discharge and sediment in transport had little to no relationship to the grain size of the bed material. Bedload samples I collected months after the breach indicate that ten times more sediment transported at 191 cms early in the hydrograph than later at 400 cms (Figure 2.7.A). This first bedload sample, I collected at 191 cms on 5/9/2008, had the highest rate of transport sampled that year. In fact, the empirical rating curve I calculated from the 2008 Deer bedload data had a negative exponent and large positive coefficient ($y=7E+07x^{-2.19}$, $R^2=0.82$) (Figure 2.7).

In 2009, bedload transport at the Deer site coarsened in particle size, had higher rates of transport when compared to 2008 and had a positive correlation to discharge (Figure 2.7).

Hysteresis occurred in the bedload samples in 2009, allowing for the development of rising ($y=2E-10x^{4.95}$, $R^2=0.93$) and falling limb ($y=2E-08x^{4.45}$, $R^2=0.74$) rating curves. When I compared the 2009 rising and falling limb rating curves, I calculated almost an order of magnitude greater rate of transport on the falling limb.

Table 2.3 Summary of regressions for bedload transport data (regression equations represent the bedload rating curve for the time period during which the data were collected).

Site and Rating Curve	Regression Equation	R^2
Turah 2006, 2008, 2009	$y=5E-10x^{5.43}$	0.82
Blackfoot Highway 200 (2006)	$y=2E-07x^{3.78}$	0.92
Black 2009	$y=1E-07x^{4.49}$	0.86
Deer 2008	$y=7E+07x^{-2.19}$	0.82
Deer 2009 Rising Limb	$y=2E-10x^{4.95}$	0.93
Deer 2009 Falling limb	$y=2E-08x^{4.45}$	0.74
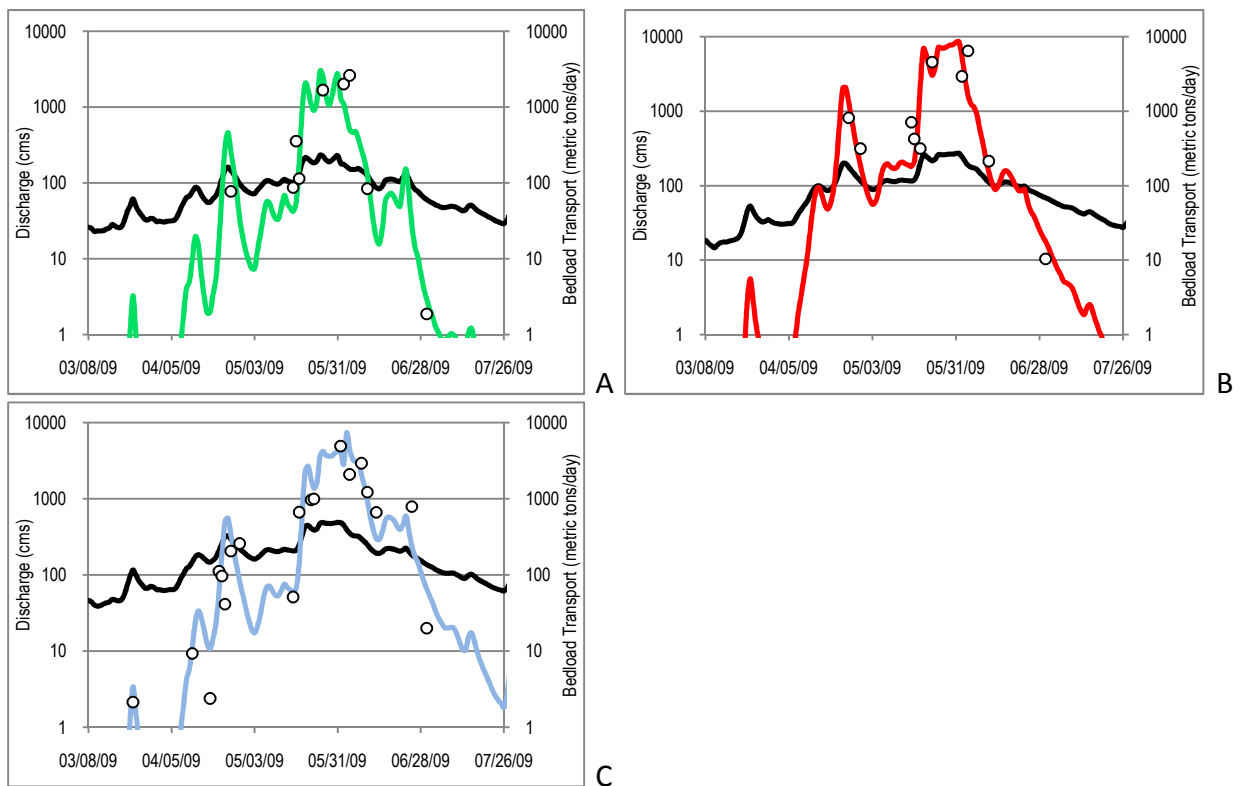
Figure 2.8 Bedload sedigraphs for the 2009 sample season derived by inserting discharge values from the USGS hydrograph into the rating curve equations found in Table 2.3 (circles represent sample data presented as daily rates of transport and black lines are the respective hydrograph discharge values). (A) Turah sedigraph in green. (B) Black sedigraph in red. (C) Deer sedigraph in blue.

Calculated sedigraphs for bedload transport are shown in Figure 2.8. Turah bedload totals for the 2009 water year totaled 30,000 t (Figure 2.8.A). At the Black site roughly 115,000 t transported in 2009 (Figure 2.8.B) while at the Deer site roughly 81,000 t transported (Figure2.8.C).

A summary of the changing grain sizes in bedload transport collected within (Black) and downstream of (Deer) the reservoir is shown in Figure 2.9. Discharges were similar for the samples detailed in Figure 2.9 (between 190 and 225 cms). At both sites these discharges are capable of transporting bedload at rates in the thousands of t/d. I combined these summary results with grain size specific transport results from Figures 2.6 and 2.7.

At the Black site dimensionless transport rates in 2008 show two distinct patterns of sediment in transport (Figure 2.6.B). Early in 2008, sand transported as the dominant grain size at lower rates than the later two samples (Figure 2.6.B and 2.9.A). These last two samples contained a mix of grain sizes, between sand and 16-32 mm, all transporting at similar rates. This mixed grain size distribution continued to coarsen in the next year, on the rising limb of the hydrograph (Figure 2.6.C and 2.9.A). On the falling limb of the 2009 hydrograph, particles greater than 64 mm were the dominant grain size in transport (Figure 2.9.A). These >64 mm particles had the highest transport rates recorded for any grain size category in the two years of sampling (Figure 2.6.D).
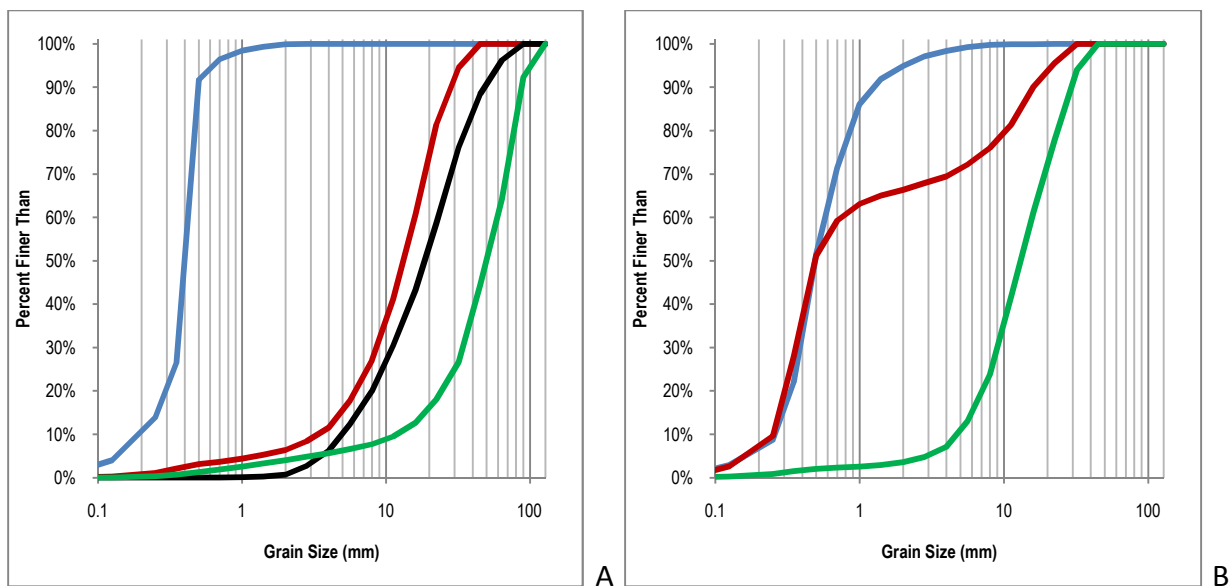
Figure 2.9 Sampled bedload transport particle size distributions at similar discharges (range is 190 and 225 cms) showing the changing caliber of sediment in transport through time. (A) Bedload samples from the Black site (Blue = 5/18/2008, Red = 5/27/2008, Black = 5/23/2009 and Green = 6/4/2009). (B) Bedload samples from the Deer site (Blue = 5/9/2008, Red = 4/21/2009 and Green = 6/13/2009). Almost identical grain size distributions were sampled at the Black site on 5/27/08 (A, Red line) when compared to the 6/13/09 Deer site sample (B, Green line).

Of the samples collected at the Deer site in 2008, sand and smaller sized particles made up >90% of the total sample weight (Figure 2.7.B and 2.9.B). Initially on the rising limb in 2009, sand was still the dominant grain size transporting (Figure 2.7.C and 2.9.B). About half way through the rising limb a more homogenous mix of grain sizes, between sand and 16-32 mm in size, transporting at similar rates showed up in the samples (Figure 2.9.B). This coarse gravel sediment was roughly the same mixture and caliber as bedload samples that were sampled at

the Black site within the reservoir in 2008 (Figure 2.6.B and 2.9). However, I noticed the one difference between these two patterns was the time they took to manifest. This change in the caliber of transporting sediment (from sand dominated to 16-32 mm dominated) took roughly one year at the Black site while taking two years to manifest at the Deer site (Figure 2.9).

Reference Shear Stress:
In order to quantify the critical shear stress I used samples of bedload transport to identify a small reference transport rate (Parker and Klingeman, 1982). The shear stress required to transport at the rate of reference transport is called the reference shear stress and is used in place of the critical shear stress (Wilcock, 1988). As discharge increases, shear stress increases and above the reference shear stress sediment transport rates increase with discharge. I have provided mobility thresholds for reference transport rates of W* = 0.002 (after Wilcock et al., 2009) in Table 2.4. This analysis is presented to demonstrate the unique transport conditions involved in dam removal and the reference shear stress (τ_r), discharge and reference Shields number (τ_r^*) at which grain motion occurred. The τ_r^* values reported in this table, which were calculated using τ_r and equation (4), are relative to the median grain size of the channel sediments and are not derived from the sediment in transport.

Table 2.4 Reference shear stress (τ_r; the shear stress τ' at which a dimensionless transport rate W*=.002 is achieved), reference Shields number (τ_r^*) for the D50 of the bed material, and associated discharges for each sample unit. Results shown are for the condition where τ'/τ_r=1, or where grain stress and reference stress are equal.

Site/Year	τ_r (Pa)	τ_r^*	Discharge (cms)	D50/D65 (mm)
Turah 2008-2009	26-30	0.026-0.030	63-73	61/75
Black 2008 [a]	5	0.62	34	.5/1
Black 2009	18-21	0.022-0.025	50-65	51/71
Deer 2008-Early 2009 [a]	3.3	0.002	68	90/120
Deer Later 2009	6.0	0.004	113	90/120

a. Calculations represent the pulse of sand that evacuated the reservoir on the rising limb of the hydrograph in 2008.

The Turah τ_r calculation produced τ^* ranging between 0.027 and 0.03. The high end of this range (0.03) is a commonly accepted reference Shields number for the natural threshold between grain motion and non-motion (Buffington and Montgomery, 1997; Shields, 1936). At the Black and Deer sites the τ_r values illustrate three things:
1. Based upon our limited data in 2008, fine grained sediment (sand) was mobile within (5 Pa, 34 cms) and downstream (3.3 Pa, 68 cms) of the reservoir at about 0.8 mean annual flow (Black and Deer mean annual flow are 44 and 82 cms respectively) (USGS, 2010).
2. Coarse bedload (> 2mm) started mobilizing within the reservoir at 18 to 21 Pa (50 to 65 cms), about 1.3 mean annual flow.
3. Downstream of the reservoir in 2009, coarse bedload (> 2mm) started mobilizing at about 6 Pa (113 cms), about 1.4 mean annual flow.

Suspended Sediment Transport:

USGS total daily suspended sediment sedigraphs through the 2008 and 2009 water years for all gauges are supplied in Figure 2.10. I present this graph to demonstrate the elevated transport rates exiting the reservoir after removal. Overall the dam removal increased suspended sediment transport rates downstream by about five times in 2008 and double in 2009. The Clark Fork and Blackfoot Rivers contributed about 51,000 and 56,000 t of suspended sediment to the reservoir during the 2008 water year and about 75,000 and 56,000 t in 2009 respectively (Figure 2.10). Below the reservoir a total of 463,000 metric tons of sediment transported as suspended load in the 2008 water year with rates as high as 42,100 metric tons of suspended sediment transporting in a single day (Figure 2.10). In 2009, 200,000 t of suspended sediment transported past the Deer Site.
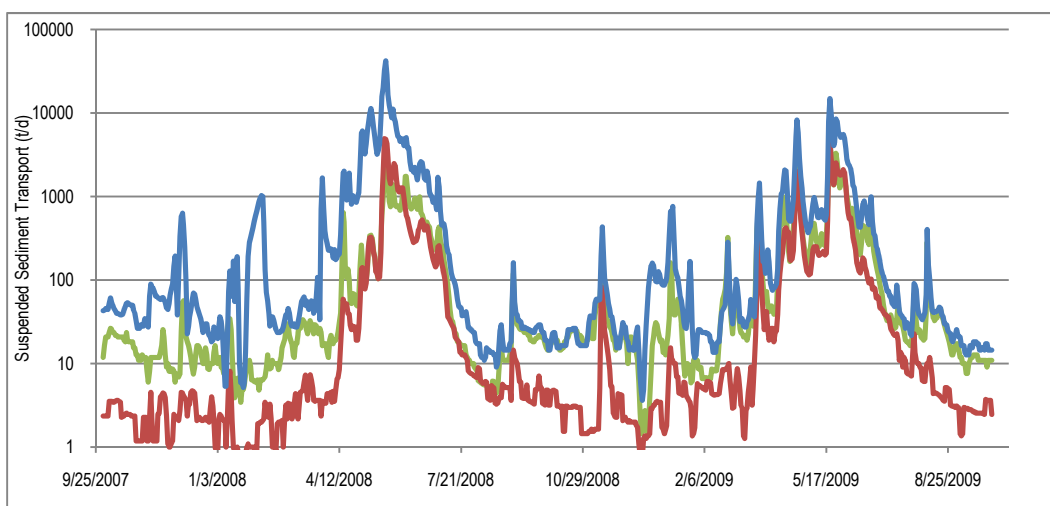
Figure 2.10 USGS suspended sediment sedigraphs for the Turah Gauge (green), Blackfoot Gauge upstream of the reservoir (red) and Clark Fork above Missoula Gauge (blue).
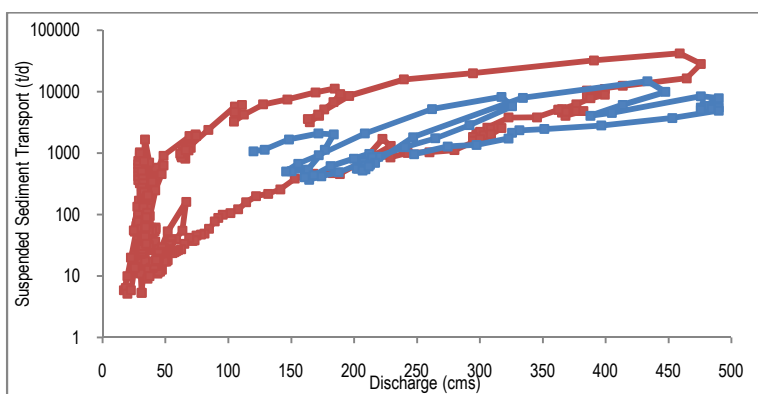
Figure 2.11 USGS Clark Fork above Missoula Gauge 2008 and 2009 hysteresis graph. Comparison between 2008 (red) and 2009 (blue) daily suspended sediment transport results.

I have shown a suspended sediment hysteresis graph of the USGS Clark Fork above Missoula Gauge in Figure 2.11. This graph is meant to show the extreme differences in transport rates recorded between rising and falling limbs and between years. 2008 suspended sediment transport rates on the rising limb are between 1 and 2 orders of magnitude greater than falling limb rates. A pattern of hysteresis is also evident in the 2009 suspended sediment results, at much lower rates than the 2008 results.

Selected USGS suspended sediment results from the Clark Fork above Missoula Gauge (Deer site) and the Clark Fork Bypass near Bonner-station within the reservoir (bypass channel) are summarized in Figure 2.12. This figure illustrates the concentrations of fine grained sediment in transport entering the bypass channel (i.e., illustrating erosion from the Clark Fork Arm of the reservoir) and transporting past the Deer site. These changes in fine grained concentration can help shed light on the processes of transport for sand and smaller particles and the timing of fine grained sediment erosion out of the reservoir. Notice the large differences in suspended sediment concentrations recorded at the Deer site between 2008 and 2009 (Figure 2.12.A-B).

USGS measurements show that the highest concentration of fine grained suspended sediment occurred with the 2008 peak in discharge (Figure 2.12.A). This peak in concentration, coinciding with the peak in the hydrograph, also occurred in the bypass channel on the same day (Figure 2.12.C). Further, the sampled total daily suspended sediment weight from the bypass channel was 110% that sampled 4 km downstream at the Deer site, suggesting to me that with the peak in the hydrograph the vast majority of the sediment sampled at the Deer site came from the Clark Fork Arm of the reservoir. This also indicates to me that with the peak in the hydrograph the Blackfoot Arm did not contribute substantial fine sediment to the downstream suspended sediment totals.

The peak in coarse grained suspended sediment concentration at the Deer site occurred on the rising limb of the hydrograph. At about 180 cms, particles >.062 mm made up about 80% of the suspended sediment sample weight (Figure 2.12.A). This peak in coarse suspended sediment did not show up in the bypass channel sample data (Figure 2.12.C). At the Deer site in 2008, concentrations in coarse grained suspended sediment increased consistently above about 60-80 cms (4/29/2008). This increase in coarse grained concentrations continued to rise until the 5/8/2008 sample, 770 mg/l. After this date, sampled bedload and coarse suspended sediment concentrations, sand, continued to decline even with increasing discharge. Fine grained suspended sediment concentrations remained fairly consistent between 100 to 200 mg/l from the time the dam was removed to the peak in the hydrograph.
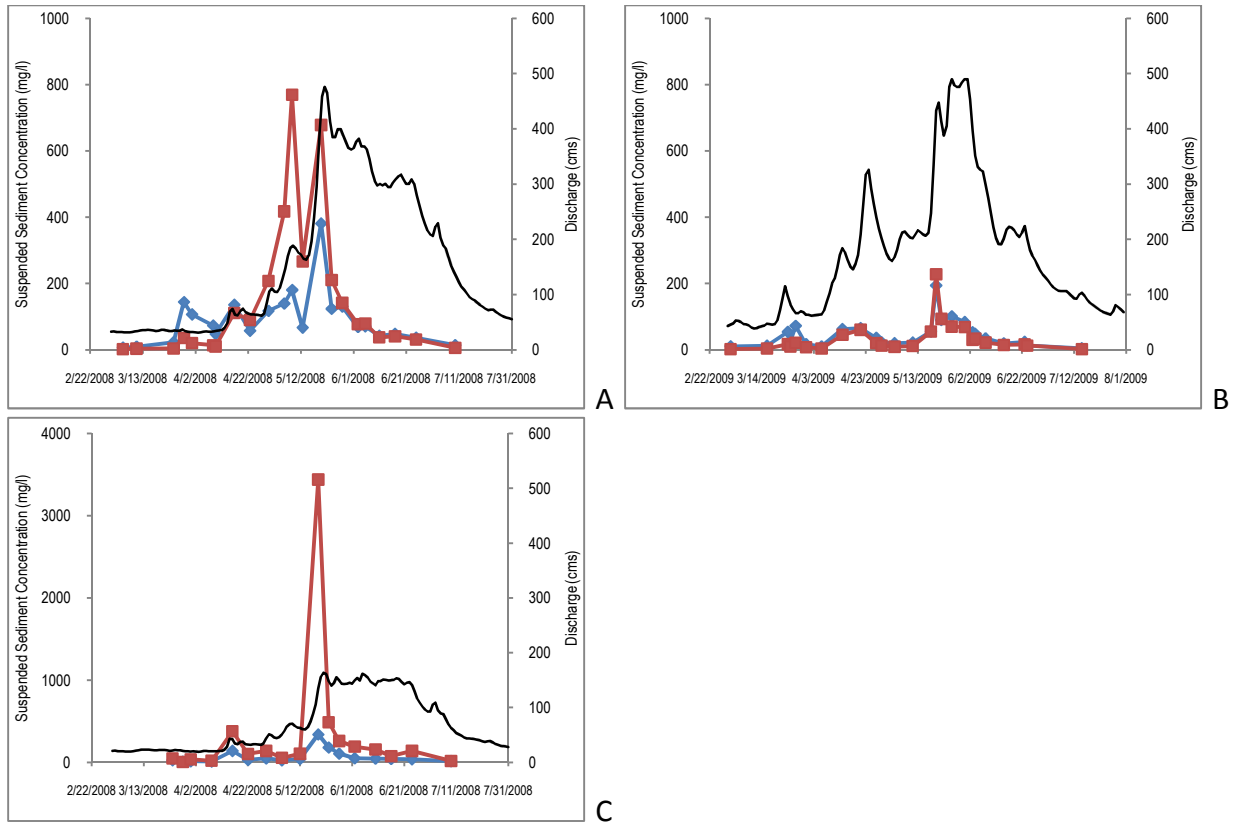
Figure 2.12 USGS suspended sediment concentrations by particle size. Concentrations for particles <.062 mm (blue) and >.062 mm (red) are graphed with the hydrograph (black). Secondary axis is in cms. (A) 2008 USGS Clark Fork above Missoula Gauge. (B) 2009 USGS Clark Fork above Missoula Gauge. (C) 2008 Clark Fork Arm of the reservoir samples collected from the Duck Bridge that spanned the bypass channel, notice the different scale of the primary Y axis (these samples represent the suspended sediment exiting the Clark Fork Arm of the reservoir).
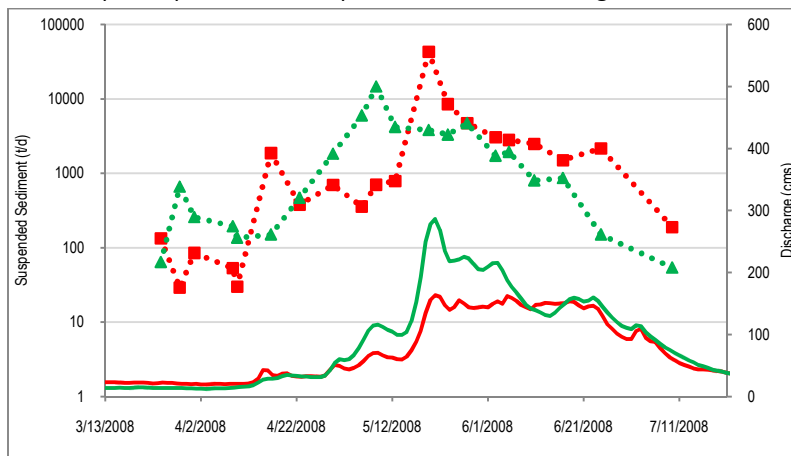
Figure 2.13 Raw daily suspended sediment transport sample results of the Clark Fork Arm Bypass Channel (red) and Blackfoot Arm (green) of the reservoir with respective hydrographs. Blackfoot values are an estimate derived from a subtraction between the Clark Fork Arm measurements and the downstream Clark Fork above Missoula Gauge sampled data.

24

If the Deer site sample data for total daily suspended sediment is subtracted from the Clark Fork Arm suspended values, I can estimate the transport values for the Blackfoot Arm of the reservoir (Figure 2.13) This figure shows that elevated transport of suspended sediment occurred at moderate rates (~10^2 t/d) just after removal and then at much higher rates (~10^3-10^4 t/d) that were not sampled within the Clark Fork Arm of the reservoir. Fine sediments that evacuated from the Clark Fork Arm did so almost entirely with or just after the peak in the hydrograph while it appears that Blackfoot Arm of the reservoir transport most of its fine sediment out of the impoundment early on the rising limb of the hydrograph.

Sediment Budget:

Suspended and bedload sediment transport totals for the 2008 and 2009 water years are found in Table 2.5. I derived these totals by summing daily values from the bedload and suspended sedigraphs. The sediment budget also accounts for the estimated mass of sediment that filled a large scour hole that was present immediately downstream of the dam before removal but filled during the 2008 hydrograph. I have added the conservative estimated weight of sediment to fill the scour hole in 2008 to the 2008 sediment budget totals (Table 2.5). For further details on these calculations refer to Appendix A.

Table 2.5 Suspended and bedload sediment transport totals for the 2008 and 2009 water years (range on bedload values were derived from bootstrapping analysis). To account for additional output from the reservoir, a conservative estimated weight of the sediment that filled the scour hole downstream of the dam is added to the 2008 sediment budget.

	2008		2009	
	Bedload (t)	Suspended (t)	Bedload (t)	Suspended (t)
Turah	21,000 14,000-37,000 [a.]	51,000	24,000 15,000-39,000 [a.]	75,000
Blackfoot	4,000 1,000-9,000 [a.]	56,000	5,000 2,000-12,000 [a.]	56,000
IN TOTAL	**25,000**	**107,000**	**29,000**	**131,000**
Deer	>25,000	463,000	75,000 43,000-124,000 [a.]	200,000
Scour Hole	140,000	X	X	X
OUT TOTAL	**>165,000**	**463,000**	**75,000**	**200,000**
OUT-IN	**>140,000**	**356,000**	**46,000 26,000-73,000 [a.]**	**69,000**
	Total Sediment Out of Reservoir in 2008	**>500,000 t**	**Total Sediment Out of Reservoir in 2009**	**120,000 t 100,000-150,000 [a.]**

a. Range was derived from random bootstrap sampling of the data 1000 times and represents the 90% confidence interval.

Table 2.6 Volumetric and sediment budget calculation comparisons to validate both methods.

	2008		2009	
	Volume (m^3) [c.]	Mass (t)	Volume (m^3)	Weight (t)
Upper Clark Fork Volumetric Calculation [a.]	180,000 ± 30,000	250,000	15,000	20,000
Blackfoot Volumetric Calculation [b.]	160,000	220,000	80,000	110,000
Volume Calculation Total	**470,000 t**		**130,000 t**	
Sediment Budget Total	**>500,000 t**		**120,000 t** **100,000-150,000 t**	

a. Volumetric estimate obtained from Brinkerhoff (2009) and Wilcox et al., (2008), based on comparison of pre-removal topography and post-removal LiDAR data.
b. Volumetric estimate obtained from Epstein (2009) and Wilcox et al., (2008), based on comparison of pre-removal topography and post-removal ground survey data.
c. Bulk density conversion is 1.4 metric tons (t) per cubic meter (m^3) (Wilcox et al., 2008), based on bulk densities used in various EPA reports regarding Milltown sediments.

I have compared the bedload and suspended sediment budget with other estimates of storage change derived from independent methods. Surveys of topographic change calculated the volumetric change in the reservoir for the 2008 and 2009 water years (Brinkerhoff, 2009; Epstein, 2009; Wilcox et al., 2008) (Table 2.6). To compare these volume estimates with my estimates I applied a conversion of 1.4 metric tons per cubic meter (Wilcox et al., 2008). Overall, volume calculations are 94% of the sediment budget total in 2008 and 108% in 2009. This result adds robustness to the sediment budget and volumetric estimates and the methods used to develop them. Additional results can be found in Appendix A.

Discussion:
Fine Grained Reservoir Sediment:
Blackfoot Arm:
The rates and magnitudes of reservoir sediment transport varied with grain size. The wash load (silt) that evacuated the reservoir provided a time marker for sand and silt erosion within the impoundment. Elevated rates of silt transport indicated threshold driven erosion of mostly Blackfoot Arm sediments early on the rising limb of the 2008 hydrograph. The coarse grained suspended sediment (sand) that eroded with these silts transported out of the reservoir and deposited within the downstream channel, probably filling the scour hole. Once the threshold for sand bedload transport was exceeded downstream of the dam the sand moved as a distinct wave. As the sand bedload moved downstream, discharge increased, resulting in higher rates of bedload transport and higher concentrations of coarse grained suspended sediment. The peak in sand concentration represented the threshold for total suspension of sand in the water column, at about 180 cms. This marked the peak of the sand and silt transport out of the Blackfoot Arm of the reservoir. A peak in sand concentration before the peak in the hydrograph

is described as a Class 2a hysteresis loop (Williams, 1989). This type of hysteresis loop indicates that on the rising limb of the hydrograph the sand and silt supply within the Blackfoot Arm of the reservoir started to become limited. Bedload results (Figure 2.6.A and B) and water surface elevation measurements collected on 5/15/08 within the reservoir also indicate that most of the sand and silt had evacuated the Blackfoot Arm by about this date (Epstein, 2009).

Clark Fork Arm:
Within the Clark Fork Arm of the reservoir the sand and silt in transport also indicated a threshold driven pattern of erosion. However, this pattern was different than that of the Blackfoot Arm in that the majority of fine grained Clark Fork Arm sediments transported all at once, with the peak in the hydrograph. This type of hysteresis is classified as a Class 2b hysteresis loop (Williams, 1989), and is typical of a transport limited suspended sediment regime. This indicates that, if the peak in discharge had been greater than it was in 2008 even more Clark Fork Arm sediment would have evacuated the reservoir.

Channel Geometry:
Channel geometry differences between the two arms of the reservoir led to dissimilar patterns in fine grained entrainment and transport. Within the confined Blackfoot the only source of fine grained sediment was within the active channel bed. Within the Clark Fork Arm, little profile adjustment was possible because the bypass channel entrance elevation was designed to be in line with the upstream river profile (Envirocon, 2004b). However, large volumes of readily available sediment were stored within the bank material in the Upper Clark Form Arm of the reservoir. This difference, in the location of available sediment, resulted in low to moderate discharges on the rising limb of the hydrograph eroding the confined Blackfoot downward and peak discharges eroding massive amounts of bank sediment from the unconfined Clark Fork (Figure 2.14).

Figure 2.14 Erosion within the Clark Fork Arm of the reservoir in 2008. Photo taken in July 2008 (Wilcox et al., 2008).

Reservoir Channel Erosion:

When the above results are compared to other large volume sediment transport scenarios a possible pattern emerges as to reservoir channel evolution. In the case of the Marmot removal, 12 hours after the breach, reservoir sediments had eroded down to nearly the pre dam profile (Major et al., 2008a). It was further documented that incision of the channel destabilized banks, causing constant channel erosion through bank failures in the first 24 hours (Major et al., 2008a). After the eruption of Mount St. Helens, Major (2004) and Major and Mark (2006) document that with high volumes of sediment available for river transport, small discharges effectively transport suspended sediment during profile adjustment, similar to the Blackfoot erosion on the rising limb in 2008 and the Sandy River the 12 hours after removal. Major (2004) and Major and Mark (2006) further describe that as the profile becomes more developed, moderate magnitude discharges emerge as the dominant sediment transporting flows. Further, if land-sliding (bank failures) deliver sediment to the channel, then large discharges become the more dominant transporting flow, similar to the erosion of Upper Clark Fork Arm bank sediments in 2008.

Coarse Grained Reservoir Sediment:

Bedload Transport Patterns:

Patterns of bedload transport within and downstream of the reservoir varied temporally while upstream transport remained consistent during the three years of sampling. Within the reservoir, transport adjusted with changing channel geometry, hydrology, grain size, and sediment volume. Within the Blackfoot Arm of the reservoir, bedload results indicated a rapidly changing caliber of sediment in transport, with slightly increasing rates of transport through time. If we try to track this sediment to the downstream sample site we see that sand and smaller particles dominated the transport regime throughout 2008 and into 2009 (Figure 2.15). The first substantial quantity of coarse bedload sediment appeared in the samples near the 2009 peak discharge with the most abundant particle size by weight being about 16 mm. As shown in the results, the sediment caliber and transport rate changed twice as fast at the Black site when compared to the Deer site (Figure 2.15). We see an increase in the time it took for the grain sizes in bedload transport to coarsen and smaller rates of transport the further we are from the sediment source (Figure 2.15). This implied that the bedload exiting the reservoir was segregating by grain size. As the gravel and cobble bedload moved, the finer gravels were transported further distances than the coarse cobble particles (Church and Hassan, 1992).
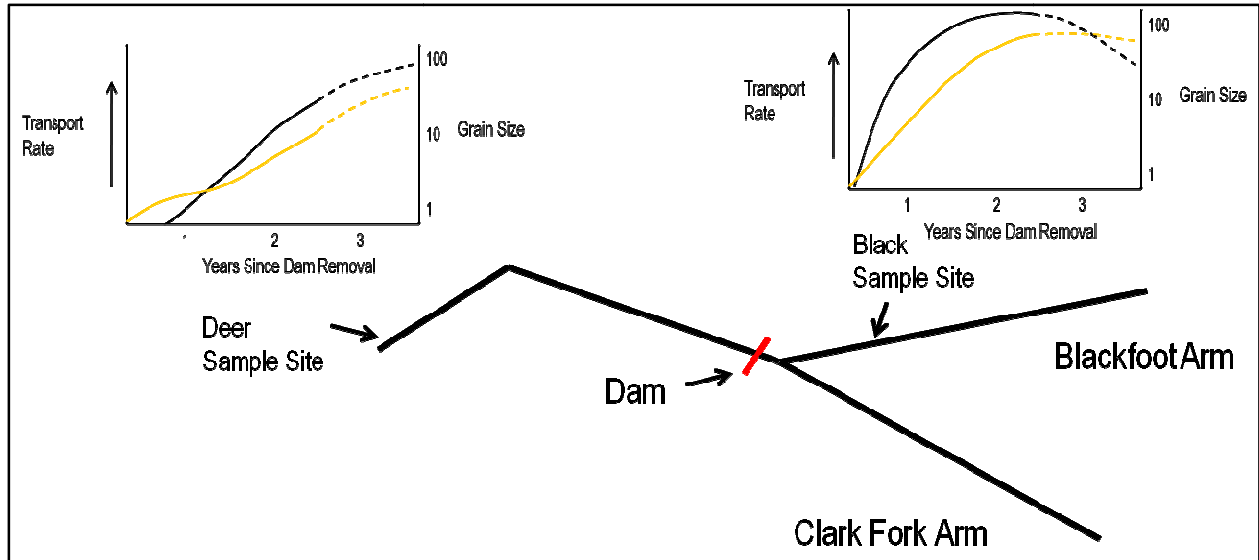
Figure 2.15 Planform illustration of the translating and dispersing wave of non-sand bedload sediment within (Black, Upper right) and downstream (Deer, Upper left) of the reservoir. Conceptual sketch where solid yellow line represents the most abundant grain size by weight in each sample and the black line represents the dimensionless transport rate. Dotted lines are estimated values and the primary axis are at the same scale.

Sediment Wave Dynamics:

One study suggests that reservoir sediment may transport downstream as a distinct wave or gradually over time (Doyle et al., 2002). Milltown Reservoir sediments transported as a series of distinct waves and the speed at which the waves moved downstream was dependent upon the grain size of the sediment. Silt sediments transported as multiple waves in suspension and, once eroded within the reservoir, were sampled at the downstream gauge within days. Sand that transported probably as bedload early in the hydrograph reached a threshold discharge and moved as a large wave in suspension. Coarse grained sediments transported as a distinct wave, with smaller bedload particles transporting further distances than the coarse grains. This finding is demonstrated by the pattern of coarsening grain size with time since removal at the Deer site.

Studies of large sediment inputs suggest two different geometries, or combinations thereof, by which bedload sediment waves move (Figure 2.16) (Gilbert, 1917; James, 2010; Lisle et al., 2001; Sklar et al., 2009). I propose that in the following discussion:
1. The bedload transport rate will represent the thickness of the bedload wave.
2. Bedload samples containing fine gravel as the most abundant particle by weight are assumed to represent the leading edge of the wave.
3. Bedload samples with a D50 similar to the above reservoir surface bed material D50 are assumed to represent the middle of the wave.
4. Bedload samples containing the coarsest reservoir sediment as the most abundant particle by weight are assumed to represent the trailing edge of the wave.

When the bedload results from the Black and Deer sites were interpreted with respect to the wave forms in Figure 2.16, it appeared the Milltown bedload sediment dispersed and translated

29

downstream (Figure 2.15). The leading edge of the wave was interpreted as the small gravel sampled at the Black site in 2008 and the Deer site in 2009. Once this small gravel showed up in bedload transport at both sites, the Black bedload samples increased in transport rate and most abundant particle by weight twice as fast as the bedload samples collected at the Deer site. This was interpreted as a flattening and elongation of the bedload wave as it dispersed downstream (Figure 2.15).
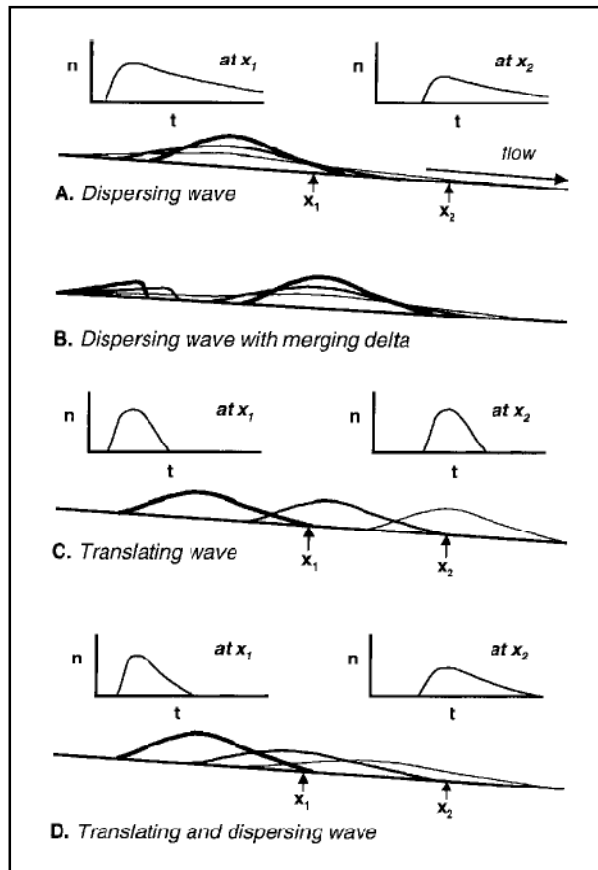
Figure 2.16 Patterns of transporting sediment waves (Lisle et al., 2001). The bottom-most figure (D), showing a translating and dispersing wave, is similar to Figure 2.15.

From the Deer bedload data, results indicated that channel roughness could have been a possible mechanism for bedload wave dispersion. With the trailing edge composed of coarser material, bed roughness increased, promoting lower rates of transport and shorter transport periods through time. The leading edge of the sediment wave, as sampled at the Deer site in 2009, was composed of mostly fine gravel. This fine gravel, once in transport, probably reduced bed roughness and promoted increased transport rates and distance of transport downstream.

Although natural bedload waves typically disperse there is evidence that the coarse Milltown sediments translated downstream (Lisle et al., 2001). Translation has been shown to occur when the sediment in transport is much smaller than the bed material and the channel has Froude numbers << 1 (Lisle et al., 2001; Sklar et al., 2009) . Calculations using WinXSPRO

indicated that at 500 cms (roughly the peak flow of the 2008 and 2009 hydrographs downstream of the reservoir), the channel at the Deer site had a Froude number of approximately 0.37. Further, in 2009 at the Deer site, the most abundant particle by weight in transport was 16-22 mm, much smaller than the D50 of the bed material at 90 mm. This would indicate based upon work by Sklar et al., (2009) that the Milltown sediments translated downstream. Supporting this were the Shields number calculations for the most abundant particle by weight in the 2009 Black bedload samples. Calculations showed that these grain sizes had a τ^* < and in some cases << 0.03, thus demonstrating that the most abundant particle size by weight in transport was larger than it theoretically should have been, possibly due to a sand content in the reservoir sediments increasing transport efficiencies (Wilcock et al., 2001). This may have signaled the translation of the coarser trailing edge of the bedload wave. I interpret this as an indication that the Milltown bedload wave moved by dispersion and translation downstream.

Sources of Error:
Sampling Error:
With each sample there were several possible sources of error in my measurements. My use of several different samplers, though necessary in this case, could have added uncertainty due to the documented differences between sampler capture efficiencies (capture efficiencies of some bedload samplers can result in measurements being off by an order of magnitude). The variety of sampler sizes and the bag mesh size I used produce uncertainty in the grain size specific results (each sampler type and size is more efficient at capturing a certain range of grain sizes. Further, although the use of a stay line is a standard practice in bedload sampling, a stayline was used for only a subset of the samples (at Black) for logistical and safety reasons. One major source of error associated with bedload sampling is letting the sampler dig into the channel bottom as it is moving upstream. Even though I took great care to avoid this it was still very difficult to sample at peak flow with a slow winch and numerous logs. If the sampler does dredge the channel bottom the sample could substantially over represent the transport (especially at low flow). The leverage methods described above for removing outliers attempted to filter out erroneous data arising from the types of sampling error discussed here.

Probably the greatest source of error in the analysis was the number of samples collected. The limited sampling in 2008 and to some extent in 2009 was unavoidable. The intensity of sampling associated with the cable-suspended sampler method was low, between 0.0002 and 0.0044 for all the samples collected, but this was the only way that sampling of this kind could be done. To address this and other sources of sampler error and transport variability, repeat samples were collected in 2010 at the Black and Deer sites. These results are not discussed here but will follow in future publications. The USGS flow data used in this analysis also contain some error, the magnitude of which is unknown.

Calculation Uncertainty:
To address the error in the sediment rating curve calculations, I used a bootstrapping method to sample from the data set and calculate the rating curve and subsequent transport totals

1000 times. The resulting median bedload transport totals were then reported with a 90% confidence interval of the transport totals for the data sets evaluated.

Sediment Budget:

Sediment budget calculations did not take into account all the sediment that evacuated the reservoir by year. There is about 4 km of river length between the dam site and my downstream sample location. I assume a portion of the sediment that evacuated the reservoir after the dam was removed in 2008 and traveled as bedload did not reach my sample site that year. I attempted to partially quantify this volume of sediment by estimates of the volume required to fill the scour hole. I did not collect measurements of the deposit, and measurements were not collected to quantify the portion of the hole that did not fill with sediment. The 140,000 t estimated weight to fill the scour hole and other mass to volume conversions rely upon my conversion factor of 1.4 metric tons per cubic meter. It is probable that this conversion factor is inaccurate. All my suspended sediment results were obtained from the USGS and like any sampling are subject to error. The USGS reports provide information on suspended sediment error analysis (Dodge et al., 2009; Lambing and Sando, 2009). This discussion of error highlights the challenges of accurate measurement and calculations of bedload sediment fluxes and sediment budgets, which, even when based on intensive field campaigns such as for the Milltown study, may have substantial error.

Figure 2.17 Photo taken of the scour hole deposit (bottom left) in the summer of 2008 (looking SSE) (Clark Fork Coalition, 2009).

Conclusion:

Findings from my study can inform future dam removals and provide insights into large river transport processes. The dimensionless transport and shear values along with reference shear stress values I have calculated can be applied to different dam removal scenarios than Milltown. I have identified thresholds and patterns of suspended sediment erosion and transport (that depended upon the discharge and channel geometry of the reservoir sediments) that can allow for prediction of fine grained erosion and reservoir channel evolution throughout

the hydrograph. The translating and dispersing bedload wave form I have illustrated here could be a consistent occurrence in situations where reservoir sediments that are finer than the bed material, transport in channels downstream of reservoirs that have low Froude numbers and are in a degraded and armored state. The spatial and temporal perturbation caused by the dam removal has allowed for a clear picture of the transitions between fine grained bedload and suspended sediment transport. Furthermore, the Milltown Reservoir sediments I sampled in bedload transport have shown a size selective transport distance with little interference from the channel between the sediment source and the sample site. It has also provided insight to the processes for the dispersion of bed material waves. In conclusion, results suggest that transport of Milltown sediments was determined by the channel geometry, hydrology and grain size and location of the reservoir sediment; which in turn determined distance, processes and timing of transport. It is intended that my study benefit future dam removal projects and give society confidence in deciding where and how to maximize limited resources.

Chapter 3: Dam Removal Sediment Transport Modeling

Introduction:

In recent years, numerical sediment transport models have been used more regularly to predict the impacts associated with dam removal. With a growing trend expected in dam removal there is a need to validate and develop these models to more accurately predict how reservoir sediment will erode, where this sediment will be deposited and its impact to the channel (Doyle et al., 2002). With any model prediction, data can help us understand the limitations of the model and identify erroneous assumptions made by modelers. This validation can help researchers and decision makers have more confidence in evaluating the modeling efforts of future dam removals (Doyle et al., 2002; Nelson et al., 2002; Pizzuto, 2002; Rathburn and Wohl, 2001). Further, it can show the benefits of using one model over another.

In the case of the Milltown Dam removal, the risks associated with downstream transport of contaminated reservoir sediments were predicted by applying a one-dimensional model (Envirocon, 2004b). The HEC-6 sediment transport model, developed by the United States Army Corps of Engineers, was used to evaluate various scenarios for removing Milltown Dam (Envirocon, 2004b). The model underwent several revisions for calibration and prediction of the volume of sediment that would be transported for a 4-year period surrounding the breach. This 4-year model period included the initial reservoir drawdown and simulated sediment transport from December 1, 2004 to December 31, 2008 (Envirocon, 2004b). Four scenarios were evaluated:

1. "No action", where the dam remains in place.
2. 85% wet and 15% dry removal, where 85% of the sediments would be dredged out and 15% would be removed in the dry.
3. Dry removal without bypass channel, where the Clark Fork sediments would all be vulnerable to river scour during removal of the dried sediments.
4. Dry removal with full bypass channel, where a bypass channel would be constructed to protect the most contaminated sediments while they were excavated and moved off site.

With Scenario 4 came several flow scenarios where different hydrographs (low flow (1992), average annual flow (1999) and 25 year flood (1975)) were used to simulate the sediment transport associated with the Milltown Dam removal (Envirocon, 2004b).

Modeling of sediment transport associated with the Milltown Dam removal had several unique challenges. With the multiple stage drawdown and the various scenarios, the actual application of the model occurred well before the dam was removed. Adding to the difficulty, the dam consisted of two arms, the Blackfoot and Clark Fork. These arms of the reservoir were different in that contaminants within the Clark Fork Arm resulted in the lower half of that arm of the reservoir being protected by a bypass channel so that contaminants could be moved by rail during removal action (Envirocon, 2004b). Within the Blackfoot Arm was another dam constructed in 1884 and removed in 2005 prior to the Milltown removal (Epstein, 2009). The

two arms of the reservoir also had different channel geometries, the Blackfoot being confined and the Clark Fork being unconfined (Wilcox et al., 2008).

Here I review the HEC-6 results and identify possible limitations of the model and error in user assumptions. I then apply DREAM (Dam Removal Express Assessment Model) to the Milltown Dam removal, using the original HEC-6 modeling assumptions and inputs, to compare the resulting predictions. Next, I modify DREAM inputs to closely simulate the measured sediment transport results. Finally, I test the sensitivity of DREAM-1 to the sediment input parameters.

HEC-6 Model:
The HEC-6 model is a one-dimensional model that simulates bed and suspended sediment transport using stream cross-sectional and longitudinal geometry, sediment particle characteristics, hydrology and sediment loading assumptions (Gee, 1995). With these data it calculates water and channel surface profiles by computing the interaction between substrate and the flowing water-sediment mixture. It calculates the change in sediment load, bed elevation, water surface elevation and thalweg elevation for each cross-section in the vertical direction only (Gee, 1984, 1995).

The HEC-6 model is reportedly limited when lateral movement and bank erosion occur at a cross-section, erosion occurs at different rates across the channel, the channel is multi-threaded and varying properties exist between bed material layers (Gee, 1984, 1995). Further, modeling environments where rapid fluctuations occur between subcritical and supercritical flow are not represented by the model (Rathburn and Wohl, 2001). Furthermore, the selection of sediment transport equations has a significant influence on the HEC-6 computed bed profiles and the model's predictive capability is reduced where highly non-uniform flow occurs (Tingsanchali and Supharatid, 1996). On the South Fork of the Salmon River, ID, the model over-predicted at low flow and under-estimated transport at high flow (Havis et al., 1996). On the North Fork Cache la Poudre, CO, the HEC-6 model predicted with 50% accuracy the scour and deposition of three pools after a reservoir sediment release and it was found that the present construct of the model does not reflect the physical processes operating along that river (Rathburn and Wohl, 2001). The HEC-6 model is now considered legacy software by the Hydrological Engineering Center and its sediment transport functionality has been transferred to HEC-RAS.

DREAM:
DREAM-1 and -2 (Dam Removal Express Assessment Models) were developed for the simulation of sediment transport pulses in rivers and are equipped to address issues following dam removal (Cui and Cluer, 2008). DREAM is similar to HEC-6, in that it is a one-dimensional model that simulates cross-sectional and reach averaged erosion and deposition, but it assumes a trapezoidal shaped channel in the reservoir sediments after removal. DREAM-1 applies to fine sediment transport and can be used when the reservoir deposits are primarily fine grained. DREAM-2 applies to fine and coarse reservoir sediment transport and was used to predict the sediment transport associated with the 2007 removal of Marmot Dam on the Sandy River, OR

(Cui et al., 2006a; Cui et al., 2006b; Major et al., 2008b). The initial sediment transport data findings from the Marmot removal indicate that the DREAM-2 predictions have been relatively accurate (Cui et al., 2008; Cui and Wilcox, 2008).

Methods

HEC-6 Model:

The input and output files for the HEC-6 modeling of the Milltown Dam removal were provided to UM by EMC[2], a subcontractor to Envirocon who performed the modeling. Additional HEC-6 files were retrieved from the Envirocon FTP site (Envirocon, 2010). The Milltown Reservoir Dry Removal Scour Evaluation Addendum 1 (Envirocon, 2004b) details some of the assumptions that were made by the modelers and presents model predictions for a 4-year period surrounding the dam removal (Envirocon, 2004b). This modeling assumed that the reservoir drawdown would begin in December 2004, the dam would be breached in March 2006, and all contaminated sediment excavation and channel reconstruction would be complete by the end of 2008. The actual dam removal and associated remediation efforts followed a delayed time schedule compared to the model assumptions, with dam breaching in March 2008. For this reason the observations from one year after removal are compared to the HEC-6 model results for one year after the simulated breach. This analysis follows methods of previous research assessing the accuracy and limitations of the HEC-6 model (Gee, 1984, 1995; Rathburn and Wohl, 2001; Tingsanchali and Supharatid, 1996).

DREAM:

Reservoir sediment erosion and downstream transport for the one-year period following beaching of Milltown Dam were simulated using DREAM-1 (Cui and Cluer, 2008). DREAM is proprietary software and a copy was provided for this study by the model developer. Here I describe the type of input data required by DREAM-1 and the sources of my input data (Table 3.1; actual values used are presented in Appendix B):

1) Reservoir sediment and downstream channel widths and elevations were derived from the original HEC-6 input cross-sections. Instead of a complete HEC-6 cross-section, DREAM-1 required reservoir sediment widths at one elevation and with one reservoir sediment thickness (Cui, 2002). When running DREAM-1 with the original HEC-6 input, values were averaged when direct transfer of data was not possible.

2) Sediment thicknesses for the Blackfoot Arm used results from Envirocon (2004a). Upper Clark Fork Arm thicknesses used a combination of values from Titan (1995) and Harding Lawson and Associates (1986).

3) Bed material grain size distributions were determined from pebble counts (Wolman, 1954). Data used for the Blackfoot reach were obtained from the HEC-6 input data, verified with pebble count results from Chapter 2, while Upper Clark Fork Arm pebble count results came from River Designs Group and WestWater Consultants (2006) for the CFR 3C reach pebble count at cross-sections XS3 and 139+00.

4) The various reports detailing the grain size distributions within the reservoir were collected from bore holes, test pits and tile probes. Blackfoot and Upper Clark Fork Arm values came from the HEC-6 modeling inputs and were checked with Envirocon (2004a)

and Titan (1995) respectively. The DREAM-1 sediment characteristics are more general than the HEC-6 input data. When running DREAM-1 with the original HEC-6 input, values were averaged when direct transfer of data was not possible.

5) Like the final HEC-6 results, discharge values input to DREAM-1 were collected by the USGS during the 1999 water year (considered the average annual flow) (Envirocon, 2004b). The USGS 12334550 Clark Fork at Turah Bridge near Bonner, MT Gauge discharge data were used to model the Clark Fork Arm of the reservoir. The USGS 12340000 Blackfoot River near Bonner, MT Gauge was used to model the Blackfoot Arm and the USGS 12340500 Clark Fork above Missoula MT Gauge discharge values were used for the model reaches from the confluence within the reservoir to the gauge downstream (USGS, 2010).

6) The sediment supply and associated grain-size distribution coming into the reservoir were derived from sediment transport rating curves applied to the 1999 hydrograph. Suspended sediment values were totaled from the USGS website for the 1999 water year while the bedload input to the reservoir was derived from rating curves detailed in Table 2.3.

Table 3.1 Type of data and data sources input to the DREAM-1 model.

DREAM Input Data Type	Data Used	Data Sources
Geometry Data	HEC-6 cross-sections	(Envirocon, 2010)
Bed Material Grain Size Distributions	Pebble count results	(Envirocon, 2010; River Design Group and WestWater Consultants, 2006) Results from Chapter 2
Reservoir Sediment Grain Size Distributions	Results from tile probes, bore holes and test pits	(Envirocon, 2004a, 2010; Titan, 1995)
Reservoir Sediment Thicknesses	Results from tile probes, bore holes and test pits	(Envirocon, 2004a, 2010; Harding Lawson Associates, 1986; Titan, 1995)
Reservoir Sediment Elevations	HEC-6 cross-sections and results from tile probes, bore holes and test pits	(Envirocon, 2004a, 2010; Harding Lawson Associates, 1986; Titan, 1995)
Discharge Data	Daily discharge values for the 1999 water year (considered average annual flow)	(USGS, 2010)
Suspended Sediment Entering Reservoir	Daily suspended sediment values from USGS gauge data	(USGS, 2010)
Bedload Sediment Entering Reservoir	Bedload rating curve results from Chapter 2	(River Design Group and WestWater Consultants, 2006) Results from Chapter 2

The DREAM-1 domain extended from the upstream reaches of the reservoir to the downstream USGS Clark Fork River above Missoula Gauge (about 100 m downstream of the Deer Creek Bridge). This allowed for comparison between the sample data and model outputs. The unique geometry of the reservoir required modeling of each arm separately and a combined model downstream. The Blackfoot Arm of the reservoir was modeled to the downstream model

boundary, treating the Clark Fork Arm as a tributary. This setup was considered the most plausible because the mostly immobile bypass channel provided a barrier or break between model domains. As a general rule all DREAM-1 model results assume the channel eroded in the reservoir were trapezoidal in shape, with its bottom width slightly narrower than the downstream bankfull width and the bank slopes equal to an angle of repose of 35 degrees (Cui, 2002). However, if the reservoir sediment width was narrower than the downstream bankfull width then the reservoir width was applied to the calculation.

Five different runs of DREAM-1 were completed, each using different input variables (Table 3.2). Run 1 used the HEC-6 input, as described above. Run 2 was designed to evaluate how to mimic the sampled sediment budget and volumetric estimates of reservoir sediment erosion in 2008. This entailed adjustment of the depth of the reservoir sediments and the bed material grain size in the Clark Fork Arm. The depth of sediment data was obtained from two reports detailing the sediments in the Upper Clark Fork Arm of the reservoir (Harding Lawson Associates, 1986; Titan, 1995). These details were not found in the HEC-6 input data or reports. The bed material grain size distribution was obtained from a report detailing the Clark Fork channel upstream of and within the reservoir (River Design Group and WestWater Consultants, 2006). The grain size distribution that produced the closest results to the observed sampling was the CFR 3C reach pebble count at cross-sections XS3 and 139+00. These pebble counts are located at the interface between the upstream channel and impounded reservoir waters. This grain size distribution represented a combination between the upstream channel and reservoir sediments.

Runs 3-5 were performed to evaluate the sensitivity of DREAM-1 to the sediment input values (Table 3.2). This sensitivity analysis was applied to the Clark Fork Arm modeling only. Run 3 used all the same input values as Run 2, only the reservoir sediment width was decreased by 50%. Run 4 included a change in the bed material grain size distribution by one phi class, meaning the percent finer than values were adjusted to reflect a grain size distribution that was coarser by one phi class. Run 5 represented a decrease in the proportion of wash load at each cross-section by 10%.

An important step in the modeling of long-term, large-scale sediment transport is the "zero process," in which known pre-dam removal conditions are reproduced (Cui and Wilcox, 2008). I completed the zero process for each model run. Once the zero process was completed the incremental elevation of the run was checked. If there were trends of aggradation/degradation at any location during the simulation the zero process was run again (Cui, 2002). Once the results indicated that the channel was aggrading and degrading around the initial channel bed elevation, I concluded that the zero process had been performed successfully (Cui, 2002). If the zeroing process did not reach an equilibrium then the input parameters, like sediment supply from upstream, were adjusted until the zero process was successful (Cui, 2002).

Table 3.2 Description of DREAM-1 model runs made and the different input data sources between them (input data files are supplied in Appendix A)

DREAM-1 Input Data	Run 1	Run 2	Run 3	Run 4	Run 5
Upstream of Dam Geometry Data	HEC-6 input data	HEC-6 input data supplemented with results from other reports	50% reduction in Run #2 sediment widths (Clark Fork Arm of reservoir)	HEC-6 input data supplemented with results from other reports	HEC-6 input data supplemented with results from other reports
Downstream of Dam Geometry Data	HEC-6 input data	HEC-6 input data supplemented with results from other reports	HEC-6 input data supplemented with results from other reports	HEC-6 input data supplemented with results from other reports	HEC-6 input data supplemented with results from other reports
Bed Material Grain Size Distribution	Averaged from HEC-6 input data	Averaged from HEC-6 input data, and pebble counts from other studies	Averaged from HEC-6 input data, and pebble counts from other studies	One phi class coarser bed material of Run #2 percent finer values (Clark Fork Arm of reservoir)	Averaged from HEC-6 input data, and pebble counts from other studies
Proportion of Wash Load in Reservoir Sediments	Averaged from HEC-6 input data	Averaged from HEC-6 input data and other sediment sampling reports	Averaged from HEC-6 input data and other sediment sampling reports	Averaged from HEC-6 input data and other sediment sampling reports	10% decrease in Run #2 wash load proportions (Clark Fork Arm of reservoir)
Reservoir Sediment Thickness	HEC-6 input data	Averaged or extrapolated sediment results from previous studies	Averaged or extrapolated sediment results from previous studies	Averaged or extrapolated sediment results from previous studies	Averaged or extrapolated sediment results from previous studies
Discharge Data	HEC-6 input data	HEC-6 input data	HEC-6 input data	HEC-6 input data	HEC-6 input data
Sediment Supply Data	USGS and UMT	USGS and UMT	USGS and UMT	USGS and UMT	USGS and UMT

Results:

HEC-6 Model Results:

Comparison between modeled and empirical results focused on sediment transport the year after the dam was removed. The four year totals predicted by HEC-6 under flow scenario A, conservative scour model, are presented in Figure 3.1 and Table 3.3 to illustrate where and how much scour was predicted.
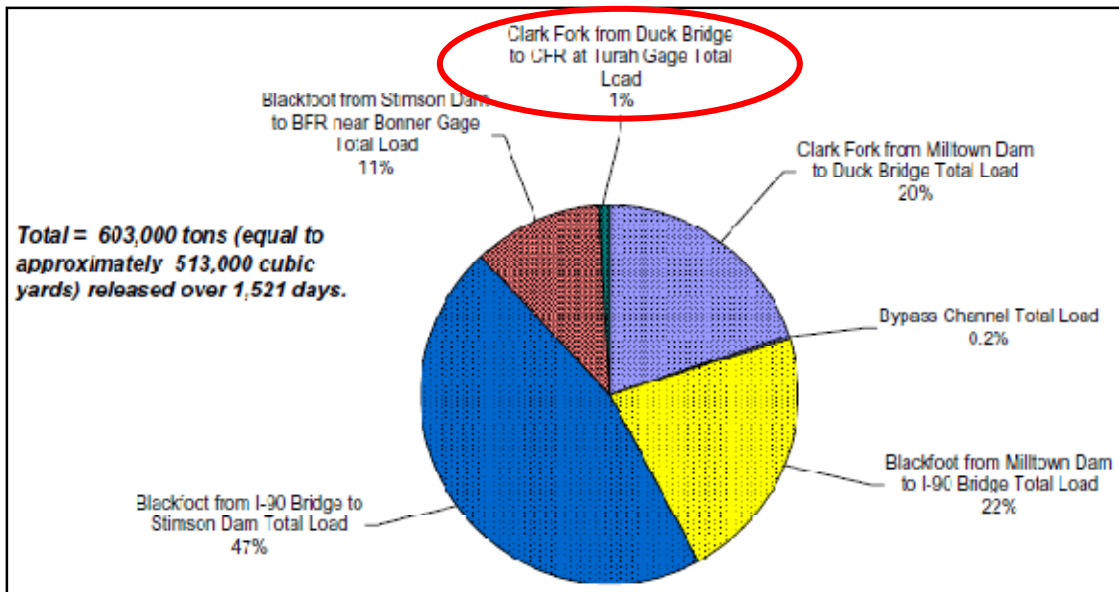
Figure 3.1 HEC-6 predicted four year sediment transport totals after the Milltown Dam removal, flow scenario A conservative scour model (Envirocon, 2004b) (weight reported in figure is short tons). Circled in red is the proportion of the total sediment transport to come from the Upper Clark Fork Arm of the reservoir. Conversion from short tons to metric tons is shown in Table 3.3.

Table 3.3 HEC-6 predicted 4 year sediment transport totals reported in short ton and metric tons (values were calculated by multiplying the total mass reported by Envirocon, by the percentages reported in the figure above).

Location and Proportion of Total Scour	HEC-6 Prediction (short tons)	HEC-6 Prediction (metric tons)
Blackfoot Upstream of Stimson Dam 11%	66,000	60,100
Blackfoot from Stimson Dam to I-90 Bridge 47%	283,000	257,000
Blackfoot from I-90 Bridge to Milltown Dam 22%	132,000	121,000
Clark Fork Upstream of Duck Bridge 1% *	6,000 *	5,400 *
Clark Fork Bypass Channel 0.2%	1,200	1,100
Clark Fork from Duck Bridge to Milltown Dam 20%	120,000	110,000
4 Year total Load	603,000	547,000

* Total sediment predicted to come from the Upper Clark Fork Arm of the Milltown

The HEC-6 model results from March 2008 to March 2009 were obtained from the HEC-6 output files on the Envirocon ftp site (Envirocon, 2010) while the four year totals were obtained from the scour report detailing the reservoir erosion and downstream transport associated with the Milltown removal (Figure 3.1 and Table 3.3)(Envirocon, 2004b). HEC-6 predicted that 220,000 metric tons of sediment would scour from the Milltown Reservoir the year following the breach (Envirocon, 2010). Assuming the percentages of how much scour was predicted in each location (Table 3.3) in the four year scour prediction can be translated to the one year prediction, ~1% (~2,200 t) was to come from the Upper Clark Fork Arm of the reservoir (Envirocon, 2004b, 2010).

The sediment budget and volumetric calculations are compared to the HEC-6 model results in Table 3.4. The difference between the observed and predicted sediment transport totals in 2008 correlated with the transport of Upper Clark Fork Arm sediments. The volumetric calculations for this section of the reservoir were further validated by the USGS suspended sediment data from Duck Bridge (located at the upstream end of the bypass channel and the downstream extent of the Upper Clark Fork Arm sediments)(Dodge et al., 2009). A single empirical rating curve derived from the Duck Bridge data indicated that about 270,000 metric tons of suspended sediment transported past that bridge in 2008. Subtracting the 2008 suspended sediment mass measured at the upstream Turah Bridge site (50,000 t) from this total suggested that approximately 220,000 t eroded from the Clark Fork Arm in 2008, accounting for suspended sediment only. The resulting sediment mass was 88% that of volumetric estimates of Upper Clark Fork Arm erosion in 2008 (Brinkerhoff, 2009; Wilcox et al., 2008). Volumetric and sediment budget values for this arm of the reservoir were two orders of magnitude higher than the HEC-6 predictions.

Table 3.4 Empirical and predicted sediment transport of Milltown Reservoir sediments, March, 2008 to March 2009 (Envirocon, 2010).

	Sediment Budget [a]	Topographic Change Estimates [b]	HEC-6 Prediction [e]
Upper Clark Fork Arm	~220,000 t [c]	250,000 t	2,200
Blackfoot Arm	~290,000 t [d]	220,000 t	218,000 t [d]
2008 Sediment Transport Totals	> 500,000 t	470,000 t	220,000 t

a. Sediment budget values are from Table 2.5, calculated suspended sediment totals from the Bypass Channel are subtracted from the totaled sediment budget in Table 2.5 for the 2008 water year to obtain Blackfoot values.
b. See Table 2.6.
c. Accounts for suspended sediment transport only, measurements collected from the Duck Bridge.
d. Includes reservoir sediments between the confluence and dam.
e. Assuming the percentages of the four year scour prediction can be translated to the one year prediction, ~1% of the total scour predicted in 2008 was to come from the Upper Clark Fork Arm. Taking 1% of 220,000 t results in an estimated 2,200 t of sediment was predicted to come from the Upper Clark Fork Arm of the reservoir

DREAM-1 Model Results:
When the original assumptions and input data from the HEC-6 modeling effort were applied to DREAM-1, the results were similar (Figure 3.2 and Table 3.5)(Envirocon, 2010). Within the Blackfoot Arm of the reservoir DREAM-1 predictions were 111% the original HEC-6 predicted totals in 2008. Within the Clark Fork Arm DREAM predicted net aggradation when the assumed reservoir sediment thickness was set at 0.003 m. This result was not surprising because the HEC-6 input geometry was a detailed cross-section with highs and lows in topography while the DREAM input was a single averaged elevation value for the entire reservoir width (a flat channel the width of the reservoir sediments)(Cui, 2002). For instance, in a confined reservoir setting the active channel represents the reservoir width while in an unconfined reservoir setting the average elevation of the deposits will more than likely be above what could be

considered the active channel or the lows in topography where water would naturally flow. When both arms of the reservoir were totaled for Run 1 the result was 108% the predicted total of the original HEC-6 modeling effort.

Table 3.5 Total sediment transport predicted by the DREAM-1 and HEC-6 models for the year following the dam removal. Differences between runs are described in Table 3.2. (All values are reported in metric tons, conversion factor from model output to metric tons is 1.4 t/m^3).

	HEC-6	Run 1	Run 2	Run 3	Run 4	Run 5
Blackfoot Arm*	218000*	245000*	X	X	X	X
Upper Clark Fork Arm	2200	-7800	92000	92000	85000	92000

* includes reservoir sediments between the confluence and dam

A

B
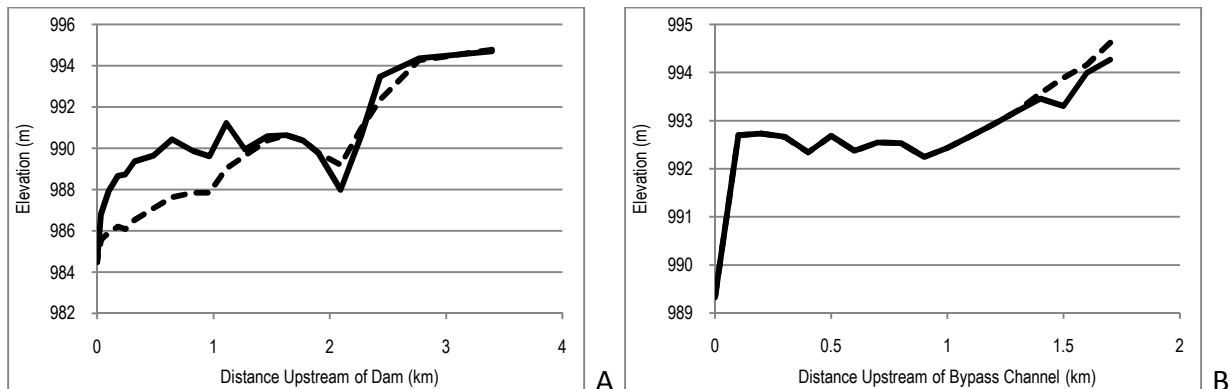
Figure 3.2 Results from the Blackfoot (A) and upper Clark Fork (B) Arms of the reservoir for DREAM-1 model Run 1. The original HEC-6 input values were used in this run to assess the differences between the DREAM-1 and HEC-6 models (Solid line represents the average initial elevation (NAVD 88) of reservoir sediments and dotted line represents the bottom elevation of the assumed trapezoidal channel after one year. (A) In the Blackfoot results the significant drop in the river profile at about 2.1 km represents the scour hole below the Stimson Dam, removed in 2005 (Epstein, 2009). (B) Steep drop at 0 km is artifact of the model switching from upstream geometry to downstream geometry).

Combining the Blackfoot results from Run 1 with the improved input data and assumptions for the Clark Fork Arm Run 2 increased the total transport out of the reservoir, more closely representing the observed transport results (Figure 3.3 and Table 3.5). This outcome was the result of increased scour predicted in the Upper Clark Fork Arm. An estimated 66,000 m^3 would be scoured from this arm of the reservoir or about 92,000 t of material.

When combined with the Blackfoot results the Run 2 DREAM-1 prediction was 65 and 71% the sampled sediment budget and volumetric estimates respectively (Tables 3.4 and 3.5). While this result was encouraging it was not all together accurate. The reservoir sediments within the Upper Clark Fork Arm were not flat prior to dam removal. In fact the reservoir deposit had a developed channel within the reservoir and the longitudinal profile was closely in line with the upstream channel (Envirocon, 2004b). The trapezoidal channel assumed by the DREAM model was already present before dam removal action.
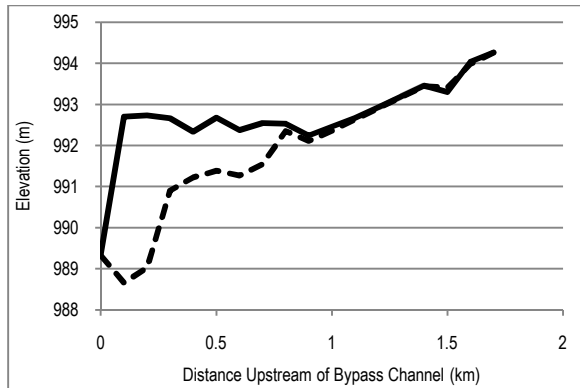
Figure 3.3 Results from the Upper Clark Fork Arm of the reservoir for DREAM-1 model Run 2. From the original HEC-6 input values two variables were adjusted in Run 2 to closely mimic the sampled sediment budget and volumetric estimates of reservoir sediment erosion in 2008; the depth of the reservoir sediments and the bed material grain size. (Solid line represents the average initial elevation (NAVD 88) of reservoir sediments and dotted line represents the bottom elevation of the assumed trapezoidal channel after one year. Steep drop at 0 km is artifact of the model switching from upstream geometry to downstream geometry).
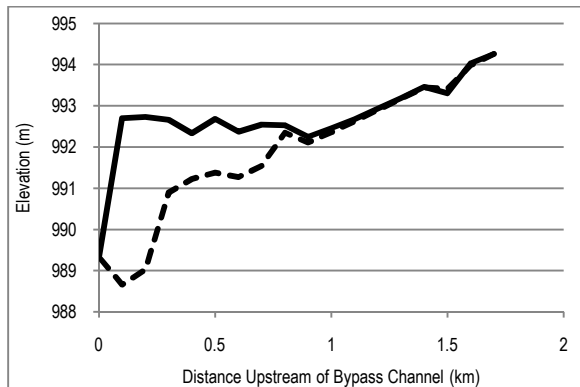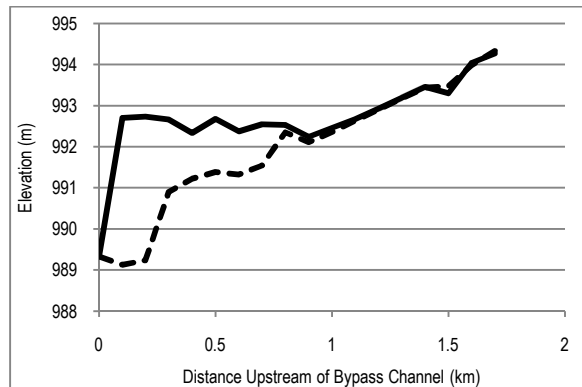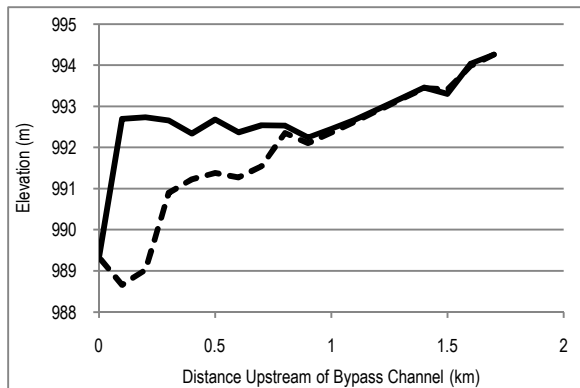
Figure 3.4 Sensitivity results preformed on the Upper Clark Fork Arm of the reservoir for DREAM-1 model Runs 3-5 (A-C respectively). A. Run 3 reservoir sediment width within the Clark Fork Arm of the reservoir was decreased by 50%. B. Run 4 the bed material grain size distribution in the Clark Fork Arm of the reservoir was coarsened by one phi class. Run 5 the proportion of wash load of each cross-section was decreased by .1 (Solid line represents the average initial elevation (NAVD 88) of reservoir sediments and dotted line represents the bottom elevation of the assumed trapezoidal channel after one year. Steep drop at 0 km is artifact of the model switching from upstream geometry to downstream geometry).

43

Sensitivity Analysis Results:
Sensitivity results of model Runs 3-5 are presented in Figure 3.4. There was no difference in predicted scour depth or volume between Run 2, 3 and 5 (Table 3.5). The only difference between the outputs from these runs was the suspended sediment concentrations. The decreased proportion of wash load present in Run 5 resulted in lower suspended sediment concentrations while the depth of scour stayed the same; indicating the proportion of sand and smaller sized particles in the reservoir sediments had no influence on the scour functionality of DREAM-1. However, when the bed material grain size distribution was coarsened by one phi class (Run 4) the scour depths decrease, resulting in a 7% reduction in the predicted scour volume. The sensitivity of DREAM-1 to the sediment properties required as input was determined by the single grain size distribution that represents the bed material upstream, within and downstream of the reservoir; assuming the reservoir sediment widths were wider than the downstream bankfull channel width. Additional results such as DREAM-1 output tables and predicted volume and weight of sediment erosion can be found in Appendix B.

Discussion:

Upper Clark Fork Arm Modeling:
Comparison between the original model predictions and empirical results indicated the HEC-6 model predictions for the Milltown Dam removal were inaccurate in the Upper Clark Fork Arm of the reservoir. When DREAM-1 was run with the original input data and assumptions of the HEC-6 modeling effort the resulting prediction was similar. The minor differences between these outputs were mostly a function of the input geometry required by each model being different. When the HEC-6 assumptions were corrected in subsequent DREAM-1 runs the predicted scour in the Clark Fork Arm increased. However, the resulting trapezoidal channel predicted by DREAM was simply a recreation of the channel that existed within the reservoir sediments before removal. These results indicated that although the original assumptions made by the modelers could have been the source of some error in the Upper Clark Fork Arm predictions, there is some inherent limitation of both models when applied to wide alluvial reservoir settings.

As stated in Chapter 2, the majority of sediment that eroded from the Upper Clark Fork Arm of the reservoir was the result of bank erosion, when lateral movement of the channel occurred (Figure 3.5). Bank pin erosion tests conducted before the removal indicated that the average bank erosion hazard index (BEHI) and near bank stress (NBS) of these sediments were very high, with one bank described as extreme (River Design Group and WestWater Consultants, 2006). Despite these unstable banks, some several meters in height, the possibility of bank failure in the Upper Clark Fork Arm during and after the removal was not addressed in the scour reports or modeling effort (Envirocon, 2004b, 2010).

One-dimensional sediment transport models do not simulate multidimensional effects such as lateral scour or deposition (Cui and Wilcox, 2008; Ferguson, 2003; Gee, 1984, 1995; Rathbun and Wohl, 2001). Since both the HEC-6 and DREAM models are one-dimensional and the erosion of the Upper Clark Fork Arm of the Milltown Dam removal was mostly due to lateral

bank scour; it is more than likely that the inability of the one-dimensional models to quantify lateral bank scour was the main source of error in the original HEC-6 prediction and the adjusted DREAM-1 predictions.
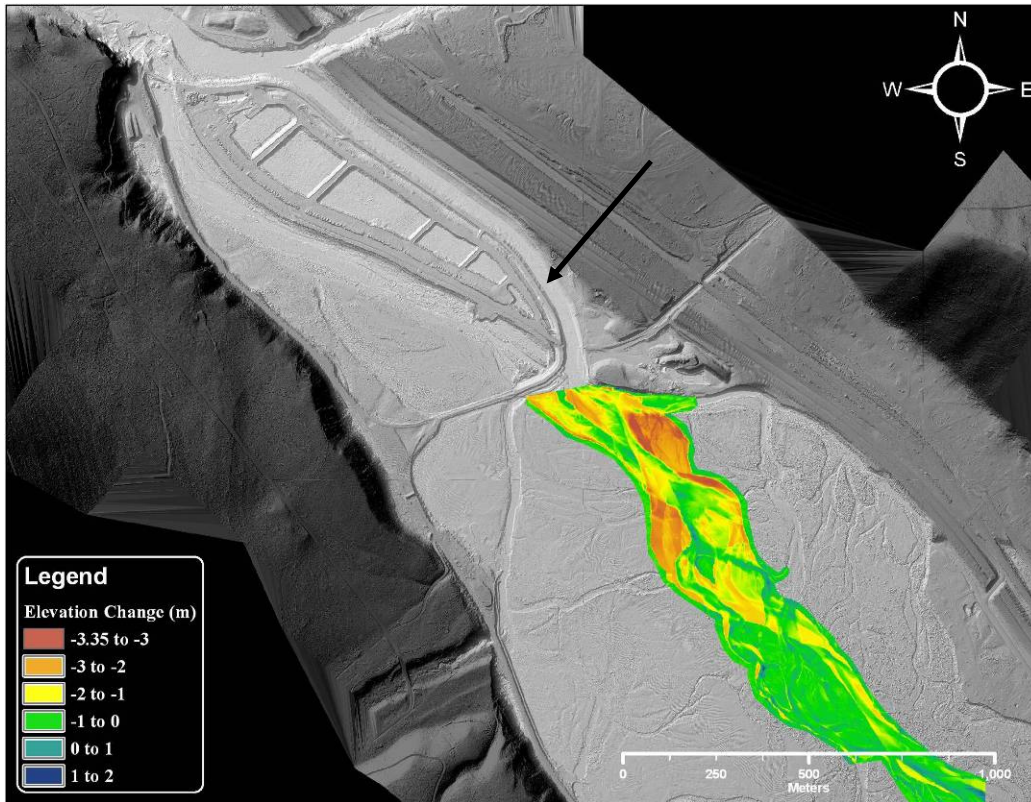
Figure 3.5 Volumetric DEM differencing calculation for erosion within the Upper Clark Fork Arm of the reservoir (Wilcox et al., 2008). Black arrow points to the bypass channel with an average width of about 40 m. (Total scour = 180,000 ±30,000 m^3)

Sediment transport models applied to dam removal are typically one-dimensional (Cui and Wilcox, 2008). If one-dimensional models are to be used where lateral channel scour is a possibility, supplementary methods to estimate lateral erosion should be added to the modeling effort. Although not applied in this study, the model developed by Cantelli et al., (2007) could possibly have accounted for channel widening within the Milltown Reservoir after the dam removal. Their model uses the initial downward erosion and narrowing of reservoir sediments as calibration to calculate the rate of channel widening (Cantelli et al., 2007). Coupling this model or others with the hourly, daily or weekly DREAM-1 input and output data (changing elevation and slope, hydrology and bank characteristics, such as height and grain size distribution) could help predict reservoir erosion in future dam removals where wide, fine grained reservoir deposits are present.

Blackfoot Arm Modeling:
Blackfoot Arm modeling results indicated that both the HEC-6 and DREAM-1 models were relatively accurate. Both models predicted similar sediment transport in the confined reservoir

45

setting. Differences between the outputs could have been the result of simplified channel geometry when converting from HEC-6 to DREAM-1. Also, some of the cross-sections were removed from the HEC-6 input to simplify the input to DREAM-1, allowing for a good zeroing run. As stated in Chapter 2, the scour associated with the Blackfoot Arm of the reservoir was the result of profile adjustment. When this result is combined with the accuracy of both one-dimensional models in predicting the Blackfoot scour volumes it implies that the functionality of both models is well suited when they are applied to confined reservoir settings.

DREAM-1 Model:
When managing the HEC-6 and DREAM input and output files the DREAM model was much easier to apply and interpret. Change to input values were simple in DREAM and the results from a changed simulation could be calculated and viewed in minutes. These factors, combined with the accuracy of the modeling results for the Blackfoot Arm of the reservoir made the DREAM model very applicable to confined reservoir settings, as was the case in the Marmot Dam removal. Further, if the DREAM model is supplemented with some type of bank erosion model (e.g., Cantelli et al. 2007), DREAM could also be applied to wide, fine grained alluvial reservoir settings.

When using DREAM-1, three input parameters were problematic:
1. When modeling wide alluvial reservoir deposits the simplicity of the reservoir geometry data entered does not account for an already developed channel. This can lead to over estimation of the volume of erosion out of the reservoir because the model may predict erosion where a channel was already present. Wide sections of the reservoir make the average elevation of the reservoir sediments higher in elevation than a pre-existing reservoir channel. A possible solution would be to subtract the preexisting channel from the volume of scour predicted by DREAM-1.
2. Currently the Parker (1990) equation is used in DREAM-1. This equation does not allow for sand-sized particles to transport as bedload. This results in sand that would normally transport at lower discharges to not transport until the threshold of motion is achieved for the coarser bed material grain size distribution input. For example, the single bed material grain size distribution input to the model could have a D50 of 70 mm. This grain sized distribution would then determine the scour potential of reservoir sediments composed entirely of sand.
3. The sediment properties entered into DREAM-1 only account for the grain size distribution of the upstream bed material and the proportion of wash load in each cross-section. This leaves a gap if the reservoir sediments are predominantly finer than the bed material of the upstream channel but coarser than sand in grain size, possibly resulting in a misrepresentation of reservoir erosion potential. A possible solution for numbers 2 and 3 above is to use a variety of upstream pebble counts and compare them to the reservoir sediments to best represent the upstream bed material and reservoir sediment grain size distributions together.

Input data used for the various DREAM-1 simulations could have introduced error to the predictions of reservoir sediment transport. In both the Blackfoot and Clark Fork Rivers several pebble counts were collected upstream of the reservoir. It is possible that the input pebble count used for the DREAM-1 model runs was flawed or not the best representation of the bed material. Geometry data entered into DREAM were also suspect. Averaged values from sparse sediment depth maps within the Upper Clark Fork Arm could have misrepresented the thickness of the reservoir deposit, resulting in erroneous sediment transport estimates. The bed material elevations underlying the reservoir sediments were a result of methods that may not have taken into account logs that deposited in the Blackfoot Arm of the reservoir. These logs would have prevented tile probes from reaching the historic channel below the reservoir sediments, thus misrepresenting the depth of reservoir sediments.

Conclusion:

Both HEC-6 and DREAM-1 model predictions for the Milltown Dam removal were inaccurate when applied to the unconfined Clark Fork Arm of the reservoir. Although the models were well suited when applied to the confined Blackfoot the inherent inability of the one-dimensional models to quantify lateral bank scour was the primary source of error. Even though the bank sediments in the Upper Clark Fork Arm of the reservoir were very unstable, the possibility of bank failure during and after the removal was not addressed in the original scour reports or modeling effort. Supplementing current one-dimensional models with a model capable of predicting lateral bank scour could help future dam removals where wide, fine grained reservoir deposits are present. Overall the DREAM-1 model was easy to use and produced acceptable results in a confined reservoir setting and if coupled with a bank erosion model could possibly be applied to unconfined reservoir settings.

References:

ASCE, 2009, 2009 Report Card for America's Infrastructure, Facts about Dams, p. 14-23.

Babbitt, B., 2002, What goes up, may come down: BioScience, v. 52, p. 656–658.

Brinkerhoff, D. J., 2009, Erosion and Deposition Following the Removal of Milltown Dam, Clark Fork River, Montana, unpublished thesis (Undergraduate), University of Montana, Missoula.

Buffington, J. M., and D. R. Montgomery, 1997, A systematic analysis of eight decades of incipient motion studies, with special reference to gravel-bedded rivers: Water Resources Research, v. 33, p. 1993–2029.

Bunte, K., K. W. Swingle, and S. R. Abt, 2007, Guidelines for using bedload traps in coarse-bedded mountain streams: Construction, installation, operation, and sample processing., *in* F. S. U.S. Department of Agriculture, Rocky Mountain Research Station, ed., Fort Collins, CO, p. 91.

Bushaw-Newton, K. L., D. D. Hart, J. E. Pizzuto, J. R. Thomson, J. Egan, J. T. Ashley, T. E. Johnson, R. J. Horwitz, M. Keeley, J. Lawrence, D. Charles, C. Gatenby, D. A. Kreeger, T. Nightengale, R. L. Thomas, and D. J. Velinsky, 2002, An integrative approach towards understanding ecological responses to dam removal: The Manatawny Creek Study: Journal of the American Water Resources Association, v. 38, p. 1581-1599.

Cantelli, A., M. Wong, G. Parker, and C. Paola, 2007, Numerical model linking bed and bank evolution of incisional channel created by dam removal: Water Resources Research, v. 43, p. 16.

Church, M., and M. A. Hassan, 1992, Size and distance of travel of unconstrained clasts on a streambed: Water Resources Research, v. 28, p. 299-303.

Cui, Y. T., 2002, Dam Removal Express Assessment Models, User's Manual (Version 2.0): Stillwater Sciences, v. October, 2002, p. 31.

Cui, Y. T., C. Braudrick, W. E. Dietrich, B. Cluer, and G. Parker, 2006a, Dam Removal Express Assessment Models (DREAM). Part 2: Sample runs/sensitivity tests: Journal of Hydraulic Research, v. 44, p. 308-323.

Cui, Y. T., and B. Cluer, 2008, Dam Removal Express Assessment Models (DREAM-1 and -2): applications and examinations: Proceedings of the World Environmental and Water Resources Congress.

Cui, Y. T., B. Orr, A. Wilcox, J. Vick, C. Podolak, and P. Wilcock, 2008, Marmot Dam removal: predictions and observations: Presentation at the 2008 AGU Fall Meeting.

Cui, Y. T., G. Parker, C. Braudrick, W. E. Dietrich, and B. Cluer, 2006b, Dam Removal Express Assessment Models (DREAM). Part 1: Model development and validation: Journal of Hydraulic Research, v. 44, p. 291-307.

Cui, Y. T., and A. Wilcox, 2008, Development and application of numerical modeling of sediment transport associated with dam removal: ASCE Manual 110, v. 110, p. 995-1020.

Dietrich, W. E., T. Dunne, N. F. Humphrey, and L. M. Reid, 1982, Construction of sediment budgets for drainage basins, U.S. Department of Agriculture: Sediment Budgets and Routing in Forested Drainage Basins: Proceedings of the Symposium; 31 May - 1 June 1982, Corvallis, Oregon. Gen. Tech. Rep. PNW-141, Pacific Northwest Forest and Range Experiment Station, Forest Service, 1982, p. 5-23.

Dodge, K. A., M. I. Hornberger, and J. L. Dyke, 2009, Water-Quality, Bed Sediment, and Biological Data (October 2007 through September 2008) and Statistical Summaries of Long-Term Data for Streams in the Clark Fork Basin, Montana, *in* U. S. G. S. United Stated Department of the Interior, Prepared in cooperation with the U. S. Environmental Protection Agency, ed., p. 139.

Doyle, M. W., E. H. Stanley, and J. M. Harbor, 2002, Geomorphic analogies for assessing probable channel response to dam removal: Journal of the American Water Resources Association, v. 38, p. 1567-1579.

Edwards, T. K., and G. D. Glysson, 1999, Field methods for measurement of fluvial sediment, *in* U. Department of the Interior, ed., Revision Copyright 2007, American Geological Institute, p. 89.

Efron, B., and R. J. Tibshirani, 1994, An Introduction to the Bootstrap: Boca Raton, FL: CRC Press.

Emmett, W. W., 1980, A field calibration of the sediment-trapping characteristics of the Helley-Smith bedload sampler, *in* U. S. G. S. U.S. Department of the Interior, Professional Paper, 1139, ed.

Envirocon, 2004a, Draft, Remedial Design Data summary Report #1, Milltown Reservoir Sediments Site, Prepared by Envirocon, Inc. for the Atlantic Richfield Company, p. 215, 10 Appendixes.

Envirocon, 2004b, Milltown Reservoir Dry Removal Scour Evaluation – Addendum 1, Proposed Plan Updated Scour Evaluation, October version, Prepared by Envirocon, Inc. and EMC2 for the Atlantic Richfield Company, p. 121, 3 Appendixes.

Envirocon, 2010, ftp://milltown.envirocon.com/, Open Access FTP Site, Accessed 02/02/2010.

Epstein, J., 2009, Upstream response to dam removal: The Blackfoot river, Montana, unpublished thesis (M.S.), University of Montana.

Ferguson, R. I., 2003, The missing dimension: effects of lateral variation on 1-D calculations of fluvial bedload transport: Geomorphology, v. 56, p. 1-14.

Gee, D. M., 1984, Role of Calibration in the Application of HEC-6 model: US Army Corps of Engineers, Hydrologic Engineering Center Tech. Pap. No. 102, p. 26.

Gee, D. M., 1995, HEC-6: Reservoir Sediment Control Applications: US Army Corps of Engineers, Hydrologic Engineering Center Tech. Pap. No. 148, p. 18.

Gilbert, G. K., 1917, Hydraulic Mining Debris in the Sierra Nevada, *in* U. S. G. S. Professional Paper 105, Department of the Interior, ed., Washington, D.C., p. 154.

Gomez, B., 1991, Bedload Transport: Earth-Science Reviews, v. 31, p. 89-132.

Graf, W. L., E. Wohl, T. Sinha, and J. L. Sabo, 2010, Sedimentation and sustainability of western American reservoirs: Water Resources Research, v. 46, W12535.

Gran, K. B., and D. R. Montgomery, 2005, Spatial and temporal patterns in fluvial recovery following volcanic eruptions: Channel response to basin-wide sediment loading at Mount Pinatubo, Philippines: GSA Bulletin, v. 117, p. 195–211.

Gran, K. B., and D. R. Montgomery, 2006, Channel bed evolution and sediment transport under declining sand inputs: Water Resources Research, v. 42, p. 14.

Grant, G., 2001, Dam removal: Panacea or Pandora for rivers? Invited commentary: Hydrological Processes, v. 15, p. 1531-1532.

Grant, G. E., J. C. Schmidt, and S. L. Lewis, 2003, A Geological Framework for Interpreting Downstream Effects of Dams on Rivers: In: O'Connor JE and Grant GE (Eds). A peculiar river: geology, geomorphology and hydrology of the Deschutes River. Washington, DC: American Geophysical Union, Water Science and Application 7., v. 10/1029/007WS13.

Hall, H. T., 2000, Regional Director of Federal Energy Regulatory Commission letter to Jim Stilwell - Montana Power Company.

Harding Lawson Associates, 1986, Milltown Reservoir Feasibility Study, Prepared by Harding Lawson Associates for Montana Department of Health and Environmental Sciences, p. 198, 39 Tables.

Hart, D. D., T. E. Johnson, K. L. Bushaw-Newton, R. J. Horwitz, A. T. Bednarek, D. F. Charles, D. A. Kreeger, and D. J. Velinsky, 2002, Dam removal: Challenges and opportunities for ecological research and river restoration: Bioscience, v. 52, p. 669-681.

Havis, R. N., C. V. Alonso, and J. G. King, 1996, Modeling sediment in gravel-bedded streams using HEC-6: Journal of Hydraulic Engineering-ASCE, v. 122, p. 559-564.

Heinz Center, 2002, H. John Heinz III Center for Science, Economics and the Environment. 2002. Dam Removal: Science and Decision Making. Washington, DC, p. 221.

Heinz Center, 2003, H. John Heinz III Center for Science, Economics and the Environment. 2003. Dam Removal Research: Status and Prospectus. Washington, DC, p. 151.

James, L. A., 2010, Secular Sediment Waves, Channel Bed Waves, and Legacy Sediment: Geography Compass, v. 4, p. 576-598.

Lambing, J. H., and S. K. Sando, 2009, Estimated Loads of Suspended Sediment and Selected Trace Elements Transported through the Milltown Reservoir Project Area Before and After the Breaching of Milltown Dam in the Upper Clark Fork Basin, Montana, Water Year 2008, *in* U. S. G. S. United States Department of the Interior, Prepared in cooperation with the U. S. Environmental Protection Agency, ed., p. 30.

Lisle, T. E., Y. Cui, G. Parker, J. E. Pizzuto, and A. M. Dodd, 2001, The dominance of dispersion in the evolution of bed material waves in gravel-bed rivers: Earth Surface Processes and Landforms, v. 26, p. 1409–1420.

Major, J. J., 2004, Posteruption suspended sediment transport at Mount St. Helens: Decadal-scale relationships with landscape adjustments and river discharges: Journal of Geophysical Research, v. 109, p. 22.

Major, J. J., and L. E. Mark, 2006, Peak flow responses to landscape disturbances caused by the cataclysmic 1980 eruption of Mount St. Helens, Washington: Geological Society of America Bulletin, v. 118, p. 938-958.

Major, J. J., J. E. O'Connor, G. E. Grant, K. R. Spicer, H. M. Bragg, A. Rhode, D. Q. Tanner, C. W. Anderson, and J. R. Wallick, 2008a, Initial fluvial response to the removal of Oregon's Marmot Dam: EOS Trans. AGU, p. 241-242.

Major, J. J., J. E. O'Connor, K. R. Spicer, H. M. Bragg, J. R. Wallick, R. L. Kittleson, K. K. Lee, D. Cushman, D. Piatt, D. Q. Tanner, T. Hale, M. A. Uhrich, and A. Rhode, 2008b, Event-Based Monitoring of Sediment Flux Following Removal of Oregon's Marmot Dam: EOS Trans. AGU, 89(53), Fall Meeting Supplemental Abstract H41I-05.

Major, J. J., J. E. O'Connor, C. J. Podolak, M. K. Keith, K. R. Spicer, J. R. Wallick, H. M. Bragg, S. Pittman, P. R. Wilcock, A. Rhode, and G. E. Grant, 2009, Evolving fluvial response of the Sandy River, Oregon, following removal of Marmot Dam: 2nd Joint Federal Interagency Conference, p. 11.

Moog, D. B., and P. J. Whiting, 1998, Annual hysteresis in bed load rating curves: Water Resources Research, v. 34, p. 2393-2399.

Moore, J. N., 1985, Source of metal contamination in Milltown Reservoir, Montana: An interpretation based on Clark Fork River bank sediment, *in* H. Report to the USEPA: District VII, MT., ed.

Moore, J. N., and E. M. Landrigan, 1999, Mobilization of metal contaminated sediment by ice-jam floods: Environmental Geology, v. 37, p. 96–101.

Moore, J. N., and W. W. Woessner, 2003, Arsenic contamination in the water supply of Milltown, Montana, *in* A. H. Welch, Stollenwerk, K. G., ed., Arsenic in Ground Water, Kluwer Academic Publishers, p. 329-350.

Nelson, J. M., J. P. Bennett, and S. M. Wiele, 2002, Flow and sediment-transport modeling, *in* G. M. Kondolf, and H. Piegay, eds., Tools in fluvial geomorphology, John Wiley & Sons, Chichester, United Kingdom (GBR), p. 539-576.

Parker, G., and P. C. Klingeman, 1982, On why gravel bed streams are paved: Water Resources Research, v. 18, p. 1409–1423.

Pejchar, L., and K. Warner, 2001, A river might run through it again: Criteria for consideration of dam removal and interim lessons from California: Environmental Management, v. 28, p. 561-575.

Pizzuto, J., 2002, Effects of dam removal on river form and process: Bioscience, v. 52, p. 683-691.

Poff, N. L., B. P. Bledsoe, and C. O. Cuhaciyan, 2006, Hydrologic variation with land use across the contiguous United States: Geomorphic and ecological consequences for stream ecosystems: Geomorphology, v. 79, p. 264-285.

Poff, N. L., and D. D. Hart, 2002, How dams vary and why it matters for the emerging science of dam removal: Bioscience, v. 52, p. 659-668.

Rathburn, S. L., and E. E. Wohl, 2001, One-dimensional sediment transport modeling of pool recovery along a mountain channel after a reservoir sediment release: Regulated Rivers: Research and Management, v. 17, p. 251-273.

River Design Group, and WestWater Consultants, 2006, Geomorphic Data Summary Report, Restoration Plan for the Clark Fork River and Blackfoot River near Milltown Dam, Prepared For: State of Montana NRDP and Montana FWP, In consultation with the USFWS and Confederated Salish and Kootenai Tribes, p. 14, 14 Appendixes.

Schmidt, J. C., and P. R. Wilcock, 2008, Metrics for assessing the downstream effects of dams: Water Resources Research, v. 44, p. 19.

Shields, A., 1936, Anwendung der Aehnlichkeitsmechanik und der Turbulenzforschung auf die Geschiebebewegung, *in* U. S. D. o. A. English title: Application of similarity principles and turbulence research to bed-load movement [translated by W.P. Ott and J.C. van Uchelen, Soil Conservation Service Cooperative Laboratory, California Institute of Technology, Pasadena, 1936], ed., p. 36.

Shuman, J. R., 1995, Environmental considerations for assessing dam removal alternatives for river restoration: Regulated Rivers: Research and Management, v. 11, p. 249-261.

Sklar, L. S., J. Fadde, J. G. Venditti, P. Nelson, M. A. Wydzga, Y. Cui, and W. E. Dietrich, 2009, Translation and dispersion of sediment pulses in flume experiments simulating gravel augmentation below dams: Water Resources Research, v. 45, p. 14.

Stanley, E. H., and M. W. Doyle, 2003, Trading off: the ecological removal effects of dam: Frontiers in Ecology and the Environment, v. 1, p. 15-22.

Tingsanchali, T., and S. Supharatid, 1996, Experimental investigation and analysis of HEC-6 river morphological model: Hydrological Processes, v. 10, p. 747-761.

Titan, 1995, Milltown Reservoir Sediments Operable Unit, Final Draft Remedial Investigation Report: Prepared by Titan Environmental Corporation for the Atlantic Richfield Company, v. 1-3.

USFWS, 1998, Klamath River and Columbia River bull trout population segments: status summary. Prepared by the USFWS bull trout listing team, *in* U. S. F. a. W. Service, ed., Boise, Idaho.

USFWS, 2002, Chapter 3, Clark Fork River Recovery Unit, Montana, Idaho, and Washington, *in* U. S. F. a. W. Service, ed., Bull Trout (Salvelinus confluentus) Draft Recovery Plan: Portland, Oregon, p. 285.

USGS, 2010, http://waterdata.usgs.gov, Accessed 2008-2010.

Wilcock, P. R., 1988, Methods for estimating the critical shear stress of individual fractions in mixed-size sediment: Water Resources Research, v. 24, p. 1127–1135.

Wilcock, P. R., S. T. Kenworthy, and J. C. Crowe, 2001, Experimental study of the transport of mixed sand and gravel: Water Resources Research, v. 37, p. 3349-3358.

Wilcock, P. R., J. Pitlick, and Y. Cui, 2009, Sediment transport primer: estimating bed-material transport in gravel-bed rivers, *in* F. S. United States Department of Agriculture, Rocky Mountain Research Station, ed., Fort Collins, CO, p. 64.

Wilcox, A. C., D. Brinkerhoff, and C. Woelfle-Erskine, 2008, Initial geomorphic responses to removal of Milltown Dam, Clark Fork River, Montana, USA, EOS Trans. AGU, 89(53), Fall Meeting Supplemental Abstract H41I-07.

Williams, G. P., 1989, Sediment concentration versus water discharge during single hydrologic events in rivers: Journal of Hydrology, v. 111, p. 89-106.

Wolman, M. G., 1954, A method of sampling coarse river-bed gravel: Transactions of American Geophysical Union, v. 35, p. 951-956.

Appendix A: Dam Removal Sediment Transport

Introduction:

Sediment Transport Summary:

Sediment transport is commonly divided into two transport processes, suspended and bedload transport. Suspended transport moves fine sediment mostly within the water column while bedload transport moves coarse sediment while it is still in contact with the bed material. Where these two processes overlap can sometimes be difficult to identify (Wilcock et al., 2009). Depending upon discharge, grain sizes between about .1 to 8 mm can move by both processes within a given storm or runoff event, making it difficult to consistently sample them through one method (Figure 2.1). However, this transition between bedload and suspended transport can be useful if both suspended and bedload are collected together. The patterns and thresholds within the channel can be further understood by correlating this transition.
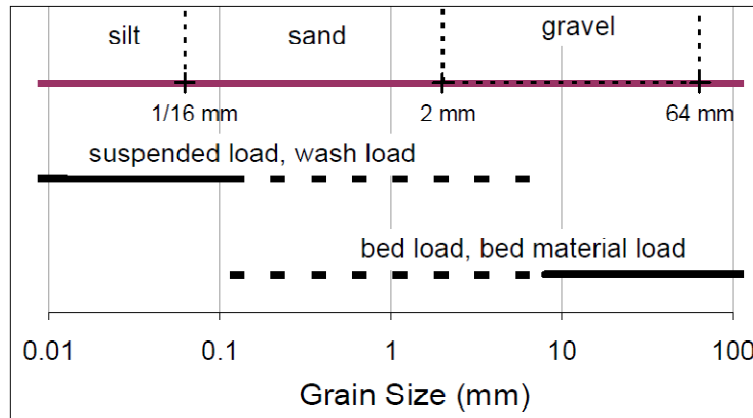
Figure A.1 Typical relationship between grain size and transport processes (Wilcock et al., 2009).

Sediment transport is a function of the driving and resisting forces within a channel. Not all driving hydraulic forces within the channel are applied to the channel sediment. The force that does come in contact with river sediments is known as shear stress. Assuming steady, uniform flow and a width to depth ratio greater than 20, shear stress can be expressed as:

$$\tau = \rho g d S$$

(1)

where τ is shear stress, ρ is the density of water, g is the acceleration of gravity, d is water depth and S is slope. When the shear stress is greater than the resisting forces exerted by the grain, the grain moves (Church, 2002). The shear stress required to move a particle is called the critical shear stress and it varies depending upon particle characteristics like grain size. Sometimes the orientation of particles with each other can increase the critical shear stress required to move the particle. To represent the shear stress to grain size ratio we can calculate the Shields number (Shields, 1936). The Shields number is a dimensionless ratio and it can be expressed in the form:

$$\tau^* = \frac{\tau}{(\rho_s - \rho)gD}$$

(2)

where τ^* is Shields number, ρ_s is sediment density and D is grain diameter (often the grain diameter used is the D50, or median grain size). In theory, once the Shields number for a particle larger than sand reaches a value around .03 to .05 the resisting force of the particle is exceeded by the shear stress (Shields, 1936).

In order to quantify the critical shear stress we can use samples of bedload transport to identify a small reference transport rate (Parker and Klingeman, 1982). The shear stress required to transport at the rate of reference transport is called the reference shear stress and is used in place of the critical shear stress (Wilcock, 1988). As discharge increases, shear stress increases and above the reference shear stress sediment transport rates increase with discharge.

Sediment in transport can be quantified by a rate of transport at a certain discharge. Several observations of the rate of transport at different discharges can be used to mathematically represent the relationship between discharge and bedload transport (i.e. a bedload rating curve). There are three general methods to develop bedload transport rating curves (Wilcock et al., 2009). 1) Empirical rating curves derived through a regression of sample data. 2) Formulas that incorporate calibration with sample data. 3) Uncalibrated transport formulas that do not use sample data to produce rating curves. Each method has advantages and disadvantages. Empirical rating curves can be used in cases where the underlying assumptions of current formulas are not met, but this requires a significant sampling effort. Also, empirically derived rating curves can be sensitive to outliers or erroneous samples. Calibrated formulas can often provide the most accurate results for the least effort, but the underlying assumptions of the formulas can bias the rating curve if they are not met under the sediment transport regime being modeled. With limited resources uncalibrated formulas can be effective at predicting transport but only if the underlying assumptions of the formula are met (Wilcock et al., 2009).

Formulas of sediment transport rely upon dimensionless relationships of known sediment transport regimes. Sample data are used to derive the relationships between a dimensionless transport rate q^* (Einstein transport parameter)(Einstein, 1950) and dimensionless shear stress τ^* (Shields Number). The dimensionless transport rate q^* represents the ratio of the volumetric transport rate qs to the product (wD), where w is the grain fall velocity (Wilcock et al., 2009). The dimensionless transport rate more commonly used today is:

$$W^* = \frac{(s-1)gq_s}{(\tau/\rho)^{\frac{3}{2}}}$$

(3)

where W^* is the dimensionless transport parameter, s is the ratio of ρ_s/ρ and q_s is the unit bedload flux. With these two dimensionless variables the transport rate is scaled by the size and weight of the grain in transport while the shear stress is scaled to the grain weight. This allows for a sediment transport formula to be scaled to rivers of different sizes. Formula inputs, like bed material grain size distributions, slope, channel geometry, scale the formula to different channel settings. Problems can arise when applying these formulas to transport regimes that are different than the regime the formula was derived from (Wilcock et al., 2009).

Methods:

WinXSPRO Input Data:

Table A.1 WinXSPRO input cross-sections (orange cells represent high water marks from the 2009 spring runoff and yellow cells represent the water surface elevations the day of the surveys (Feb. 10, 2010)).

Turah		Black		Deer	
Distance from Left Bank (m)	Arbitrary Elevation (m)	Distance from Left Bank (m)	Arbitrary Elevation (m)	Distance from Left Bank (m)	Arbitrary Elevation (m)
0.00	6.59	0.00	15.24	0.00	15.24
1.52	6.68	2.32	14.71	1.56	15.07
3.05	6.22	8.81	12.24	10.17	10.13
4.57	5.63	16.62	10.85	14.09	8.66
6.10	5.09	23.10	8.93	15.96	8.18
7.62	4.33	29.65	7.41	18.32	8.14
7.92	4.08	32.98	6.87	19.48	6.92
8.53	3.53	36.12	6.57	20.61	6.69
9.14	3.32	41.09	5.15	21.36	6.41
10.67	2.95	44.46	4.52	24.91	4.62
12.19	2.84	46.90	4.10	29.26	3.51
13.72	2.71	52.06	3.43	33.55	3.33
15.24	2.57	53.67	2.97	37.93	3.29
16.76	2.61	56.25	2.91	42.20	2.97
18.29	2.79	59.18	3.07	46.58	2.86
19.81	2.55	62.81	3.43	50.98	3.59
20.42	2.46	65.79	3.51	55.32	5.18
21.33	2.44	69.04	3.47	59.67	6.54
21.94	2.68	73.09	3.21	60.77	6.96
22.25	2.68	77.16	3.07	62.84	7.60
22.86	2.65	79.08	2.97	66.89	8.76
24.38	2.50	80.98	2.58	71.94	11.06
25.91	2.90	85.28	2.41	75.98	13.02
27.43	3.03	89.22	2.49	78.59	13.88
28.95	3.40	90.07	2.97		
30.48	3.70	91.88	3.20		
31.39	3.83	93.51	3.90		
31.70	4.05	94.98	4.21		
32.00	4.23	97.69	5.13		
33.53	4.50	99.57	6.71		
35.05	4.63	101.34	7.24		
36.57	4.75	106.29	8.70		

38.10	4.66	110.79	10.50
39.62	4.53	120.43	11.86
41.15	4.51	127.36	13.36
42.67	4.56	130.17	14.52
42.97	4.66	134.04	14.86
43.28	4.63		
43.89	4.72		
44.19	4.69		
45.72	4.60		
47.24	4.60		
48.77	4.60		
50.29	4.53		
51.14	4.64		
52.67	3.66		
53.89	3.23		
56.93	2.83		
59.98	2.80		
63.03	2.64		
66.08	2.63		
69.13	2.29		
72.17	2.20		
75.22	2.26		
76.59	2.65		
77.66	3.71		
79.79	5.10		
81.47	6.31		
83.75	6.66		
86.86	6.65		
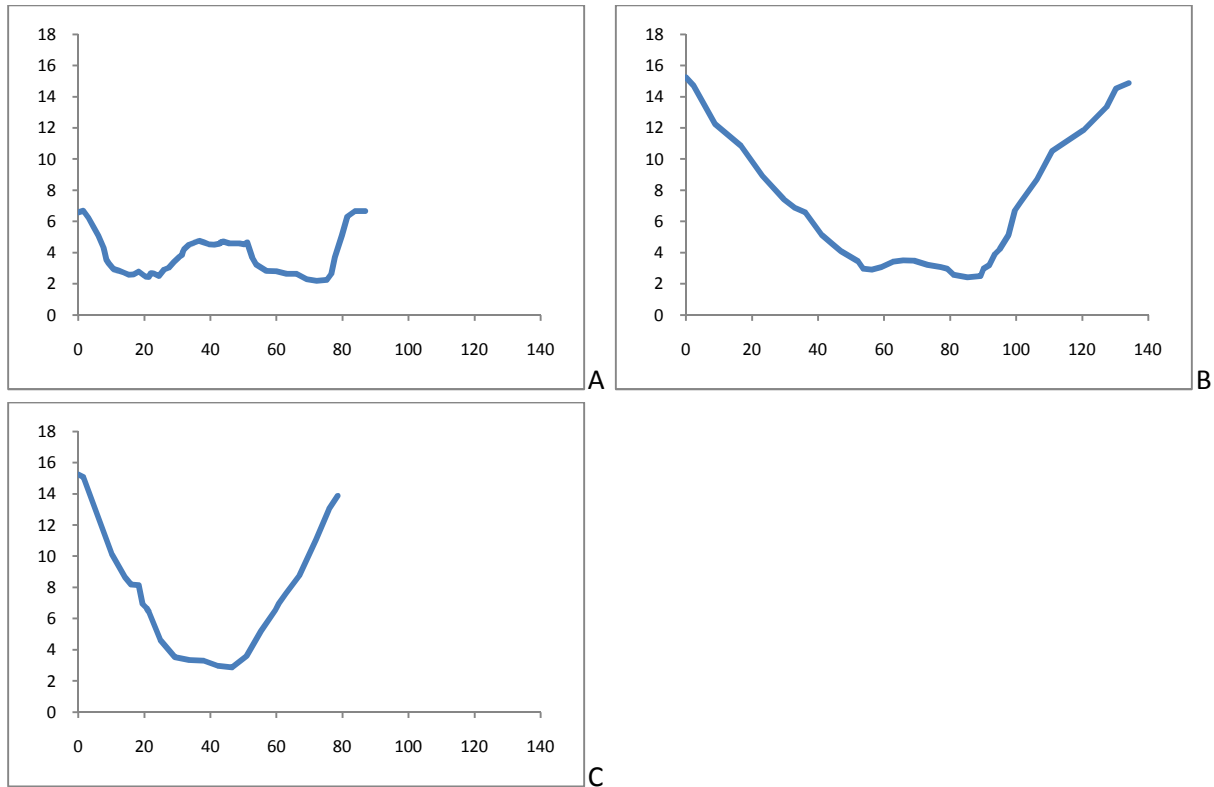
Figure A.2 WinXSPRO cross-sections.

Calibrated and Uncalibrated Rating Curves:

The Bedload Assessment in Gravel-bedded Streams (BAGS) software package was used as an interface to calculate the calibrated and uncalibrated rating curve models. BAGS is an interactive software package written in Visual Basic for Applications within a Microsoft Excel workbook (Wilcock et al., 2009). Four models from the BAGS software were used to derive bedload rating curves. Bedload transport models calculate transport rate as a function of excess stress and reference stress. All four transport models that were used have been derived from the same or similar empirical data sets resulting in very similar mechanics, but the models differ in three ways. The Wilcock and Bakke models allow for calibration with bedload sample data while the Parker and Wilcock-Crowe models are uncalibrated. All the models require bed material surface particle size distributions for input except for the Bakke model which uses sub-surface particle size distributions. The models all output multiple grain size fractions in their results except for the Wilcock model which only calculates two grain size fractions, larger than sand or sand and smaller.

The calibrated and uncalibrated models were applied to the sample data and sample sites for two reasons. Limited data collected in 2008 requires the use of calibrated models to produce results that are more robust. The calibrated Wilcock and Bakke models were originally derived from a different transport regime, but the models are very sensitive to the calibration data and applying the sample data to the calibration of those models will allow for more confidence in

the 2008 sediment transport results. The uncalibrated models were run to highlight the differences between normal and dam removal sediment transport conditions. The two uncalibrated models run here are commonly used for estimating sediment transport when sample data are not available.

The final empirical and calibrated rating curves were graphed with the sample data to determine the best fit curve for the sampled transport regime. Methods for determining the rating curve used in calculations of rates, magnitudes and sediment budgets depended upon the number of samples collected and the consistency between discharge and transport rates over time. In general, the 2009 sampling effort was assumed to have sufficient data to produce accurate empirical rating curves.

Sediment Budget:
Simply calculating the reservoir sediment budget using the downstream sediment sampling location does not account for all the sediment out of the reservoir. The downstream sample site has roughly 4 km of channel between it and the reservoir. This includes a large scour hole that was present just downstream of the dam structure, a sink for reservoir sediments (Envirocon, 2004). To account for the storage of reservoir sediment between the dam and the downstream sample site the volume of sediment required to fill the scour hole needs to be accounted for. Based upon photographs and observations it is assumed that the scour hole located just downstream of the spillway filled mostly with sediment during the 2008 spring runoff. To calculate this volume of sediment, pictures and observations of the filled scour hole were used to derive an interpolated surface (assumed to be the same elevation as the channel downstream of the scour hole, at about 987 m) that was subtracted from bathymetry data collected prior to the breach. The bathymetry and interpolated surface were converted to point features in ArcGIS 9.3.1. A raster was created of each surface using the kriging function, with an output cell size of 1 meter. The raster calculator tool was used to clip the surfaces to the scour-hole dimensions and subtract one raster from the other. The resulting raster was converted to a point feature and the attribute table summary statistics tool totaled the vertical height of square meter cells that made up the volume. This quantity was added to flux of sediment out of the reservoir.

Legend

Elevation (m)

- 971.6 - 973.4
- 973.4 - 975.1
- 975.1 - 976.8
- 976.8 - 978.6
- 978.6 - 980.3
- 980.3 - 982.0
- 982.0 - 983.7
- 983.7 - 985.4
- 985.4 - 987.1

N

Meters
0   20   40   80

0 10 20   40   60   80 Meters

Upper right: Scour hole before removal
Middle: Estimated surface of fill after removal
Colors are at the same elevation scale in meters
Projection: NAD_1983_UTM_Zone_12N
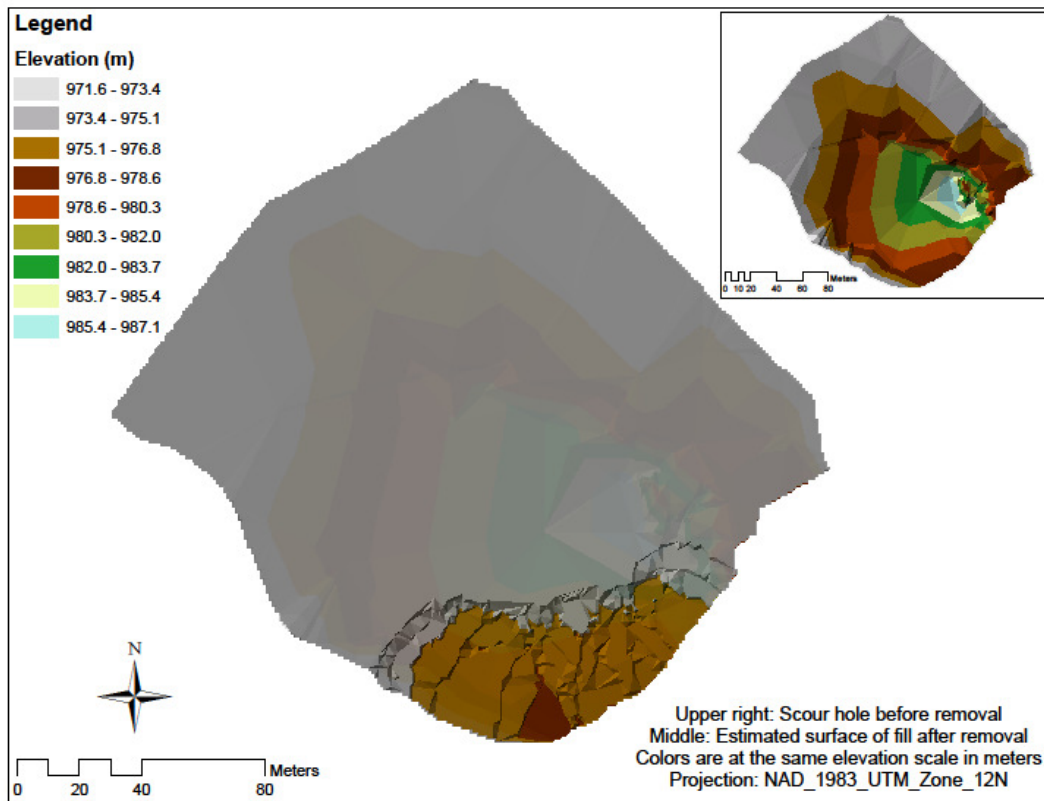
Figure A.3 Map exported from ArcGIS showing the scour hole before removal and an interpolated surface derived from observations and photos.

Results:

Bedload Samples

Table A-2 Turah bedload sampling results (All grain weights are in kg, LP = largest particle in the sample and MAPBW = most abundant particle by weight in each sample).

Turah Site Sample Dates	Duration (min)	Sampler Width (inch)	Width (meters)	Discharge (cms)	Total Bedload Transport (metric tons/day)	>128 (mm)	>90 (mm)	>64 (mm)	>45 (mm)	>32 (mm)	>22.4 (mm)	>16 (mm)	>11.2 (mm)	>8 (mm)	>5.6 (mm)	>4 (mm)	>2.8 (mm)	>2 (mm)	>1.4 (mm)	>1 (mm)	>0.7 (mm)	>0.5 (mm)	>0.35 (mm)	>0.25 (mm)	>0.125 (mm)	>0.062 (mm)	<.062 (mm)	L P (mm)	MAPBW (mm)
5/10/2008	30	6	46.6	67.5	3.0	0	0	0	0	0	0	0	0	0	0	0	0	0	0	0	0.004	0.023	0.07	0.086	0.013	0.002	0.003	0.85	0.3
5/17/2008	30	6	46.6	94.9	6.2	0	0	0	0	0	0	0	0.003	0	0.002	0.002	0.003	0.004	0.005	0.03	0.015	0.048	0.131	0.141	0.026	0.006	0.004	13.6	0.3
5/18/2008	30	6	46.6	107.6	8.6	0	0	0	0	0.179	0	0.027	0	0	0	0	0	0.002	0.002	0.009	0.013	0.046	0.126	0.148	0.027	0.004	0.004	38.5	38.5
5/26/2008	30	6	48.5	154.3	227.1	0	1.44	2.462	4.311	1.77	1.666	1.144	0.515	0.248	0.119	0.041	0.027	0.022	0.021	0.054	0.13	0.396	0.447	0.334	0.078	0.016	0.014	110	54.5
5/27/2008	30	6	48.5	150.1	359.5	0	0	4.23	3.209	4.606	2.747	3.333	1.923	1.104	0.605	0.23	0.107	0.05	0.025	0.037	0.124	0.445	0.414	0.296	0.049	0.006	0.009	83	38.5
4/18/2009	30	3	46.6	52.7	0.8	0	0	0	0	0	0	0	0	0	0	0	0	0	0	0	0	0.004	0.007	0.009	0.006	0	0	0.6	0.3
4/25/2009	30	3	46.6	131.5	77.7	0	0	0	0.143	0.456	0.796	0.619	0.299	0.08	0.008	0.004	0.007	0.01	0.008	0.012	0.015	0.035	0.062	0.057	0.033	0	0	54.5	27.2
5/16/2009	30	12	46.6	101.1	87.2	0	2.528	5.033	1.441	1.168	0.97	0.104	0.06	0.053	0.036	0.018	0.023	0.02	0.018	0.021	0.027	0.069	0.125	0.114	0.031	0.007	0.004	104	77
5/17/2009	30	12	46.6	109.3	356.0	1.756	11.929	11.237	15.079	4.81	1.826	0.456	0.127	0.114	0.1	0.087	0.099	0.093	0.074	0.058	0.054	0.123	0.207	0.177	0.053	0.009	0.006	155	54.5
5/18/2009	30	12	46.6	146.7	114.3	0	5.31	5.414	3.245	0.478	0.315	0.13	0.04	0.023	0.029	0.022	0.016	0.014	0.01	0.011	0.02	0.08	0.164	0.175	0.05	0.003	0	102	77
5/26/2009	20	12	51.8	211.8	1676.8	17.689	37.947	11.298	14.791	15.155	13.137	9.578	6.954	4.568	2.83	1.768	0.809	0.301	0.114	0.036	0.012	0.004	0	0	0	0	0	163	109
6/2/2009	5	12	51.8	191.7	2021.9	7.874	10.655	9.313	6.205	3.064	1.301	0.711	0.504	0.219	0.227	0.127	0.089	0.052	0.04	0.039	0.054	0.201	0.339	0.238	0.034	0.007	0.003	153	109
6/4/2009	5	12	49.4	160.0	2626.6	8.06	17.602	11.849	9.375	6.206	1.717	0.558	0.297	0.041	0.004	0.003	0.004	0.006	0.008	0.016	0.036	0.122	0.181	0.164	0.039	0.007	0.003	137	109
6/10/2009	10	12	49.1	122.9	84.3	0	2.972	0	0	0.306	0	0.019	0.009	0	0.007	0.007	0.012	0.016	0.014	0.016	0.022	0.051	0.074	0.084	0.023	0.003	0	112	109
6/25/2009	10	12	47.5	85.5	212.3	3.861	2.334	0.567	2.005	0.181	0.037	0.034	0.024	0.021	0.022	0.02	0.03	0.028	0.024	0.023	0.029	0.059	0.074	0.06	0.014	0.002	0	133	154
6/30/2009	10	12	46.6	57.2	1.9	0	0	0	0	0	0	0	0	0	0.002	0.002	0	0.003	0.003	0.003	0.004	0.016	0.025	0.023	0.004	0	0	6.8	0.42

Table A-3 Black bedload sampling results (All grain weights are in kg, LP = largest particle in the sample and MAPBW = most abundant particle by weight in each sample).

Black Site Sample Dates	Duration (min)	Sampler Width (inch)	Width (meters)	Discharge (cms)	Total Bedload Transport (metric tons/day)	>128 (mm)	>90 (mm)	>64 (mm)	>45 (mm)	>32 (mm)	>22.4 (mm)	>16 (mm)	>11.2 (mm)	>8 (mm)	>5.6 (mm)	>4 (mm)	>2.8 (mm)	>2 (mm)	>1.4 (mm)	>1 (mm)	>0.7 (mm)	>0.5 (mm)	>0.35 (mm)	>0.25 (mm)	>0.125 (mm)	>0.062 (mm)	<.062 (mm)	LP (mm)	MAPBW (mm)
5/17/2008	30	6	50.3	163.8	201.6	0	0	0	0	0	0	0	0	0.014	0.002	0.079	0.122	0.171	0.226	0.437	0.893	6.345	3.088	0.877	0.403	0.049	0.023	9.6	0.6
5/18/2008	30	6	50.3	197.1	64.1	0	0	0	0	0	0	0	0	0	0	0	0.004	0.023	0.035	0.082	0.19	2.639	0.51	0.4	0.126	0.026	0.01	3.4	0.6
5/26/2008	30	6	56.4	220.6	2612.5	0	0	3.29	4.054	8.894	12.967	18.609	21.112	21.582	19.112	10.469	6.287	3.742	2.235	2.4	3.154	5.111	2.722	1.021	0.254	0.044	0.043	80	9.6
5/27/2008	30	6	56.4	226.0	2334.6	0	0	0	7.139	17.349	27.199	25.661	18.511	12.225	8.215	4.103	2.613	1.503	1.143	0.933	0.717	1.336	1.385	1.034	0.281	0.053	0.051	54.5	27.2
4/25/2009	30	3	53.0	173.6	812.3	0	0	0.671	3.283	5.216	4.726	3.738	2.544	1.316	0.723	0.366	0.318	0.255	0.206	0.188	0.162	0.226	0.205	0.116	0.047	0.003	0.006	77	38.5
4/29/2009	30	3	50.0	112.4	313.4	0	0	0.454	2.257	1.506	1.704	0.947	0.742	0.621	0.425	0.253	0.192	0.144	0.127	0.122	0.113	0.144	0.111	0.056	0.024	0.006	0.006	77	54.5
5/16/2009	30	12	50.0	116.1	711.8	0	9.743	19.963	13.744	11.611	8.431	5.796	4.789	2.964	2.453	1.711	1.623	1.339	1.25	1.348	1.148	1.208	0.796	0.406	0.068	0.012	0.017	115	77
5/17/2009	20	12	50.0	121.8	425.6	0	0	5.034	9.895	10.866	5.711	1.875	0.706	0.151	0.069	0.016	0.016	0.012	0.019	0.059	0.175	0.518	0.568	0.285	0.047	0.007	0.012	79	38.5
5/19/2009	20	3	54.3	218.3	314.5	0	0	0	0.6	0.891	0.59	0.477	0.491	0.407	0.421	0.314	0.273	0.193	0.143	0.129	0.147	0.32	0.391	0.219	0.117	0.006	0.005	54.5	38.5
5/23/2009	15	12	55.5	216.4	4552.2	0	9.811	20.289	32.075	45.709	39.872	33.497	27.292	20.055	15.683	9.282	5.151	1.214	0.362	0.134	0.03	0.013	0.003	0.002	0.005	0.008	0.053	103	38.5
6/2/2009	10	12	57.3	243.1	2931.0	5.074	31.346	18.634	13.68	9.602	7.036	5.75	4.883	3.483	2.497	1.294	0.847	0.632	0.532	0.526	0.509	0.758	0.663	0.393	0.082	0.02	0.025	153	109
6/4/2009	5	12	53.9	190.2	6426.7	9.816	40.330	19.925	22.373	10.858	6.795	3.987	2.216	1.424	1.254	0.983	1.021	0.975	0.906	0.852	0.696	0.773	0.502	0.293	0.065	0.014	0.016	169	109
6/11/2009	10	12	49.7	109.9	4628.3	19.242	27.995	25.473	11.716	5.068	2.426	1.31	0.792	0.552	0.509	0.424	0.408	0.366	0.307	0.284	0.328	0.668	0.436	0.23	0.039	0.019	0	163	109
6/30/2009	10	12	45.1	68.5	10.4	0	0	0	0	0.078	0.019	0.015	0.012	0	0.001	0.004	0.005	0.005	0.008	0.02	0.047	0.122	0.104	0.041	0.005	0	0	38.5	0.6

Table A-4 Deer bedload sampling results (All grain weights are in kg, LP = largest particle in the sample and MAPBW = most abundant particle by weight in each sample).

Deer Site Sample Dates	Duration (min)	S. Width (inch)	C. Width (meters)	Discharge (cms)	Total Bedload Transport (metric tons/day)	>128 (mm)	>90 (mm)	>64 (mm)	>45 (mm)	>32 (mm)	>22.4 (mm)	>16 (mm)	>11.2 (mm)	>8 (mm)	>5.6 (mm)	>4 (mm)	>2.8 (mm)	>2 (mm)	>1.4 (mm)	>1 (mm)	>0.7 (mm)	>0.5 (mm)	>0.35 (mm)	>0.25 (mm)	>0.125 (mm)	>0.062 (mm)	<.062 (mm)	L P (mm)	MAPBW (mm)
5/9/2008	30	6	44.2	191.2	985.2	0	0	0	0	0	0.035	0.015	0.124	0.335	0.636	0.905	1.532	2.158	4.06	10.435	14.122	20.817	9.415	4.129	1.768	0.208	0.082	27.2	0.6
5/10/2008	30	6	44.2	184.6	533.6	0	0	0	0	0	0	0	0.003	0.156	0.015	0.225	0.298	0.411	1.061	2.568	4.515	16.392	8.06	3.121	1.278	0.155	0.076	13.6	0.6
5/17/2008	30	6	48.5	261.1	566.6	0	0	0	0.207	0.075	0.193	0.301	0.554	0.987	0.996	1.782	2.154	2.726	3.149	4.05	3.883	4.677	6.011	3.399	1.624	0.129	0.222	54.5	0.42
5/18/2008	30	6	48.5	312.4	166.8	0	0	0	0	0	0	0	0	0	0	0.019	0.048	0.032	0.093	0.237	0.379	2.557	4.465	1.912	1.005	0.1	0.079	4.8	0.42
5/26/2008	30	6	54.9	399.3	171.6	0	0	0	0	0.492	0.914	0.603	0.478	0.362	0.288	0.261	0.207	0.167	0.132	0.164	0.337	1.484	2.611	1.016	0.298	0.071	0.046	38.5	0.42
5/27/2008	30	6	54.9	399.3	133.8	0	0	0.263	0	0	0	0	0.143	0.047	0.081	0.063	0.064	0.056	0.084	0.141	0.348	4.636	1.257	0.384	0.087	0.025	0.066	77	0.6
3/23/2009	30	3	43.6	121.5	2.1	0	0	0	0	0	0	0	0	0	0	0	0	0	0	0	0.001	0.003	0.014	0.035	0.025	0	0	0.85	0.3
4/12/2009	30	3	43.6	157.7	9.3	0	0	0	0	0	0	0	0.003	0.001	0.004	0.003	0	0	0	0	0.005	0.043	0.13	0.098	0.047	0.002	0.003	13.6	0.3
4/18/2009	30	3	43.6	144.1	2.4	0	0	0	0	0	0	0	0	0.001	0	0	0	0	0	0.001	0.003	0.016	0.029	0.024	0.013	0	0	9.6	0.42
4/21/2009	30	3	45.4	219.5	112.3	0	0	0	0	0.173	0.216	0.345	0.206	0.152	0.107	0.06	0.06	0.053	0.076	0.15	0.318	0.912	0.718	0.275	0.103	0	0	38.5	19.2
4/22/2009	30	3	48.5	280.1	96.9	0	0	0	0	0.17	0.204	0.205	0.169	0.042	0.026	0.016	0.019	0.026	0.049	0.085	0.217	0.863	0.647	0.273	0.148	0.008	0.006	38.5	0.6
4/23/2009	30	3	48.5	334.2	41.3	0	0	0	0	0.073	0.193	0.187	0.148	0.048	0.027	0.02	0.018	0.017	0.015	0.028	0.045	0.115	0.188	0.139	0.087	0.004	0	38.5	27.2
4/25/2009	30	3	48.5	288.9	205.6	0	0	0	1.193	1.264	0.977	1.066	0.623	0.329	0.225	0.098	0.063	0.043	0.048	0.062	0.077	0.251	0.24	0.115	0.057	0.003	0.001	54.5	38.5
4/28/2009	30	3	45.4	216.1	258.9	0	0	0	0.439	0.549	1.057	1.164	1.326	1.179	0.871	0.502	0.404	0.271	0.205	0.183	0.248	0.305	0.224	0.088	0.034	0	0	54.5	13.6
5/16/2009	30	12	45.4	206.2	51.4	0	0	0	0.471	1.471	1.14	0.687	0.378	0.265	0.257	0.179	0.143	0.104	0.072	0.066	0.314	0.407	0.774	0.369	0.073	0.006	0.004	54.5	38.5
5/18/2009	30	12	45.4	266.2	667.6	0	0	0	0.912	9.352	15.361	19.828	17.178	11.121	7.071	3.096	1.871	1.023	0.672	0.59	0.75	1.585	1.522	1.037	0.305	0.038	0.038	54.5	19.2
5/22/2009	20	12	54.9	410.6	966.1	0	0	3.031	1.232	6.885	11.572	13.43	13.306	9.812	6.907	4.301	2.378	1.003	0.413	0.17	0.055	0.023	0.012	0.008	0.001	0	0.003	89	89
5/23/2009	20	12	54.9	390.8	995.1	0	0	5.003	7.351	8.214	9.827	11.265	10.125	8.117	7.207	4.803	2.554	1.167	0.613	0.327	0.135	0.051	0.014	0.007	0	0	0	87	87
6/1/2009	5	12	56.7	487.1	4924.4	0	5.550	3.753	7.227	8.827	10.483	9.599	9.337	7.302	6.299	4.296	3.547	2.798	2.312	2.349	2.269	3.004	1.751	1.014	0.162	0.027	0.022	107	107
6/4/2009	5	12	53.0	348.3	2087.7	0	0	1.185	4.125	6.221	6.506	6.063	4.57	3.281	2.511	1.773	1.459	1.116	0.783	0.607	0.386	0.343	0.307	0.311	0.084	0.013	0.017	77	27.2
6/8/2009	10	12	51.2	291.7	2935.7	1.394	3.733	11.352	9.649	10.874	12.349	14.289	14.547	11.329	8.999	5.684	4.826	3.924	3.069	2.304	1.174	0.744	0.533	0.422	0.121	0.013	0.023	135	135
6/10/2009	10	12	48.5	243.6	1211.8	0	2.551	5.746	6.872	8.345	11.803	7.587	4.211	2.033	0.94	0.401	0.223	0.223	0.226	0.202	0.185	0.29	0.488	0.455	0.118	0.014	0.015	115	115
6/13/2009	10	12	44.2	191.2	664.8	0	0	0	1.897	5.184	5.285	6.204	5.692	3.42	1.896	0.734	0.393	0.2	0.11	0.091	0.09	0.15	0.207	0.207	0.061	0.008	0.008	54.5	19.2
6/25/2009	10	12	44.2	178.7	789.9	0	0	0.395	0	1.345	2.11	5.46	6.249	4.866	3.354	2.136	1.815	1.513	1.332	1.547	1.793	2.597	0.981	0.269	0.059	0.004	0.004	77	13.6

| 6/30/2009 | 10 | 12 | 43.3 | 135.4 | 20.1 | 0 | 0 | 0 | 0 | 0.164 | 0.25 | 0.239 | 0.159 | 0.02 | 0.024 | 0 | 0 | 0 | 0 | 0 | 0.008 | 0.03 | 0.045 | 0.037 | 0.005 | 0 | 0 | 38.5 | 27.2 |

W* Calculations

Table A-5 Turah dimensionless transport calculations.

Turah Site Sample Dates	Bedload Transport (m3/s, 1650kg/m3)	Unit Bedload Flux (m2/s)	Shear WinXSPRO (N/m2)	W* all	>128 W*	>90 W*	>64 W*	>45 W*	>32 W*	>22.4 W*	>16 W*	>11.2 W*	>8 W*	>5.6 W*	>4 W*	>2.8 W*	>2 W*	sand W*
			W*i (Wilcock et al. 2009 (BAGS Primer, equation 2.31))															
			y = 2E-07x3 - 0.001x2 + 0.347x + 2.810															
5/10/2008	2.071E-05	4.441E-07	21.75	0.0022	0	0	0	0	0	0	0	0	0	0	0	0	0	0.0022
5/17/2008	4.327E-05	9.280E-07	26.90	0.0034	0	0	0	0	0	0	0	0.0000	0	0.0000	0.0000	0.0000	0.0000	0.0034
5/18/2008	6.048E-05	1.297E-06	28.82	0.0043	0	0	0	0	0.0013	0	0.0002	0	0	0	0	0	0.0000	0.0043
5/26/2008	1.593E-03	3.287E-05	33.28	0.0876	0	0.0085	0.0145	0.0254	0.0104	0.0098	0.0067	0.0030	0.0015	0.0007	0.0002	0.0002	0.0001	0.0899
5/27/2008	2.521E-03	5.203E-05	33.04	0.1402	0	0	0.0252	0.0191	0.0274	0.0164	0.0198	0.0115	0.0066	0.0036	0.0014	0.0006	0.0003	0.1402
4/18/2009	5.358E-06	1.149E-07	18.34	0.0007	0	0	0	0	0	0	0	0	0	0	0	0	0	0.00074858
4/25/2009	5.448E-04	1.168E-05	31.61	0.0337	0	0	0	0.0018	0.0058	0.0101	0.0079	0.0038	0.0010	0.0001	0.0001	0.0001	0.0001	0.0337
5/16/2009	6.117E-04	1.312E-05	27.88	0.0456	0	0.0097	0.0193	0.0055	0.0045	0.0037	0.0004	0.0002	0.0002	0.0001	0.0001	0.0001	0.0001	0.0456
5/17/2009	2.497E-03	5.355E-05	29.05	0.1750	0.0063	0.0431	0.0406	0.0544	0.0174	0.0066	0.0016	0.0005	0.0004	0.0004	0.0003	0.0004	0.0003	0.1750
5/18/2009	8.016E-04	1.719E-05	32.83	0.0468	0	0.0160	0.0163	0.0098	0.0014	0.0009	0.0004	0.0001	0.0001	0.0001	0.0001	0.0000	0.0000	0.0468
5/26/2009	1.176E-02	2.270E-04	35.34	0.5530	0.0714	0.1532	0.0456	0.0597	0.0612	0.0530	0.0387	0.0281	0.0184	0.0114	0.0071	0.0033	0.0012	0.5530
6/2/2009	1.418E-02	2.737E-04	34.99	0.6769	0.1291	0.1747	0.1527	0.1017	0.0502	0.0213	0.0117	0.0083	0.0036	0.0037	0.0021	0.0015	0.0009	0.6769
6/4/2009	1.842E-02	3.732E-04	34.55	0.9406	0.1347	0.2941	0.1980	0.1566	0.1037	0.0287	0.0093	0.0050	0.0007	0.0001	0.0001	0.0001	0.0001	0.9406
6/10/2009	5.911E-04	1.205E-05	30.72	0.0362	0	0.0296	0	0	0.0030	0	0.0002	0.0001	0	0.0001	0.0001	0.0001	0.0002	0.0362
6/25/2009	1.489E-03	3.132E-05	25.30	0.1260	0.0515	0.0311	0.0076	0.0267	0.0024	0.0005	0.0005	0.0003	0.0003	0.0003	0.0003	0.0004	0.0004	0.1260
6/30/2009	1.314E-05	2.817E-07	19.43	0.0017	0	0	0	0	0	0	0	0	0	0.0000	0.0000	0	0.0001	0.0017

Table A-6 Black dimensionless transport calculations.

Black Site Sample Dates	Bedload Transport (m3/s, 1650kg/m3)	Unit Bedload Flux (m2/s)	Shear WinXSPRO (N/m2)	W* all	>128 W*	>90 W*	>64 W*	>45 W*	>32 W*	>22.4 W*	>16 W*	>11.2 W*	>8 W*	>5.6 W*	>4 W*	>2.8 W*	>2 W*	sand W*
					W*i (Wilcock et al. 2009 (BAGS Primer, equation 2.31))														
			y = 2.969x0.476																
5/17/2008	1.414E-03	2.812E-05	33.63	0.0738	0	0	0	0	0	0	0	0	0.0001	0.0000	0.0005	0.0007	0.0010	0.0738
5/18/2008	4.494E-04	8.937E-06	36.72	0.0206	0	0	0	0	0	0	0	0	0	0	0	0.0000	0.0001	0.0206
5/26/2008	1.833E-02	3.250E-04	38.74	0.6899	0	0	0.0154	0.0190	0.0417	0.0608	0.0873	0.0990	0.1012	0.0896	0.0491	0.0295	0.0175	0.6899
5/27/2008	1.638E-02	2.904E-04	39.19	0.6060	0	0	0	0.0329	0.0800	0.1254	0.1183	0.0853	0.0564	0.0379	0.0189	0.0120	0.0069	0.6060
4/25/2009	5.698E-03	1.074E-04	34.57	0.2706	0	0	0.0075	0.0365	0.0581	0.0526	0.0416	0.0283	0.0146	0.0080	0.0041	0.0035	0.0028	0.2706
4/29/2009	2.199E-03	4.399E-05	28.11	0.1511	0	0	0.0069	0.0343	0.0229	0.0259	0.0144	0.0113	0.0094	0.0065	0.0038	0.0029	0.0022	0.1511
5/16/2009	4.993E-03	9.989E-05	28.54	0.3353	0	0.0361	0.0740	0.0510	0.0431	0.0313	0.0215	0.0178	0.0110	0.0091	0.0063	0.0060	0.0050	0.3353
5/17/2009	2.985E-03	5.972E-05	29.20	0.1938	0	0	0.0271	0.0532	0.0584	0.0307	0.0101	0.0038	0.0008	0.0004	0.0001	0.0001	0.0001	0.1938
5/19/2009	2.206E-03	4.066E-05	38.55	0.0869	0	0	0	0.0085	0.0126	0.0084	0.0068	0.0070	0.0058	0.0060	0.0045	0.0039	0.0027	0.0869
5/23/2009	3.193E-02	5.756E-04	38.38	1.2390	0	0.0467	0.0965	0.1525	0.2174	0.1896	0.1593	0.1298	0.0954	0.0746	0.0441	0.0245	0.0058	1.2390
6/2/2009	2.056E-02	3.588E-04	40.58	0.7106	0.0333	0.2057	0.1223	0.0898	0.0630	0.0462	0.0377	0.0320	0.0229	0.0164	0.0085	0.0056	0.0041	0.7106
6/4/2009	4.508E-02	8.357E-04	36.10	1.9722	0.1536	0.6309	0.3117	0.3500	0.1699	0.1063	0.0624	0.0347	0.0223	0.0196	0.0154	0.0160	0.0153	1.9722
6/11/2009	3.247E-02	6.535E-04	27.80	2.2817	0.2227	0.3239	0.2948	0.1356	0.0586	0.0281	0.0152	0.0092	0.0064	0.0059	0.0049	0.0047	0.0042	1.1409
6/30/2009	7.265E-05	1.611E-06	22.21	0.0079	0	0	0	0	0.0013	0.0003	0.0002	0.0002	0	0.0000	0.0001	0.0001	0.0001	0.0079

Table A-7 Deer dimensionless transport calculations.

Deer Site Sample Dates	Bedload Transport (m3/s, 1650kg/m3)	Unit Bedload Flux (m2/s)	Shear WinXSPRO (N/m2)	W* all	>128 W*	>90 W*	>64 W*	>45 W*	>32 W*	>22.4 W*	>16 W*	>11.2 W*	>8 W*	>5.6 W*	>4 W*	>2.8 W*	>2 W*	sand W*
			y = 8.873ln(x) - 17.54															
5/9/2008	6.911E-03	1.564E-04	29.07	0.5107	0	0	0	0	0	0.0003	0.0001	0.0009	0.0024	0.0046	0.0065	0.0111	0.0156	0.4692
5/10/2008	3.743E-03	8.470E-05	28.76	0.2810	0	0	0	0	0	0	0	0.0000	0.0011	0.0001	0.0016	0.0022	0.0030	0.2810
5/17/2008	3.974E-03	8.201E-05	31.84	0.2337	0	0	0	0.0013	0.0005	0.0012	0.0019	0.0035	0.0062	0.0063	0.0112	0.0136	0.0172	0.2337
5/18/2008	1.170E-03	2.414E-05	33.43	0.0639	0	0	0	0	0	0	0	0	0	0	0.0001	0.0003	0.0002	0.0639
5/26/2008	1.204E-03	2.194E-05	35.61	0.0529	0	0	0	0	0.0026	0.0049	0.0032	0.0025	0.0019	0.0015	0.0014	0.0011	0.0009	0.0529
5/27/2008	9.388E-04	1.711E-05	35.61	0.0412	0	0	0.0014	0	0	0	0	0.0008	0.0003	0.0004	0.0003	0.0003	0.0003	0.0412
3/23/2009	1.502E-05	3.447E-07	25.05	0.0014	0	0	0	0	0	0	0	0	0	0	0	0	0	0.0014
3/27/2009	4.430E-06	1.016E-07	19.71	0.0006	0	0	0	0	0	0	0	0	0	0	0	0	0	0.0006
4/12/2009	6.529E-05	1.498E-06	27.37	0.0054	0	0	0	0	0	0	0	0.0000	0.0000	0.0001	0.0000	0	0	0.0054
4/18/2009	1.676E-05	3.844E-07	26.57	0.0014	0	0	0	0	0	0	0	0	0.0000	0	0	0	0	0.0014
4/21/2009	7.874E-04	1.734E-05	30.30	0.0532	0	0	0	0	0.0023	0.0029	0.0047	0.0028	0.0021	0.0015	0.0008	0.0008	0.0007	0.0532
4/22/2009	6.795E-04	1.402E-05	32.46	0.0388	0	0	0	0	0.0021	0.0025	0.0025	0.0021	0.0005	0.0003	0.0002	0.0002	0.0003	0.0388
4/23/2009	2.895E-04	5.974E-06	34.03	0.0154	0	0	0	0	0.0008	0.0022	0.0021	0.0017	0.0005	0.0003	0.0002	0.0002	0.0002	0.0154
4/25/2009	1.442E-03	2.976E-05	32.73	0.0813	0	0	0	0.0144	0.0153	0.0118	0.0129	0.0075	0.0040	0.0027	0.0012	0.0008	0.0005	0.0813
4/28/2009	1.816E-03	3.999E-05	30.16	0.1236	0	0	0	0.0060	0.0075	0.0144	0.0159	0.0181	0.0161	0.0119	0.0069	0.0055	0.0037	0.1236
5/16/2009	3.602E-04	7.932E-06	29.74	0.0250	0	0	0	0.0016	0.0051	0.0040	0.0024	0.0013	0.0009	0.0009	0.0006	0.0005	0.0004	0.0250
5/18/2009	4.683E-03	1.031E-04	32.01	0.2915	0	0	0	0.0028	0.0292	0.0480	0.0619	0.0536	0.0347	0.0221	0.0097	0.0058	0.0032	0.2915

5/22/2009	6.777E-03	1.235E-04	35.86	0.2945	0	0	0.0120	0.0049	0.0272	0.0457	0.0531	0.0526	0.0388	0.0273	0.0170	0.0094	0.0040	0.2945
5/23/2009	6.980E-03	1.272E-04	35.42	0.3090	0	0	0.0201	0.0296	0.0331	0.0395	0.0453	0.0407	0.0327	0.0290	0.0193	0.0103	0.0047	0.3090
6/1/2009	3.454E-02	6.093E-04	37.37	1.3652	0	0.0824	0.0557	0.1073	0.1311	0.1557	0.1426	0.1387	0.1084	0.0935	0.0638	0.0527	0.0416	1.3652
6/4/2009	1.464E-02	2.761E-04	34.40	0.7007	0		0.0199	0.0694	0.1046	0.1094	0.1020	0.0769	0.0552	0.0422	0.0298	0.0245	0.0188	0.7007
6/8/2009	2.059E-02	4.022E-04	32.82	1.0948	0.0126	0.0337	0.1024	0.0871	0.0981	0.1114	0.1289	0.1312	0.1022	0.0812	0.0513	0.0435	0.0354	1.0948
6/10/2009	8.501E-03	1.754E-04	31.22	0.5147	0	0.0248	0.0559	0.0668	0.0812	0.1148	0.0738	0.0410	0.0198	0.0091	0.0039	0.0022	0.0022	0.5147
6/13/2009	4.663E-03	1.055E-04	29.07	0.3446	0	0	0	0.0205	0.0561	0.0572	0.0671	0.0616	0.0370	0.0205	0.0079	0.0043	0.0022	0.3446
6/25/2009	5.541E-03	1.254E-04	28.47	0.4224	0	0	0.0044	0	0.0150	0.0236	0.0610	0.0698	0.0543	0.0374	0.0238	0.0203	0.0169	0.4224

WinXSPRO Output Data:

Table A.8 Turah WinXSPRO output.

*****************************WinXSPRO*********************************														
C:\Users\james\Documents\thesis\Winxspro\turah2010wxs.out														
Input File: C:\Users\james\Documents\thesis\Winxspro\turah2010wxs.txt														
Run Date: 03/19/10														
Analysis Procedure: Hydraulics														
Cross Section Number: 3														
Survey Date: 02/22/10														
Subsections/Dividing positions														
B / 36.58/														
Resistance Method: Manning's n														
SECTION B A														
Low Stage n 0.200 0.033														
High Stage n 0.050 0.017														
Unadjusted horizontal distances used														
STAGE	#SEC	AREA	PERIM	WIDTH	R	DHYD	SLOPE	n	VAVG	Q	SHEAR			
(m)		(sq m)	(m)	(m)	(m)	(m)	(m/m)		(m/s)	(cms)	(N/sq m)	STAGE	ALPHA	FROUDE
1.49	B	26.02	25.64	25.02	1.02	1.04	0.001	0.2	0.16	4.17	9.95	1.49	2.871900	0.147288
1.49	A	18.73	22.45	22.07	0.83	0.85	0.001	0.033	0.85	15.95	8.18	1.52	2.846478	0.154457
1.49	T	44.75	48.08	47.08	0.93	0.95	0.001		0.45	20.12	9.12	1.55	2.820265	0.161778
1.52	B	26.78	25.74	25.1	1.04	1.07	0.001	0.195	0.17	4.58	10.71	1.58	2.793901	0.169296
1.52	A	19.4	22.69	22.29	0.86	0.87	0.001	0.033	0.9	17.47	8.8	1.62	2.767335	0.177026
1.52	T	46.19	48.43	47.39	0.95	0.97	0.001		0.48	22.05	9.82	1.65	2.743592	0.185122
1.55	B	27.55	25.85	25.19	1.07	1.09	0.0011	0.191	0.18	5.02	11.49	1.68	2.724049	0.193666
1.55	A	20.09	22.95	22.54	0.88	0.89	0.0011	0.032	0.95	19.09	9.44	1.71	2.704014	0.202466
1.55	T	47.64	48.8	47.74	0.98	1	0.0011		0.51	24.1	10.52	1.74	2.683426	0.211540
1.58	B	28.32	25.96	25.29	1.09	1.12	0.0011	0.186	0.19	5.49	12.3	1.77	2.662223	0.220910
1.58	A	20.78	23.21	22.79	0.9	0.91	0.0011	0.032	1	20.81	10.09	1.80	2.640331	0.230598
1.58	T	49.1	49.18	48.08	1	1.02	0.0011		0.54	26.3	11.25	1.83	2.617680	0.240627
1.62	B	29.09	26.08	25.38	1.12	1.15	0.0012	0.181	0.21	6	13.12	1.86	2.594129	0.251022
1.62	A	21.48	23.48	23.04	0.91	0.93	0.0012	0.031	1.05	22.64	10.76	1.89	2.569306	0.261795
1.62	T	50.57	49.55	48.42	1.02	1.04	0.0012		0.57	28.64	12	1.92	2.543346	0.272992
1.65	B	29.87	26.19	25.48	1.14	1.17	0.0012	0.177	0.22	6.55	13.97	1.95	2.516263	0.284654
1.65	A	22.18	23.67	23.22	0.94	0.96	0.0012	0.031	1.11	24.64	11.48	1.98	2.487943	0.296823
1.65	T	52.05	49.86	48.7	1.04	1.07	0.0012		0.6	31.19	12.79	2.01	2.458258	0.309541
1.68	B	30.65	26.3	25.57	1.17	1.2	0.0013	0.172	0.23	7.14	14.85	2.04	2.425473	0.322731
1.68	A	22.89	23.77	23.3	0.96	0.98	0.0013	0.03	1.17	26.84	12.27	2.07	2.388129	0.336342
1.68	T	53.54	50.07	48.87	1.07	1.1	0.0013		0.63	33.98	13.62	2.10	2.349059	0.350679
1.71	B	31.43	26.41	25.66	1.19	1.22	0.0013	0.167	0.25	7.78	15.74	2.13	2.307971	0.365807
1.71	A	23.6	23.87	23.37	0.99	1.01	0.0013	0.03	1.24	29.17	13.09	2.16	2.264144	0.381773
1.71	T	55.03	50.28	49.04	1.09	1.12	0.0013		0.67	36.95	14.48	2.19	2.218018	0.398728
1.74	B	32.21	26.53	25.76	1.21	1.25	0.0014	0.163	0.26	8.47	16.66	2.23	2.169339	0.416793
1.74	A	24.31	23.97	23.45	1.01	1.04	0.0014	0.029	1.3	31.66	13.92	2.26	2.117830	0.436107
1.74	T	56.52	50.49	49.21	1.12	1.15	0.0014		0.71	40.12	15.36	2.29	2.063178	0.456842
1.77	B	33	26.64	25.85	1.24	1.28	0.0014	0.158	0.28	9.21	17.61	2.32	2.026055	0.479927
1.77	A	25.03	24.06	23.52	1.04	1.06	0.0014	0.029	1.37	34.3	14.78	2.35	2.027847	0.506511
1.77	T	58.03	50.7	49.38	1.14	1.18	0.0014		0.75	43.51	16.27	2.38	2.010338	0.534624
1.8	B	33.79	26.75	25.95	1.26	1.3	0.0015	0.153	0.3	10.01	18.57	2.41	2.051141	0.569566
1.8	A	25.75	24.16	23.6	1.07	1.09	0.0015	0.028	1.44	37.1	15.67	2.44	1.995372	0.601532
1.8	T	59.53	50.91	49.55	1.17	1.2	0.0015		0.79	47.12	17.19	2.47	1.924775	0.636612
1.83	B	34.58	26.86	26.04	1.29	1.33	0.0015	0.148	0.31	10.88	19.56			

1.83	A	26.47	24.26	23.68	1.09	1.12	0.0015	0.028	1.51	40.08	16.58
1.83	T	61.05	51.12	49.72	1.19	1.23	0.0015		0.83	50.96	18.14
1.86	B	35.37	26.98	26.14	1.31	1.35	0.0016	0.144	0.33	11.83	20.57
1.86	A	27.19	24.36	23.75	1.12	1.14	0.0016	0.027	1.59	43.24	17.51
1.86	T	62.56	51.33	49.89	1.22	1.25	0.0016		0.88	55.06	19.12
1.89	B	36.17	27.09	26.23	1.34	1.38	0.0016	0.139	0.36	12.85	21.6
1.89	A	27.92	24.46	23.84	1.14	1.17	0.0016	0.027	1.67	46.58	18.46
1.89	T	64.09	51.55	50.07	1.24	1.28	0.0016		0.93	59.43	20.11
1.92	B	36.97	27.2	26.33	1.36	1.4	0.0017	0.134	0.38	13.96	22.65
1.92	A	28.65	24.57	23.93	1.17	1.2	0.0017	0.026	1.75	50.12	19.43
1.92	T	65.62	51.77	50.26	1.27	1.31	0.0017		0.98	64.08	21.12
1.95	B	37.78	27.31	26.42	1.38	1.43	0.0017	0.13	0.4	15.17	23.72
1.95	A	29.38	24.68	24.02	1.19	1.22	0.0017	0.026	1.83	53.88	20.42
1.95	T	67.15	52	50.44	1.29	1.33	0.0017		1.03	69.05	22.15
1.98	B	38.58	27.43	26.51	1.41	1.46	0.0018	0.125	0.43	16.49	24.82
1.98	A	30.11	24.79	24.11	1.21	1.25	0.0018	0.025	1.92	57.87	21.43
1.98	T	68.69	52.22	50.63	1.32	1.36	0.0018		1.08	74.36	23.21
2.01	B	39.39	27.54	26.61	1.43	1.48	0.0018	0.12	0.46	17.93	25.94
2.01	A	30.85	24.9	24.2	1.24	1.27	0.0018	0.025	2.01	62.1	22.46
2.01	T	70.24	52.44	50.81	1.34	1.38	0.0018		1.14	80.03	24.29
2.04	B	40.2	27.65	26.7	1.45	1.51	0.0019	0.116	0.49	19.51	27.08
2.04	A	31.59	25.05	24.33	1.26	1.3	0.0019	0.024	2.11	66.52	23.48
2.04	T	71.79	52.7	51.04	1.36	1.41	0.0019		1.2	86.03	25.37
2.07	B	41.02	27.76	26.8	1.48	1.53	0.0019	0.111	0.52	21.24	28.24
2.07	A	32.33	25.27	24.54	1.28	1.32	0.0019	0.024	2.2	71.08	24.45
2.07	T	73.35	53.03	51.34	1.38	1.43	0.0019		1.26	92.33	26.44
2.1	B	41.84	27.88	26.89	1.5	1.56	0.002	0.106	0.55	23.15	29.42
2.1	A	33.08	25.49	24.75	1.3	1.34	0.002	0.023	2.29	75.93	25.44
2.1	T	74.92	53.37	51.64	1.4	1.45	0.002		1.32	99.08	27.52
2.13	B	42.66	27.99	26.99	1.52	1.58	0.002	0.102	0.59	25.26	30.63
2.13	A	33.84	25.72	24.96	1.32	1.36	0.002	0.023	2.4	81.06	26.44
2.13	T	76.5	53.7	51.95	1.42	1.47	0.002		1.39	106.32	28.62
2.16	B	43.48	28.1	27.08	1.55	1.61	0.0021	0.097	0.63	27.6	31.85
2.16	A	34.6	25.96	25.19	1.33	1.37	0.0021	0.022	2.5	86.48	27.44
2.16	T	78.09	54.06	52.27	1.44	1.49	0.0021		1.46	114.08	29.74
2.19	B	44.31	28.21	27.18	1.57	1.63	0.0021	0.092	0.68	30.2	33.1
2.19	A	35.37	26.2	25.42	1.35	1.39	0.0021	0.022	2.61	92.24	28.46
2.19	T	79.68	54.41	52.6	1.46	1.52	0.0021		1.54	122.44	30.87
2.23	B	45.14	28.33	27.27	1.59	1.66	0.0022	0.088	0.73	33.11	34.37
2.23	A	36.15	26.44	25.65	1.37	1.41	0.0022	0.021	2.72	98.37	29.49
2.23	T	81.29	54.76	52.92	1.48	1.54	0.0022		1.62	131.48	32.01
2.26	B	45.97	28.44	27.36	1.62	1.68	0.0022	0.083	0.79	36.38	35.65
2.26	A	36.94	26.68	25.88	1.38	1.43	0.0022	0.021	2.84	104.89	30.54
2.26	T	82.91	55.11	53.25	1.5	1.56	0.0022		1.7	141.27	33.18
2.29	B	46.81	28.55	27.46	1.64	1.7	0.0023	0.078	0.86	40.07	36.96
2.29	A	37.73	26.92	26.11	1.4	1.44	0.0023	0.02	2.96	111.83	31.6
2.29	T	84.54	55.47	53.57	1.52	1.58	0.0023		1.8	151.9	34.36
2.32	B	47.65	29.38	28.27	1.62	1.69	0.0023	0.073	0.91	43.55	37.36
2.32	A	38.53	27.23	26.42	1.41	1.46	0.0023	0.02	3.09	119.02	32.59
2.32	T	86.18	56.61	54.69	1.52	1.58	0.0023		1.89	162.56	35.07
2.35	B	48.55	31.8	30.67	1.53	1.58	0.0024	0.069	0.95	46	35.91
2.35	A	39.34	27.68	26.86	1.42	1.46	0.0024	0.019	3.21	126.28	33.44

2.35	T	87.89	59.48	57.53	1.48	1.53	0.0024		1.96	172.28	34.76
2.38	B	49.52	33.94	32.79	1.46	1.51	0.0024	0.064	1	49.36	35.03
2.38	A	40.17	28.13	27.3	1.43	1.47	0.0024	0.019	3.34	134.04	34.29
2.38	T	89.68	62.07	60.09	1.44	1.49	0.0024		2.04	183.4	34.7
2.41	B	50.58	38.78	37.61	1.3	1.34	0.0025	0.059	1.01	50.99	31.96
2.41	A	41.01	28.58	27.74	1.43	1.48	0.0025	0.018	3.47	142.35	35.16
2.41	T	91.58	67.37	65.35	1.36	1.4	0.0025		2.11	193.34	33.32
2.44	B	51.75	40.41	39.21	1.28	1.32	0.0025	0.055	1.09	56.51	32.01
2.44	A	41.86	29.03	28.18	1.44	1.49	0.0025	0.018	3.61	151.25	36.04
2.44	T	93.61	69.44	67.4	1.35	1.39	0.0025		2.22	207.76	33.69
2.47	B	52.96	41.85	40.63	1.27	1.3	0.0026	0.05	1.2	63.39	32.26
2.47	A	42.72	29.48	28.63	1.45	1.49	0.0026	0.017	3.76	160.8	36.93
2.47	T	95.69	71.33	69.26	1.34	1.38	0.0026		2.34	224.18	34.19

Table A.9 Black WinXSPRO output.

****************************WinXSPRO*********************************													
C:\Users\james\Documents\thesis\Winxspro\black2010wxs.out													
Input File: C:\Users\james\Documents\thesis\Winxspro\black2010wxs.txt													
Run Date: 03/19/10													
Analysis Procedure: Hydraulics													
Cross Section Number: 2													
Survey Date: 02/18/10													
Subsections/Dividing positions													
Resistance Method: Manning's n													
SECTION A													
Low Stage n 0.031													
High Stage n 0.027													
Unadjusted horizontal distances used													
STAGE	AREA	PERIM	WIDTH	R	DHYD	SLOPE	n	VAVG	Q	SHEAR			
(m)	(sq m)	(m)	(m)	(m)	(m)	(m/m)		(m/s)	(cms)	(N/sq m)	STAGE	ALPHA	FROUDE
0.91	12.93	30.38	30.09	0.43	0.43	0.0025	0.031	0.92	11.91	10.43	0.91	1.000000	0.448836
0.94	13.86	31.35	31.05	0.44	0.45	0.0025	0.031	0.95	13.12	10.83	0.94	1.000000	0.452653
0.98	14.82	32.31	32	0.46	0.46	0.0025	0.031	0.97	14.41	11.24	0.98	1.000000	0.456383
1.01	15.81	33.28	32.95	0.48	0.48	0.0025	0.031	1	15.77	11.64	1.01	1.000000	0.460034
1.04	16.83	34.73	34.39	0.48	0.49	0.0025	0.031	1.01	17.05	11.88	1.04	1.000000	0.462568
1.07	17.91	36.7	36.36	0.49	0.49	0.0025	0.03	1.02	18.27	11.96	1.07	1.000000	0.464161
1.1	19.09	41.46	41.1	0.46	0.46	0.0025	0.03	0.98	18.77	11.28	1.10	1.000000	0.460892
1.13	20.35	41.77	41.41	0.49	0.49	0.0025	0.03	1.02	20.82	11.94	1.13	1.000000	0.466211
1.16	21.61	42.09	41.71	0.51	0.52	0.0025	0.03	1.06	22.96	12.59	1.16	1.000000	0.471332
1.19	22.89	42.4	42.02	0.54	0.54	0.0025	0.03	1.1	25.19	13.23	1.19	1.000000	0.476275
1.22	24.18	42.72	42.33	0.57	0.57	0.0025	0.03	1.14	27.52	13.87	1.22	1.000000	0.481059
1.25	25.47	43.03	42.63	0.59	0.6	0.0025	0.03	1.18	29.94	14.51	1.25	1.000000	0.485698
1.28	26.78	43.34	42.94	0.62	0.62	0.0025	0.03	1.21	32.45	15.14	1.28	1.000000	0.490206
1.31	28.09	43.66	43.24	0.64	0.65	0.0025	0.03	1.25	35.06	15.77	1.31	1.000000	0.494594
1.34	29.41	43.97	43.55	0.67	0.68	0.0025	0.03	1.28	37.75	16.39	1.34	1.000000	0.498874
1.37	30.74	44.29	43.85	0.69	0.7	0.0025	0.03	1.32	40.54	17.01	1.37	1.000000	0.503053
1.4	32.08	44.6	44.16	0.72	0.73	0.0025	0.03	1.35	43.42	17.63	1.40	1.000000	0.507140
1.43	33.44	44.91	44.47	0.74	0.75	0.0025	0.03	1.39	46.4	18.24	1.43	1.000000	0.511142
1.46	34.8	45.23	44.77	0.77	0.78	0.0025	0.03	1.42	49.47	18.85	1.46	1.000000	0.515066
1.49	36.16	45.54	45.08	0.79	0.8	0.0025	0.03	1.46	52.63	19.46	1.49	1.000000	0.518917
1.52	37.54	45.93	45.46	0.82	0.83	0.0025	0.029	1.49	55.83	20.03	1.52	1.000000	0.522589
1.55	38.94	46.31	45.84	0.84	0.85	0.0025	0.029	1.52	59.12	20.6	1.55	1.000000	0.526204
1.58	40.34	46.7	46.22	0.86	0.87	0.0025	0.029	1.55	62.51	21.17	1.58	1.000000	0.529766
1.62	41.75	47.08	46.6	0.89	0.9	0.0025	0.029	1.58	65.99	21.73	1.62	1.000000	0.533277
1.65	43.18	47.47	46.98	0.91	0.92	0.0025	0.029	1.61	69.57	22.29	1.65	1.000000	0.536742
1.68	44.62	47.86	47.36	0.93	0.94	0.0025	0.029	1.64	73.24	22.85	1.68	1.000000	0.540163
1.71	46.07	48.21	47.71	0.96	0.97	0.0025	0.029	1.67	77.04	23.41	1.71	1.000000	0.543591
1.74	47.52	48.54	48.03	0.98	0.99	0.0025	0.029	1.7	80.96	23.99	1.74	1.000000	0.547033
1.77	48.99	48.87	48.36	1	1.01	0.0025	0.029	1.73	84.99	24.57	1.77	1.000000	0.550435
1.8	50.47	49.2	48.68	1.03	1.04	0.0025	0.029	1.77	89.11	25.14	1.80	1.000000	0.553800
1.83	51.96	49.48	48.95	1.05	1.06	0.0025	0.029	1.8	93.39	25.74	1.83	1.000000	0.557206
1.86	53.46	49.75	49.22	1.07	1.09	0.0025	0.029	1.83	97.78	26.33	1.86	1.000000	0.560588
1.89	54.96	50.02	49.48	1.1	1.11	0.0025	0.029	1.86	102.27	26.92	1.89	1.000000	0.563936
1.92	56.47	50.3	49.75	1.12	1.14	0.0025	0.029	1.89	106.86	27.51	1.92	1.000000	0.567253
1.95	57.99	50.57	50.01	1.15	1.16	0.0025	0.029	1.92	111.55	28.1	1.95	1.000000	0.570541
1.98	59.52	50.84	50.28	1.17	1.18	0.0025	0.028	1.95	116.35	28.69	1.98	1.000000	0.573801

2.01	61.06	51.12	50.55	1.19	1.21	0.0025	0.028	1.99	121.24	29.27	2.01	1.000000	0.577035
2.04	62.6	51.39	50.81	1.22	1.23	0.0025	0.028	2.02	126.24	29.85	2.04	1.000000	0.580245
2.07	64.16	51.66	51.08	1.24	1.26	0.0025	0.028	2.05	131.34	30.43	2.07	1.000000	0.583433
2.1	65.72	51.94	51.34	1.27	1.28	0.0025	0.028	2.08	136.55	31.01	2.10	1.000000	0.586598
2.13	67.29	52.2	51.6	1.29	1.3	0.0025	0.028	2.11	141.87	31.59	2.13	1.000000	0.589757
2.16	68.86	52.46	51.85	1.31	1.33	0.0025	0.028	2.14	147.31	32.17	2.16	1.000000	0.592906
2.19	70.45	52.72	52.11	1.34	1.35	0.0025	0.028	2.17	152.86	32.74	2.19	1.000000	0.596036
2.23	72.04	52.98	52.36	1.36	1.38	0.0025	0.028	2.2	158.51	33.32	2.23	1.000000	0.599149
2.26	73.64	53.24	52.61	1.38	1.4	0.0025	0.028	2.23	164.27	33.89	2.26	1.000000	0.602246
2.29	75.25	53.5	52.86	1.41	1.42	0.0025	0.028	2.26	170.14	34.46	2.29	1.000000	0.605327
2.32	76.86	53.76	53.12	1.43	1.45	0.0025	0.028	2.29	176.12	35.03	2.32	1.000000	0.608394
2.35	78.48	54.02	53.37	1.45	1.47	0.0025	0.028	2.32	182.2	35.6	2.35	1.000000	0.611448
2.38	80.11	54.29	53.62	1.48	1.49	0.0025	0.028	2.35	188.4	36.17	2.38	1.000000	0.614489
2.41	81.75	54.55	53.87	1.5	1.52	0.0025	0.028	2.38	194.71	36.73	2.41	1.000000	0.617518
2.44	83.4	54.81	54.12	1.52	1.54	0.0025	0.028	2.41	201.13	37.29	2.44	1.000000	0.620537
2.47	85.05	55.07	54.38	1.54	1.56	0.0025	0.027	2.44	207.66	37.85	2.47	1.000000	0.623545
2.5	86.71	55.33	54.63	1.57	1.59	0.0025	0.027	2.47	214.31	38.41	2.50	1.000000	0.626544
2.53	88.38	55.59	54.88	1.59	1.61	0.0025	0.027	2.5	221.07	38.96	2.53	1.000000	0.629534
2.56	90.06	55.85	55.13	1.61	1.63	0.0025	0.027	2.53	227.94	39.52	2.56	1.000000	0.632516
2.59	91.74	56.11	55.39	1.64	1.66	0.0025	0.027	2.56	234.93	40.07	2.59	1.000000	0.635490
2.62	93.43	56.37	55.64	1.66	1.68	0.0025	0.027	2.59	242.03	40.62	2.62	1.000000	0.638458
2.65	95.13	56.63	55.89	1.68	1.7	0.0025	0.027	2.62	249.26	41.17	2.65	1.000000	0.641420
2.68	96.84	56.89	56.14	1.7	1.72	0.0025	0.027	2.65	256.6	41.72	2.68	1.000000	0.644375
2.71	98.56	57.15	56.4	1.72	1.75	0.0025	0.027	2.68	264.06	42.26	2.71	1.000000	0.647326
2.74	100.28	57.38	56.61	1.75	1.77	0.0025	0.027	2.71	271.73	42.83	2.74	1.000000	0.650305

Table A.10 Deer WinXSPRO output.

*******************************WinXSPRO**********************************													
C:\Users\james\Documents\thesis\Winxspro\deer2010wxs.out													
Input File: C:\Users\james\Documents\thesis\Winxspro\deer2010wxs.txt													
Run Date: 03/19/10													
Analysis Procedure: Hydraulics													
Cross Section Number: 2													
Survey Date: 02/18/10													
Subsections/Dividing positions													
Resistance Method: Manning's n													
SECTION A													
Low Stage n 0.143													
High Stage n 0.033													
Unadjusted horizontal distances used													
STAGE	AREA	PERIM	WIDTH	R	DHYD	SLOPE	n	VAVG	Q	SHEAR			
(m)	(sq m)	(m)	(m)	(m)	(m)	(m/m)		(m/s)	(cms)	(N/sq m)	STAGE	ALPHA	FROUDE
3.96	110.56	41.71	40.46	2.65	2.73	0.0005	0.148	0.29	32.1	12.99	3.96	1.000000	0.056096
3.99	111.79	41.94	40.68	2.67	2.75	0.0005	0.146	0.3	33.18	13.25	3.99	1.000000	0.057182
4.02	113.04	42.18	40.91	2.68	2.76	0.0005	0.145	0.3	34.29	13.51	4.02	1.000000	0.058291
4.05	114.29	42.41	41.14	2.69	2.78	0.0005	0.143	0.31	35.44	13.77	4.05	1.000000	0.059424
4.08	115.54	42.57	41.27	2.71	2.8	0.0005	0.141	0.32	36.68	14.06	4.08	1.000000	0.060592
4.11	116.8	42.7	41.39	2.74	2.82	0.0005	0.14	0.32	37.96	14.36	4.11	1.000000	0.061788
4.15	118.07	42.85	41.52	2.76	2.84	0.0005	0.138	0.33	39.28	14.66	4.15	1.000000	0.063009
4.18	119.33	42.99	41.64	2.78	2.87	0.0006	0.136	0.34	40.64	14.97	4.18	1.000000	0.064256
4.21	120.6	43.14	41.77	2.8	2.89	0.0006	0.135	0.35	42.05	15.27	4.21	1.000000	0.065531
4.24	121.88	43.28	41.9	2.82	2.91	0.0006	0.133	0.36	43.5	15.58	4.24	1.000000	0.066836
4.27	123.16	43.43	42.03	2.84	2.93	0.0006	0.131	0.37	45	15.89	4.27	1.000000	0.068170
4.3	124.44	43.57	42.15	2.86	2.95	0.0006	0.13	0.37	46.55	16.2	4.30	1.000000	0.069536
4.33	125.73	43.72	42.28	2.88	2.97	0.0006	0.128	0.38	48.15	16.51	4.33	1.000000	0.070935
4.36	127.02	43.86	42.41	2.9	3	0.0006	0.127	0.39	49.81	16.83	4.36	1.000000	0.072368
4.39	128.31	44.01	42.54	2.92	3.02	0.0006	0.125	0.4	51.52	17.15	4.39	1.000000	0.073836
4.42	129.61	44.15	42.66	2.94	3.04	0.0006	0.123	0.41	53.29	17.47	4.42	1.000000	0.075341
4.45	130.91	44.3	42.79	2.96	3.06	0.0006	0.122	0.42	55.12	17.8	4.45	1.000000	0.076885
4.48	132.22	44.44	42.92	2.98	3.08	0.0006	0.12	0.43	57.02	18.12	4.48	1.000000	0.078468
4.51	133.53	44.59	43.05	2.99	3.1	0.0006	0.118	0.44	58.98	18.45	4.51	1.000000	0.080094
4.54	134.84	44.73	43.17	3.01	3.12	0.0006	0.117	0.45	61	18.78	4.54	1.000000	0.081763
4.57	136.16	44.88	43.3	3.03	3.14	0.0006	0.115	0.46	63.11	19.12	4.57	1.000000	0.083477
4.6	137.48	45.02	43.43	3.05	3.17	0.0007	0.113	0.47	65.28	19.46	4.60	1.000000	0.085239
4.63	138.81	45.17	43.56	3.07	3.19	0.0007	0.112	0.49	67.54	19.8	4.63	1.000000	0.087050
4.66	140.14	45.31	43.68	3.09	3.21	0.0007	0.11	0.5	69.87	20.14	4.66	1.000000	0.088913
4.69	141.47	45.46	43.81	3.11	3.23	0.0007	0.108	0.51	72.3	20.48	4.69	1.000000	0.090831
4.72	142.81	45.6	43.94	3.13	3.25	0.0007	0.107	0.52	74.81	20.83	4.72	1.000000	0.092806
4.75	144.15	45.75	44.07	3.15	3.27	0.0007	0.105	0.54	77.41	21.18	4.75	1.000000	0.094839
4.79	145.5	45.91	44.21	3.17	3.29	0.0007	0.103	0.55	80.11	21.53	4.79	1.000000	0.096933
4.82	146.85	46.06	44.34	3.19	3.31	0.0007	0.102	0.56	82.91	21.88	4.82	1.000000	0.099092
4.85	148.2	46.21	44.48	3.21	3.33	0.0007	0.1	0.58	85.81	22.23	4.85	1.000000	0.101321
4.88	149.56	46.37	44.62	3.23	3.35	0.0007	0.099	0.59	88.84	22.58	4.88	1.000000	0.103621
4.91	150.92	46.52	44.75	3.24	3.37	0.0007	0.097	0.61	91.98	22.94	4.91	1.000000	0.105998
4.94	152.28	46.67	44.89	3.26	3.39	0.0007	0.095	0.63	95.24	23.3	4.94	1.000000	0.108454
4.97	153.65	46.83	45.02	3.28	3.41	0.0007	0.094	0.64	98.65	23.66	4.97	1.000000	0.110995
5	155.03	46.98	45.16	3.3	3.43	0.0007	0.092	0.66	102.19	24.03	5.00	1.000000	0.113624
5.03	156.41	47.13	45.3	3.32	3.45	0.0008	0.09	0.68	105.87	24.4	5.03	1.000000	0.116347

5.06	157.79	47.29	45.43	3.34	3.47	0.0008	0.089	0.7	109.72	24.77	5.06	1.000000	0.119168
5.09	159.18	47.44	45.57	3.36	3.49	0.0008	0.087	0.71	113.73	25.14	5.09	1.000000	0.122094
5.12	160.57	47.59	45.7	3.37	3.51	0.0008	0.085	0.73	117.91	25.51	5.12	1.000000	0.125131
5.15	161.96	47.75	45.84	3.39	3.53	0.0008	0.084	0.75	122.28	25.89	5.15	1.000000	0.128285
5.18	163.36	47.9	45.98	3.41	3.55	0.0008	0.082	0.78	126.84	26.27	5.18	1.000000	0.131563
5.21	164.77	48.05	46.11	3.43	3.57	0.0008	0.08	0.8	131.62	26.65	5.21	1.000000	0.134973
5.24	166.17	48.21	46.25	3.45	3.59	0.0008	0.079	0.82	136.61	27.03	5.24	1.000000	0.138523
5.27	167.58	48.36	46.39	3.47	3.61	0.0008	0.077	0.85	141.84	27.42	5.27	1.000000	0.142222
5.3	169.03	50.21	48.23	3.37	3.51	0.0008	0.075	0.85	144.03	26.87	5.30	1.000000	0.145376
5.33	170.51	51.03	49.04	3.34	3.48	0.0008	0.074	0.87	148.46	26.91	5.33	1.000000	0.149126
5.36	172.01	51.26	49.27	3.36	3.49	0.0008	0.072	0.9	154.27	27.25	5.36	1.000000	0.153302
5.39	173.52	51.5	49.49	3.37	3.51	0.0008	0.07	0.92	160.39	27.6	5.39	1.000000	0.157670
5.43	175.03	51.73	49.72	3.38	3.52	0.0008	0.069	0.95	166.82	27.95	5.43	1.000000	0.162246
5.46	176.55	51.96	49.94	3.4	3.53	0.0009	0.067	0.98	173.6	28.31	5.46	1.000000	0.167043
5.49	178.07	52.2	50.17	3.41	3.55	0.0009	0.066	1.01	180.75	28.66	5.49	1.000000	0.172079
5.52	179.61	52.43	50.4	3.43	3.56	0.0009	0.064	1.05	188.3	29.02	5.52	1.000000	0.177373
5.55	181.15	52.67	50.62	3.44	3.58	0.0009	0.062	1.08	196.27	29.38	5.55	1.000000	0.182944
5.58	182.69	52.9	50.85	3.45	3.59	0.0009	0.061	1.12	204.72	29.74	5.58	1.000000	0.188816
5.61	184.25	53.14	51.08	3.47	3.61	0.0009	0.059	1.16	213.66	30.1	5.61	1.000000	0.195013
5.64	185.81	53.37	51.3	3.48	3.62	0.0009	0.057	1.2	223.16	30.47	5.64	1.000000	0.201564
5.67	187.37	53.61	51.53	3.5	3.64	0.0009	0.056	1.24	233.25	30.84	5.67	1.000000	0.208500
5.7	188.95	53.84	51.76	3.51	3.65	0.0009	0.054	1.29	243.99	31.21	5.70	1.000000	0.215857
5.73	190.53	54.07	51.98	3.52	3.67	0.0009	0.052	1.34	255.45	31.58	5.73	1.000000	0.223674
5.76	192.12	54.31	52.21	3.54	3.68	0.0009	0.051	1.39	267.69	31.95	5.76	1.000000	0.231996
5.79	193.71	54.54	52.43	3.55	3.69	0.0009	0.049	1.45	280.8	32.33	5.79	1.000000	0.240874
5.82	195.31	54.74	52.62	3.57	3.71	0.0009	0.047	1.51	294.97	32.72	5.82	1.000000	0.250385
5.85	196.92	54.94	52.81	3.58	3.73	0.0009	0.046	1.58	310.22	33.13	5.85	1.000000	0.260579
5.88	198.53	55.14	53	3.6	3.75	0.001	0.044	1.65	326.66	33.53	5.88	1.000000	0.271530
5.91	200.15	55.31	53.16	3.62	3.76	0.001	0.042	1.72	344.51	33.95	5.91	1.000000	0.283342
5.94	201.77	55.47	53.31	3.64	3.78	0.001	0.041	1.8	363.92	34.38	5.94	1.000000	0.296111
5.97	203.4	55.63	53.46	3.66	3.8	0.001	0.039	1.89	385.01	34.81	5.97	1.000000	0.309951
6	205.03	55.79	53.61	3.67	3.82	0.001	0.038	1.99	408.01	35.25	6.00	1.000000	0.325001
6.04	206.67	55.95	53.76	3.69	3.84	0.001	0.036	2.1	433.18	35.69	6.04	1.000000	0.341429
6.07	208.31	56.11	53.9	3.71	3.86	0.001	0.034	2.21	460.83	36.13	6.07	1.000000	0.359434
6.1	209.95	56.27	54.05	3.73	3.88	0.001	0.033	2.34	491.33	36.57	6.10	1.000000	0.379248

Dimensionless Transport and Shear:

Shields number to W* graphs are presented to demonstrate the dimensionless patterns of transport above, within and downstream of the reservoir. With these calculations, the dimensionless transport to shear stress patterns within the reservoir can be tracked to the downstream sample site. Shields number calculations used 4 different particle sizes: D50 values from surface pebble counts (D50); most abundant particle by weight in the sample year (APY); most abundant particle by weight in each sample (APS); and largest particle in transport by sample (LPS) (Figures 2.15-2.17). Furthermore, D50 values are back calculated by setting τ* to .035 (a theoretical threshold for sediment mobility) and the resulting grain dimensions are reported in the text.

Shields number (τ*) calculations for the Turah site represent non-reservoir influenced results. The APS for the 2009 sample data were larger than expected, resulting in low τ* values. These

low τ* values correlate with local channel geometry adjustments where 4-5 m of bank scour was recorded. For this reason the APY value from the 2008 data set was used for both years. If the APS samples are omitted from the results in 2009, when W* is greater than about .003, the τ* values at the Turah site ranged between .02 and .05 for all the grain sizes tested. If the D50 of the bed material is back calculated to a τ* value, it produces values that cover the range of .025 to .035 (Figure 2.10). These results indicate that the bed material at the Turah site has a strong correlation to the grain size of sediments in transport.

.

Figure A.4 Turah dimensionless transport rate W*of 2008-2009 bedload samples graphed against calculated Shields number values of characteristic bedload and bed material grain sizes.

Calculations of Shields number at the Black site are highly variable between 2008 and 2009. In 2008, the APY at the Black site had a τ* of >.1 and the LPS of the first two samples of the year (W*= between .1 and .01) had τ* of .75 and .25 respectively (all these values are much higher than the τ* predicted at Turah). The LPS of the remaining two samples (W*= >.1) had τ* values within the range of .03 to .05. The 2008 D50 of the bed surface was initially sand leading to τ* values ranging between 4 and 5 (Figure 2.11.A). Setting the τ* equal to .035, for all the 2008 discharges sampled, results in a D50 grain size of 60 to 70 mm. In 2009, the Black site had τ* values mostly less than .03 for the LPS and APY, while the D50 of the bed material ranged between .03 and .05 (Figure 2.11.B), illustrating that particles larger than the predicted and calculated D50 of the bed material are making up the majority of the particle weight in transport.

Shields number calculations at the Deer site showed the most variability of all three sites. In 2008 the APY and APS had τ* ranging between 3.55 and 4.4 while the largest particle in transport of each sample sporadically ranged between .043 and .516. The D50 of the bed material had τ* ranging between .02 and .025 (Figure 2.12.A), indicating an immobile channel D50 for the range of 2008 discharges. The 2009 APY at the Deer site had τ* ranging between

.064 and .12 while the LPS had a wide range of values between 3.48 and .027 (Figure 2.12.B). The 2009 τ* D50 ranged between .014 and .026 (illustrating the armored state of the channel bed material) while the APS had the largest range, between about .005 and 6 (Figure 2.11). Through 2008 and 2009, the Deer site had similar τ* values and patterns as the 2008 Black calculations (compare Figure 2.11.A with 2.12.B). The only difference between the Black 08 and Deer 09 pattern, besides the D50 τ* values, is that the Black site completed the pattern in one year while the Deer site completed it in two years.

Figure A.5 Black dimensionless transport rate W* of bedload samples graphed against calculated Shields number values of characteristic bedload and bed material grain sizes. (A) 2008 bedload samples. (B) 2009 bedload samples.
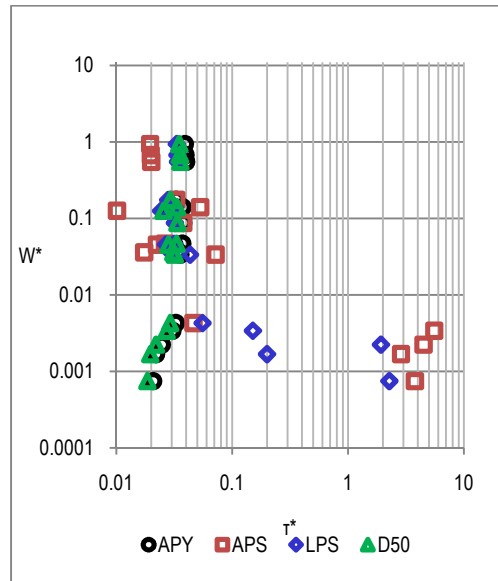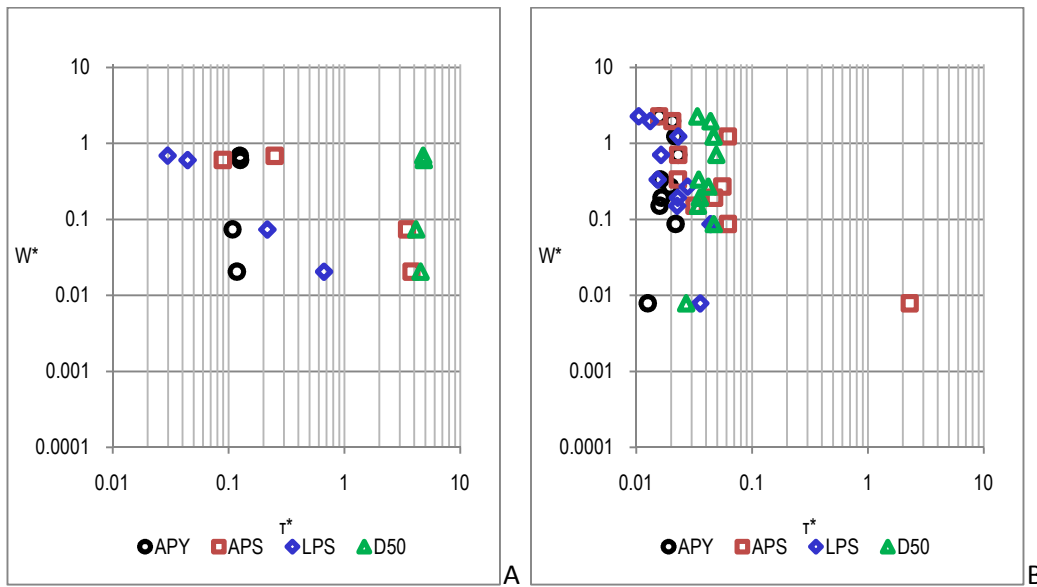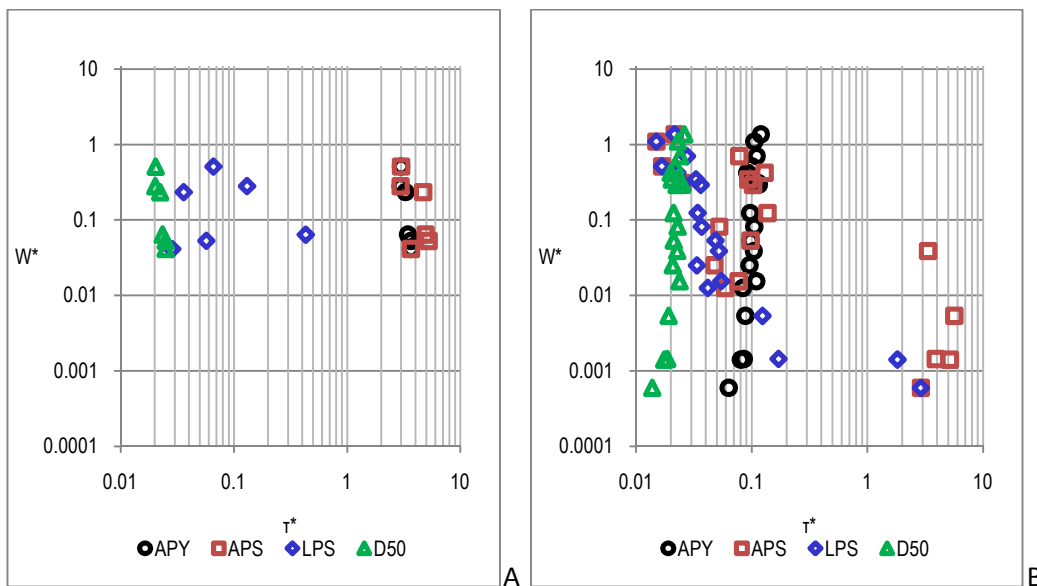

Figure A.6 Deer dimensionless transport rate W* of bedload samples graphed against calculated Shields number values of characteristic bedload and bed material grain sizes. (A) 2008 bedload samples. (B) 2009 bedload samples.

Calibrated and Uncalibrated Rating Curves:

Calibrated and uncalibrated rating curves, developed using BAGS software, are shown in Figures 2.13.A-F. Calibrated and uncalibrated rating curves fell well within the Turah bedload data collected in 2008 and 2009 (Figure 2.13.A-B). The Bakke, Parker and Wilcock and Crowe formulas predicted 106%, 80% and 70% of the flux based upon field sampling while the Wilcock formula predicted 38% of the sample flux; possibly a result of the complex channel geometry. This accuracy is attributed to the underlying assumptions of both the calibrated and uncalibrated formulas being met; sediment in transport is related to the bed material, the dimensionless thresholds of transport assumed by the formulas are met and grain sizes in transport are directly related to the hydraulic forces acting in the channel.

Before the dam removal the Black site surface and subsurface grain size distributions were more representative of a sand bedded river. No formulas of sand bedded bedload transport were used in this project. The calibrated formulas (Bakke = 160-170% and Wilcock = 117-122% sample flux) applied to the 2009 bedload data at the Black site better than the uncalibrated models (Figure 2.13.C-D). This is reflective of the elevated rates of transport within the reservoir, elevated above the current predictive methods and assumptions. The 2009 uncalibrated Black results (Parker = 13% and Wilcock and Crowe = 7% of sampled flux) were actually very similar to the empirical rating curve developed to represent the sediment transport regime entering the reservoir.

The various Deer calibrated and uncalibrated 2008 results represent sediment in transport being very different than the bed material. Uncalibrated formulas predicted between .001% and .05% of the sampled flux in 2008 and 2009. The interpretation of this result suggests that the Deer channel bed material was largely immobile throughout the two year hydrograph (Figure 2.13.E-D). Calibrated rating curves developed from all the 2008 sample data did not predict the sampled transport rates or the caliber of sediment in transport. This is due to the temporal variation in the supply of sediment and the changing process of transport (Figure 2.13.E). For instance, the Bakke formula predicted grave and cobble would transport at rates 714% of the sampled transport rates. To best represent the sample data in 2008, the transport of sand as bedload needed to take into account the strong pattern of hysteresis with a transition between rising and falling limbs. To accomplish this a second set of calibrated rating curves were applied to the 2008 Deer bedload data, treating the two high transport samples (purple dotted line) and the three lower transport samples (pink dotted line) as separate data sets (Figure 2.13.E). The resulting sand fraction of the Wilcock 01 rating curves predicted a plausible rising and falling limb of the bedload transport hysteresis with the sample data used for the transition between the two calibrated rating curves (Figure 2.13.E).

Only the calibrated models were able to repeat the Deer bedload transport regime in 2009 accurately (Figure 2.13.F). The Bakke calibrated result was 150% of the sampled transport while the Wilcock calibration was 120%. Added accuracy would have been obtained if, once again, separate rating curves were developed for the rising and falling limbs of the hydrograph because of the hysteresis pattern in the 2009 sampling results.
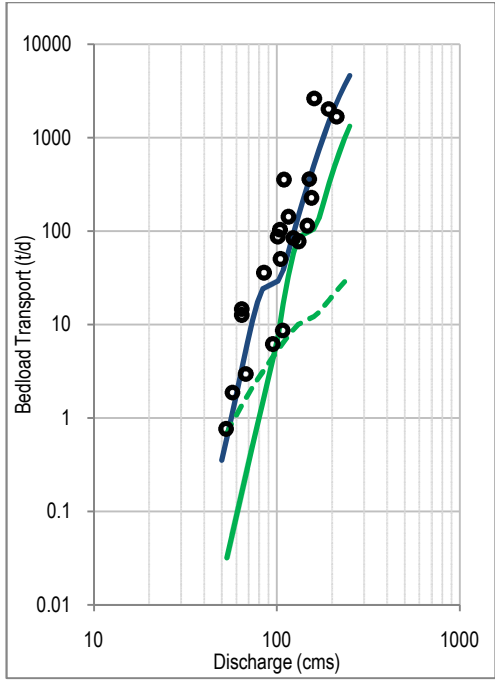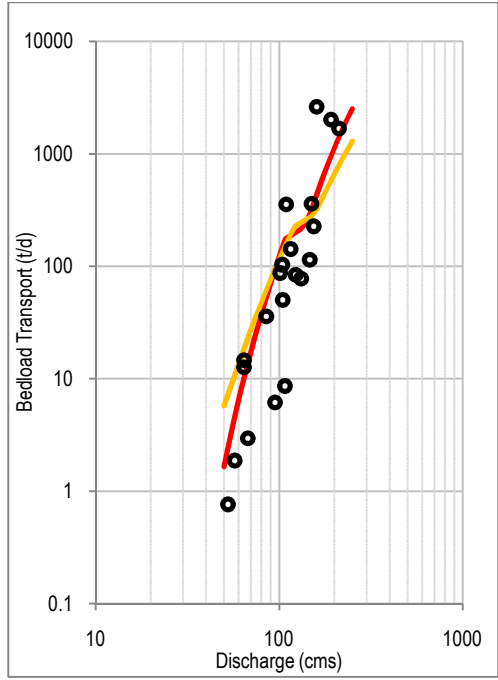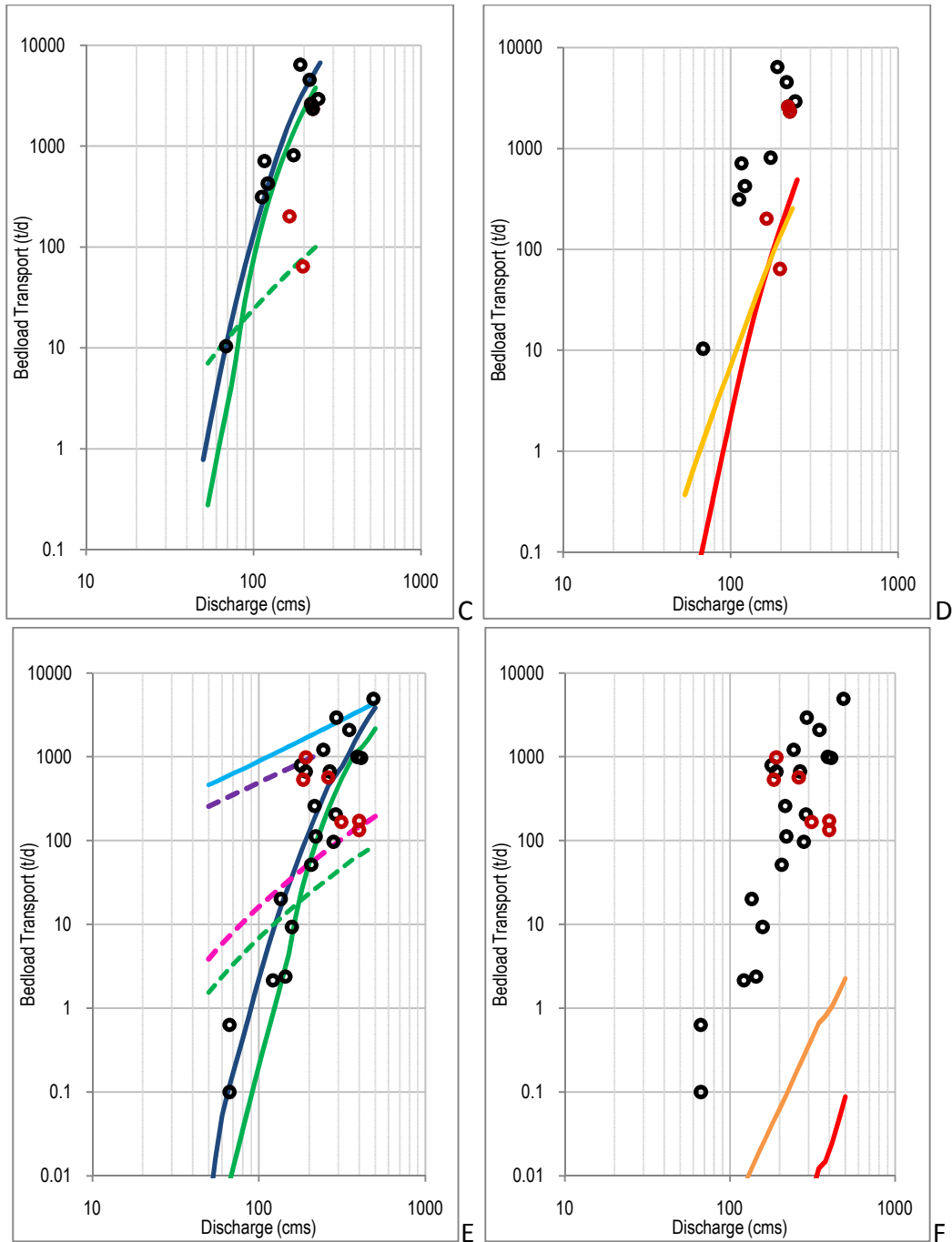
Figure A.7 Calibrated and uncalibrated rating curves presented with 2008 (red circles) and 2009 (black circles) bedload sample results. Rating curves were developed using BAGS software. Uncalibrated rating curves: Parker (red line) and Wilcock and Crowe (orange line). Calibrated rating curves: Bakke (light and dark blue lines) and Wilcock (green line and green, pink and purple dashed lines). (A) Turah calibrated rating curves. (B) Turah uncalibrated rating curves. (C) Black calibrated rating curves. (D) Black uncalibrated rating curves. (E) Deer calibrated rating curves where the light blue line is the 2008 Bakke estimate; the purple dotted line is the Wilcock sand fraction calibrated with the 2008 high transport sample and the pink dotted line Wilcock sand fraction calibrated to the 2008 three lower transport samples. (F) Deer uncalibrated rating curves.

78

Discussion:

Calibrated and Uncalibrated Rating Curves:

Rating curves of bedload sediment transport calculated using the BAGS user interface showed varying results. While calibrated rating curves generally represented the rates of transport with accuracy, the resulting grain size fractional transport rates were usually incorrect. This is the result of the formulas being dependent upon the grain size distribution of the bed material to determine the sediment supply. The unique channel conditions that dams create do not allow the accurate application of the formulas used to develop rating curves in this study. Overall, the rates of transport calculated with the Wilcock 2001 formula was used to calculate parts of the sediment budget and refine the transport to discharge relationship. Discrepancies between the sediment in transport and the surface and subsurface grain size distributions resulted in inaccurate uncalibrated rating curves, within and downstream of the reservoir. Difficulties in accurately applying the uncalibrated rating curves to the sample data within and downstream of the dam illustrates the differences between normal sediment transport and transport regimes with a dynamic sediment supply.

References:

Church, M., 2002, Geomorphic thresholds in riverine landscapes: Freshwater Biology, v. 47, p. 541–557.

Einstein, H. A., 1950, The bedload function for sediment transport in open channel flows, *in* S. C. S. U.S. Department of Agriculture, ed., Washington, D.C.

Envirocon, 2004, Milltown Reservoir Dry Removal Scour Evaluation – Addendum 1, Proposed Plan Updated Scour Evaluation, Prepared by Envirocon, Inc. and EMC2 for the Atlantic Richfield Company, p. 121, 3 Appendixes.

Parker, G., and P. C. Klingeman, 1982, On why gravel bed streams are paved: Water Resources Research, v. 18, p. 1409–1423.

Shields, A., 1936, Anwendung der Aehnlichkeitsmechanik und der Turbulenzforschung auf die Geschiebebewegung, *in* U. S. D. o. A. English title: Application of similarity principles and turbulence research to bed-load movement [translated by W.P. Ott and J.C. van Uchelen, Soil Conservation Service Cooperative Laboratory, California Institute of Technology, Pasadena, 1936], ed., p. 36.

Wilcock, P. R., 1988, Methods for estimating the critical shear stress of individual fractions in mixed-size sediment: Water Resources Research, v. 24, p. 1127–1135.

Wilcock, P. R., J. Pitlick, and Y. Cui, 2009, Sediment transport primer: estimating bed-material transport in gravel-bed rivers, *in* F. S. United States Department of Agriculture, Rocky Mountain Research Station, ed., Fort Collins, CO, p. 64.

Appendix B: Dam Removal Sediment Transport Modeling
Methods:
DREAM-1 Input Data:

Table B.1 Blackfoot Arm of reservoir Run 1 DREAM-1 input.

Channel Geometry (negative values within the reservoir, zero and positive downstream)				
X (km)	Width (m)	Base (m)	Thick (m)	Flow Index
-4.15	34.88	994.73	0.00	1
-3.39	45.48	993.60	1.10	1
-2.77	67.55	993.60	0.76	1
-2.43	60.07	992.23	1.25	1
-2.27	38.17	989.14	1.46	1
-2.09	25.50	987.90	0.09	1
-1.90	52.14	989.69	0.09	1
-1.77	62.00	989.45	0.91	1
-1.63	59.24	989.88	0.76	1
-1.46	57.82	988.51	2.07	1
-1.27	57.62	988.11	1.83	1
-1.11	61.49	989.03	2.20	1
-0.97	48.64	987.75	1.86	1
-0.82	56.88	987.81	2.07	1
-0.64	54.43	987.38	3.05	1
-0.48	60.77	986.71	2.93	1
-0.32	42.62	986.41	2.96	1
-0.24	48.48	985.95	2.77	1
-0.18	78.26	985.89	2.77	2
-0.10	86.07	985.70	2.22	2
-0.03	83.96	985.55	1.25	2
0.00	76.00	986.76	0.00	2
0.01	76.00	986.82	0.00	2
0.01	76.00	986.99	0.00	2
0.02	76.00	986.67	0.00	2
0.02	76.00	986.43	0.00	2
0.03	76.00	986.40	0.00	2
0.04	76.00	986.39	0.00	2
0.04	76.00	986.29	0.00	2
0.05	76.00	986.32	0.00	2
0.05	76.00	986.43	0.00	2
0.06	76.00	986.19	0.00	2

0.06	76.00	985.98	0.00	2
0.08	76.00	985.38	0.00	2
0.09	76.00	985.04	0.00	2
0.10	76.00	985.07	0.00	2
0.10	76.00	985.08	0.00	2
0.11	76.00	985.07	0.00	2
0.12	76.00	985.07	0.00	2
0.12	76.00	984.10	0.00	2
0.13	76.00	982.44	0.00	2
0.16	76.00	981.90	0.00	2
0.19	76.00	979.37	0.00	2
0.23	76.00	978.72	0.00	2
0.26	76.00	980.68	0.00	2
0.29	76.00	982.57	0.00	2
0.32	76.00	983.99	0.00	2
0.35	76.00	984.11	0.00	2
0.39	76.00	982.79	0.00	2
0.42	76.00	982.30	0.00	2
0.45	76.00	982.72	0.00	2
0.48	76.00	982.33	0.00	2
0.51	76.00	982.07	0.00	2
0.55	76.00	981.50	0.00	2
0.58	76.00	981.63	0.00	2
0.61	76.00	981.69	0.00	2
0.64	76.00	981.64	0.00	2
0.68	76.00	981.69	0.00	2
0.71	76.00	981.56	0.00	2
0.74	76.00	981.20	0.00	2
0.77	76.00	981.21	0.00	2
0.80	76.00	981.17	0.00	2
1.19	76.00	980.41	0.00	2
1.56	76.00	979.43	0.00	2
2.08	76.00	978.42	0.00	2
2.57	76.00	977.40	0.00	2
3.07	76.00	976.37	0.00	2
3.57	76.00	975.63	0.00	2
4.07	76.00	974.86	0.00	2
4.57	76.00	974.10	0.00	2

Bed Material	
Size (mm)	% Finer
8	0
11.3	1
16	2
22.6	8
32	23
45	44
64	60
90	79
128	95
180	100

Reservoir Sediments		
Distance (km)	Depth from Surface (m)	Fraction of wash load deposit
-4.15	0	0.13
-3.39	0	0.16
-2.38	0	0.22
-2.24	0	0.28
-2.16	0	0.33
-2.04	0	0.4
-1.87	0	0.72
-1.71	0	0.53
-1.59	0	0.73
-1.46	0	0.76
-1.32	0	0.92
-1.19	0	0.96
-1.08	0	0.97
-1.00	0	1
-0.88	0	1
-0.79	0	1
-0.68	0	0.98
-0.56	0	0.94
-0.45	0	0.96
-0.34	0	0.97
-0.24	0	0.99
-0.11	0	1
-0.06	0	0.99
-0.03	0	0.97

Sediment Supply Entering Reservoir		
Flow Index	Wash load (m3/year)	Bed Material (m3/year)
1	35000	3000
2	100000	10000

Minimal Dredging before Dam Removal

One Shot Removal

Number of weeks	Downstream Bankfull Depth
52	2.65

Discharge data from 1999 Water Year (USGS)

Table B.2 Upper Clark Fork Arm of reservoir Run 1 DREAM-1 input.

Channel Geometry (negative values within the reservoir, positive downstream)				
X (km)	Width (m)	Base (m)	Thick (m)	Flow Index
-1.8	200	994.53	0.003	1
-1.7	500	994.26	0.003	1
-1.6	600	993.99	0.003	1
-1.5	750	993.30	0.003	1
-1.4	760	993.45	0.003	1
-1.3	760	993.19	0.003	1
-1.2	840	992.93	0.003	1
-1.1	1040	992.67	0.003	1
-1	1124	992.43	0.003	1
-0.9	1162	992.24	0.003	1
-0.8	1140	992.53	0.003	1
-0.7	1134	992.54	0.003	1
-0.6	1076	992.37	0.003	1
-0.5	1000	992.68	0.003	1
-0.4	913	992.34	0.003	1
-0.3	730	992.66	0.003	1
-0.2	600	992.73	0.003	1
-0.1	573	992.70	0.003	1
0.1	40	988.97	0	1
0.2	40	988.60	0	1
0.3	40	988.24	0	1
0.4	40	987.87	0	1
0.5	40	987.50	0	1
0.6	40	987.14	0	1
0.7	40	986.77	0	1
0.8	40	986.41	0	1
0.9	40	986.04	0	1
1	40	985.68	0	1
1.1	40	985.31	0	1
1.2	40	985.07	0	1
1.3	40	984.66	0	1
1.4	40	984.31	0	1
1.5	40	983.96	0	1
1.6	40	983.61	0	1
1.7	40	983.27	0	1

1.8	40	982.92	0	1
1.9	40	982.57	0	1
2	40	982.22	0	1
2.1	40	981.87	0	1
2.2	40	981.52	0	1
2.3	40	981.18	0	1
2.4	40	980.83	0	1
2.5	40	980.48	0	1

Bed Material	
Size (mm)	% Finer
0.02	0
28	16
37	25
61	50
84	75
101	84
121	90
175	100

Reservoir Sediments		
Distance (km)	Depth from Surface (m)	Fraction of wash load deposit
-1.8	0	0.18
-1.6	0	0.34
-1.4	0	0.40
-1.2	0	0.37
-1	0	0.34
-0.8	0	0.31
-0.6	0	0.28
-0.4	0	0.26
-0.2	0	0.40
-0.1	0	0.44

Sediment Supply Entering Reservoir		
Flow Index	Wash load (m3/year)	Bed Material (m3/year)
1	28500	3300

Minimal Dredging before Dam Removal

One Shot Removal

Number of weeks	Downstream Bankfull Depth
52	2 m

Discharge data from 1999 Water Year (USGS)

Table B.3 Upper Clark Fork Arm of reservoir Run 2 DREAM-1 input.

Channel Geometry (negative values within the reservoir, positive downstream)				
X (km)	Width (m)	Base (m)	Thick (m)	Flow Index
-1.8	200	994.53	0.00	1
-1.7	500	994.26	0.00	1
-1.6	600	993.99	0.05	1
-1.5	750	993.29	0.01	1
-1.4	760	993.44	0.02	1
-1.3	760	993.17	0.02	1
-1.2	840	992.90	0.03	1
-1.1	1040	992.63	0.04	1
-1	1124	992.36	0.10	1
-0.9	1162	992.08	0.16	1
-0.8	1140	992.35	0.18	1
-0.7	1134	991.54	1.00	1
-0.6	1076	991.27	1.10	1
-0.5	1000	991.38	1.30	1
-0.4	913	991.23	1.11	1
-0.3	730	990.90	1.76	1
-0.2	600	989.02	3.71	1
-0.1	573	988.62	4.08	1
0.1	40	988.97	0.00	1
0.2	40	988.60	0.00	1
0.3	40	988.24	0.00	1
0.4	40	987.87	0.00	1
0.5	40	987.50	0.00	1
0.6	40	987.14	0.00	1
0.7	40	986.77	0.00	1
0.8	40	986.41	0.00	1
0.9	40	986.04	0.00	1
1	40	985.68	0.00	1
1.1	40	985.31	0.00	1
1.2	40	985.07	0.00	1
1.3	40	984.66	0.00	1
1.4	40	984.31	0.00	1
1.5	40	983.96	0.00	1
1.6	40	983.61	0.00	1
1.7	40	983.27	0.00	1

1.8	40	982.92	0.00	1
1.9	40	982.57	0.00	1
2	40	982.22	0.00	1
2.1	40	981.87	0.00	1
2.2	40	981.52	0.00	1
2.3	40	981.18	0.00	1
2.4	40	980.83	0.00	1
2.5	40	980.48	0.00	1

Bed Material			Reservoir Sediments			Sediment Supply Entering Reservoir		
Size (mm)	% Finer		Distance (km)	Depth from Surface (m)	Fraction of wash load deposit	Flow Index	Wash load (m3/year)	Bed Material (m3/year)
1	0		-1.8	0	0.18	1	28500	3300
2	35		-1.6	0	0.34			
4	38		-1.4	0	0.40	Minimal Dredging before Dam Removal		
8	45		-1.2	0	0.37			
16	57		-1	0	0.34	One Shot Removal		
32	75		-0.8	0	0.31			
64	93		-0.6	0	0.28	Number of weeks	Downstream Bankfull Depth	
128	100		-0.4	0	0.26	52	2 m	
			-0.2	0	0.40			
			-0.1	0	0.44	Discharge data from 1999 Water Year (USGS)		

Table B.4 Upper Clark Fork Arm of reservoir Run 3 DREAM-1 input (same as Run 2 except for the following data).

Channel Geometry (negative values within the reservoir, positive downstream)				
X (km)	Width (m)	Base (m)	Thick (m)	Flow Index
-1.8	100	994.5299	0.003	1
-1.7	250	994.2582	0.004	1
-1.6	300	993.9866	0.05	1
-1.5	375	993.2947	0.006	1
-1.4	380	993.4432	0.015	1
-1.3	380	993.1716	0.019	1
-1.2	420	992.8999	0.028	1
-1.1	520	992.6283	0.044	1
-1	562	992.3566	0.1	1
-0.9	581	992.0849	0.16	1
-0.8	570	992.3529	0.177	1
-0.7	567	991.5416	1	1
-0.6	538	991.27	1.1	1
-0.5	500	991.3807	1.3	1
-0.4	457	991.2252	1.11	1
-0.3	365	990.8991	1.761	1
-0.2	300	989.0247	3.706	1
-0.1	286	988.6163	4.081	1

Table B.5 Upper Clark Fork Arm of reservoir Run 4 DREAM-1 input (same as Run 2 except for the following data).

Bed Material	
Size (mm)	% Finer
2	0
4	35
8	38
16	45
32	57
64	75
128	93
256	100

Table B.6 Upper Clark Fork Arm of reservoir Run 5 DREAM-1 input (same as Run 2 except for the following data).

Reservoir Sediments		
Distance (km)	Depth from Surface (m)	Fraction of wash load deposit
-1.8	0	0.08
-1.6	0	0.24
-1.4	0	0.30
-1.2	0	0.27
-1	0	0.24
-0.8	0	0.21
-0.6	0	0.18
-0.4	0	0.16
-0.2	0	0.30
-0.1	0	0.34

Results:

DREAM-1 Summary Results:

Table B.7 Blackfoot Arm Run 1 DREAM-1 summary of weekly results.

Distance Upstream Dam (km)	Initial Elevation (m)	Elevation After 52 Weeks (m)	Change in Thickness (m)	Section Width (m)	Section Length (km)	Export of Sediment by Section (m3)
4.15						
3.39	994.70	994.78	0.08	45.48	0.00	0.00
2.77	994.36	994.27	-0.09	67.55	0.48	-2869.21
2.43	993.48	992.34	-1.14	60.07	0.25	-17048.15
2.27	990.60	990.95	0.35	38.17	0.17	2237.84
2.09	987.99	989.20	1.21	25.50	0.19	5695.75
1.90	989.78	989.78	0.00	52.14	0.16	0.00
1.77	990.37	990.37	0.00	62.00	0.14	0.00
1.63	990.64	990.64	0.00	59.24	0.15	0.00
1.46	990.58	990.39	-0.19	57.82	0.18	-1923.99
1.27	989.94	989.65	-0.30	57.62	0.18	-3028.75
1.11	991.23	989.03	-2.20	61.49	0.15	-20677.03
0.97	989.61	987.84	-1.77	48.64	0.14	-12446.14
0.82	989.88	987.84	-2.04	56.88	0.16	-18698.19
0.64	990.43	987.62	-2.81	54.43	0.17	-25803.09
0.48	989.64	987.08	-2.55	60.77	0.16	-24961.54
0.32	989.36	986.53	-2.83	42.62	0.12	-14571.51
0.24	988.72	986.07	-2.65	48.48	0.07	-9305.94
0.18	988.66	986.21	-2.46	78.26	0.07	-13923.14
0.10	987.92	985.91	-2.01	86.07	0.07	-12538.99
0.03	986.80	985.55	-1.25	83.96	0.06	-6754.51
0.00	984.48	984.48				
			Total Export of Reservoir Sediments (m3)			-176616.61
			Total Export of Reservoir Sediments (t)			-245497.08

Table B.8 Upper Clark Fork Arm Run 1 DREAM-1 summary of weekly results.

Distance Upstream Bypass (km)	Initial Elevation (m)	Elevation After 52 Weeks (m)	Change in Thickness (m)	Deposit Section Length (km)	Export of Sediment by Section (m3)
1.70	994.26	994.62	0.36	0.15	2148.00
1.60	993.99	994.16	0.17	0.10	668.00
1.50	993.31	993.89	0.58	0.10	2332.00
1.40	993.46	993.57	0.11	0.10	452.00
1.30	993.19	993.20	0.01	0.10	40.00
1.20	992.93	992.93	0.00	0.10	0.00
1.10	992.68	992.68	0.00	0.10	0.00
1.00	992.43	992.43	0.00	0.10	0.00
0.90	992.25	992.25	0.00	0.10	0.00
0.80	992.53	992.53	0.00	0.10	0.00
0.70	992.55	992.55	0.00	0.10	0.00
0.60	992.37	992.37	0.00	0.10	0.00
0.50	992.68	992.68	0.00	0.10	-8.00
0.40	992.34	992.34	0.00	0.10	4.00
0.30	992.66	992.66	0.00	0.10	-12.00
0.20	992.73	992.73	0.00	0.10	-12.00
0.10	992.70	992.70	0.00	0.15	-18.00
0.00	989.33	989.33			
			Total Export of Reservoir Sediments (m3)		5594.00
			Total Export of Reservoir Sediments (t)		7775.66

Table B.9 Upper Clark Fork Arm Runs 2, 3 and 5 DREAM-1, summary of weekly results.

Distance Upstream Bypass (km)	Initial Elevation (m)	Elevation After 52 Weeks (m)	Change in Thickness (m)	Deposit Section Length (km)	Export of Sediment by Section (m3)
1.70	994.26	994.26	0.00	0.15	-24.00
1.60	994.04	993.99	-0.05	0.10	-200.00
1.50	993.30	993.41	0.11	0.10	440.00
1.40	993.46	993.44	-0.01	0.10	-60.00
1.30	993.19	993.17	-0.02	0.10	-76.00
1.20	992.93	992.90	-0.03	0.10	-112.00
1.10	992.67	992.63	-0.04	0.10	-176.00
1.00	992.46	992.36	-0.10	0.10	-400.00
0.90	992.25	992.11	-0.14	0.10	-560.00
0.80	992.53	992.35	-0.18	0.10	-708.00
0.70	992.54	991.54	-1.00	0.10	-4000.00
0.60	992.37	991.27	-1.10	0.10	-4400.00
0.50	992.68	991.38	-1.30	0.10	-5200.00
0.40	992.34	991.23	-1.11	0.10	-4440.00
0.30	992.66	990.90	-1.76	0.10	-7044.00
0.20	992.73	989.03	-3.71	0.10	-14824.00
0.10	992.70	988.66	-4.03	0.15	-24210.00
0.00	989.33	989.33			
			Total Export of Reservoir Sediments (m3)		-65994.00
			Total Export of Reservoir Sediments (t)		-91731.66

Table B.10 Upper Clark Fork Arm Run 4 DREAM-1, summary of weekly results.

Distance Upstream Bypass (km)	Initial Elevation (m)	Elevation After 52 Weeks (m)	Change in Thickness (m)	Deposit Section Length (km)	Export of Sediment by Section (m3)
1.70	994.26	994.33	0.07	0.15	408.00
1.60	994.04	993.99	-0.05	0.10	-200.00
1.50	993.30	993.47	0.17	0.10	684.00
1.40	993.46	993.44	-0.01	0.10	-60.00
1.30	993.19	993.17	-0.02	0.10	-76.00
1.20	992.93	992.90	-0.03	0.10	-112.00
1.10	992.67	992.63	-0.04	0.10	-176.00
1.00	992.46	992.36	-0.10	0.10	-400.00
0.90	992.25	992.11	-0.14	0.10	-552.00
0.80	992.53	992.35	-0.18	0.10	-708.00
0.70	992.54	991.54	-1.00	0.10	-4000.00
0.60	992.37	991.32	-1.05	0.10	-4188.00
0.50	992.68	991.38	-1.30	0.10	-5200.00
0.40	992.34	991.23	-1.11	0.10	-4440.00
0.30	992.66	990.90	-1.76	0.10	-7044.00
0.20	992.73	989.23	-3.50	0.10	-13996.00
0.10	992.70	989.12	-3.57	0.15	-21444.00
0.00	989.33	989.33			
			Total Export of Reservoir Sediments (m3)		-61504.00
			Total Export of Reservoir Sediments (t)		-85490.56